

# Heterogeneous Mathematical Models in Fluid Dynamics and Associated Solution Algorithms

Marco Discacciati, Paola Gervasio, and Alfio Quarteroni

**Abstract** Mathematical models of complex physical problems can be based on heterogeneous differential equations, i.e. on boundary-value problems of different kind in different subregions of the computational domain. In this presentation we will introduce a few representative examples, we will illustrate the way the coupling conditions between the different models can be devised, then we will address several solution algorithms and discuss their properties of convergence as well as their robustness with respect to the variation of the physical parameters that characterize the submodels.

## 1 Introduction and Motivation

For the description and simulation of complex physical phenomena, combination of hierarchical mathematical models can be set up with the aim of reducing the computational complexity. This gives rise to a system of heterogeneous problems, where different kind of differential problems are set up in subdomains (either disjoint or overlapping) of the original computational domain. When facing this

---

M. Discacciati (✉)

Laboratori de Càlcul Numèric (LaCàN), Universitat Politècnica de Catalunya (UPC BarcelonaTech), Campus Nord UPC - C2, E-08034 Barcelona, Spain  
e-mail: [marco.discacciati@upc.edu](mailto:marco.discacciati@upc.edu)

P. Gervasio

Department of Mathematics, University of Brescia, Brescia, Italy  
e-mail: [paola.gervasio@unibs.it](mailto:paola.gervasio@unibs.it)

A. Quarteroni

MOX, Department of Mathematics, Politecnico di Milano, Milano, Italy

CMCS-EPFL, CH-1015 Lausanne, Switzerland

e-mail: [alfio.quarteroni@epfl.ch](mailto:alfio.quarteroni@epfl.ch)

kind of coupled problems, two natural issues arise. The former is concerned with the way interface coupling conditions can be devised, the latter with the construction of suitable solution algorithms that can take advantage of the intrinsic splitting nature of the problem at hand. This work will focus on both issues, in the context of heterogeneous boundary-value problems that can be used for fluid dynamics applications.

The outline of this presentation is as follows. After giving the motivation for this investigation, we will present two different approaches for the derivation and analysis of the interface coupling conditions: the one based on the variational formulation, the other on virtual controls. For the former we will consider at first advection–diffusion problems. After carrying out their variational analysis we propose domain decomposition algorithms for their solution, in particular those based on Dirichlet–Neumann, adaptive Robin–Neumann, or Steklov–Poincaré iterations. Then, we will focus on Navier–Stokes/Darcy or Stokes/potential coupled problem presenting their asymptotic analysis together with possible solution techniques.

For the virtual control approach, we will study the case of non-overlapping subdomains for advection–diffusion problems considering in particular possible techniques to solve the optimality system and we will present some numerical results. Then, we will consider the case of domain decomposition with overlap, namely Schwarz methods with Dirichlet/Robin interface conditions. We will investigate the virtual control approach with overlap for the advection–diffusion equations including the case of three virtual controls and we will present some numerical results. Finally, we will illustrate this framework for the case of the Stokes–Darcy coupled problem, and for the coupling of incompressible flows.

In order to motivate our investigation, we begin to analyze the advection–diffusion problem.

Let us consider a bounded domain  $\Omega \subset \mathbb{R}^d$  ( $d = 1, 2, 3$ ) with Lipschitz boundary and the advection–diffusion equation

$$\begin{cases} Au \equiv \operatorname{div}(-\nu \nabla u + \mathbf{b}u) + b_0 u = f & \text{in } \Omega \\ u = g & \text{on } \partial\Omega, \end{cases} \quad (1)$$

where  $\nu > 0$  is a characteristic parameter of the problem,  $\mathbf{b} = \mathbf{b}(\mathbf{x})$  a  $d$ -dimensional vector valued function,  $b_0 = b_0(\mathbf{x})$  and  $f = f(\mathbf{x})$  scalar functions, all assigned in  $\Omega$ , while  $g = g(\mathbf{x})$  is assigned on  $\partial\Omega$ .

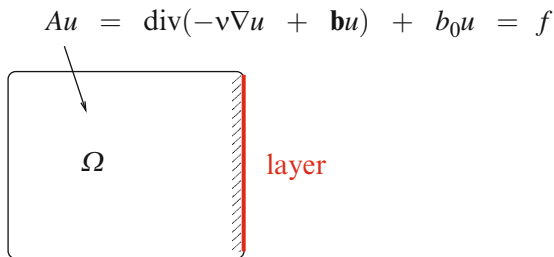
The characteristic parameter  $\nu$  can either represent the thermal diffusivity in heat transfer problems, or the inverse of the Reynolds number in incompressible fluid-dynamics, or another suitable parameter.

Denoting by

$$\mathbb{P}e_g(\mathbf{x}) = \frac{|\mathbf{b}(\mathbf{x})|}{2\nu} \quad (2)$$

the *global Péclet number*, we call (1) an *advection-dominated problem* when  $\mathbb{P}e_g(\mathbf{x}) \gg 1$ .

**Fig. 1** A simple computational domain and the localization of the boundary layer



We are interested in treating advection dominated problems with boundary layers (see, e.g., Fig. 1), that arise when boundary data are incompatible with the limit (as  $v \rightarrow 0$ ) of the advection–diffusion equation. As an example, let us consider the one-dimensional advection–diffusion equation

$$\begin{cases} -v u''(x) + b u'(x) = 0, & 0 < x < 1, \\ u(0) = 0, & u(1) = 1, \end{cases} \quad (3)$$

with  $v > 0$  and  $b > 0$ . Problem (3) can be solved exactly and its solution reads

$$u(x) = \frac{e^{bx/v} - 1}{e^{b/v} - 1}.$$

Such solution exhibits a boundary layer of width  $O(v/b)$  near to  $x = 1$  when the ratio  $v/b$  is small enough, that is when

$$\mathbb{P}e_g(\mathbf{x}) \gg 1. \quad (4)$$

In Fig. 2 we show the one-dimensional solution  $u(x)$  of (3) for two different values of the Péclet number:  $\mathbb{P}e_g(\mathbf{x}) = 0.5$  at left and  $\mathbb{P}e_g(\mathbf{x}) = 100$  at right. Only in the latter case a boundary layer occurs.

When (4) holds, the diffusive term is relevant only in a small part of the domain near to the boundary layer, while it can formally be neglected in the rest of the domain, where the advection phenomenon prevails.

The idea is then: to split the domain in two non-overlapping subdomains  $\Omega_1$  and  $\Omega_2$  where we denote by  $\Gamma = \partial\Omega_1 \cap \partial\Omega_2$  the interface between subdomains, and then to solve a reduced problem as follows (see Fig. 3):

$$\begin{cases} A_1 u_1 \equiv \operatorname{div}(\mathbf{b} u_1) + b_0 u_1 = f & \text{in } \Omega_1 \\ A_2 u_2 \equiv \operatorname{div}(-v \nabla u_2 + \mathbf{b} u_2) + b_0 u_2 = f & \text{in } \Omega_2 \\ \text{Boundary conditions} & \text{on } \partial\Omega. \end{cases} \quad (5)$$

The main question that follows is: *how to couple the subproblems?*

To answer this question one should:

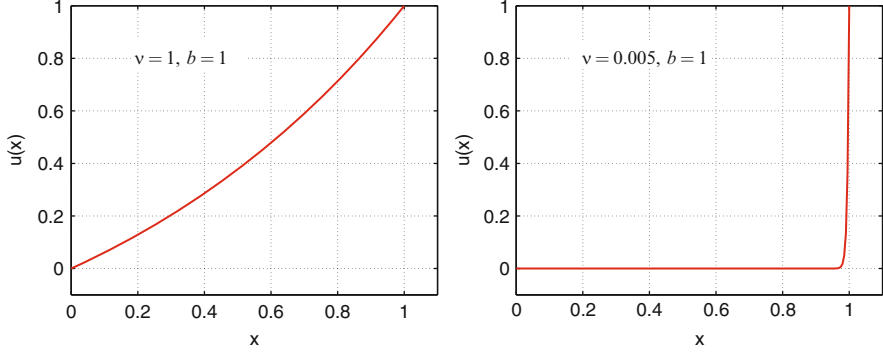


**Fig. 2** The exact solution of problem (3). The solution at right exhibits a boundary layer in  $x = 1$

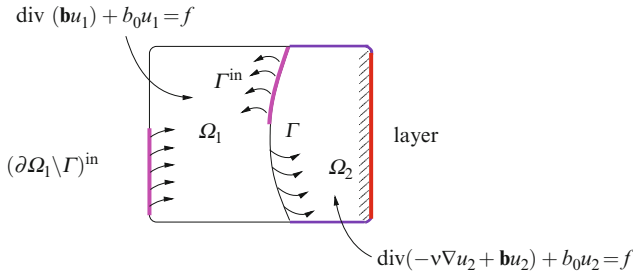


**Fig. 3** The reduced problem on the computational domain  $\Omega \subset \mathbb{R}^2$

1. Find *interface conditions* on  $\Gamma$  so that the new reduced problem is well posed and its solution is “close to” the original one; then
2. Set up *efficient solution algorithms* to solve the reduced problem.

By a singular perturbation analysis, Gastaldi et al. [30] proposed the following set of interface conditions:

$$\begin{cases} u_1 = u_2 & \text{on } \Gamma^{\text{in}} \\ \mathbf{b} \cdot \mathbf{n}_\Gamma u_1 + v \frac{\partial u_2}{\partial n_\Gamma} - \mathbf{b} \cdot \mathbf{n}_\Gamma u_2 = 0 & \text{on } \Gamma, \end{cases} \quad (6)$$

where  $\mathbf{n}_\Gamma$  is the normal vector to  $\Gamma$  oriented from  $\Omega_1$  to  $\Omega_2$  and  $\Gamma^{\text{in}} = \{\mathbf{x} \in \Gamma : \mathbf{b}(\mathbf{x}) \cdot \mathbf{n}_\Gamma(\mathbf{x}) < 0\}$  is the inflow interface for  $\Omega_1$ .

The coupled formulation (5) and (6) allows the independent solution of a sequence of hyperbolic problems in  $\Omega_1$  and elliptic problems in  $\Omega_2$ , in the framework of iterative processes between subdomains. The different possible treatments of the interface relations is what distinguishes one iterative method from another. In this respect, a very natural approach is defined as follows. Given a suitable initial guess  $\lambda^{(0)}$  on  $\Gamma^{\text{in}}$  and a suitable relaxation parameter  $\vartheta > 0$ , it iterates

between  $\Omega_1$  and  $\Omega_2$  until convergence as follows: for  $k \geq 0$  do

$$\begin{aligned}
 &\text{Solve} \quad \begin{cases} A_1 u_1^{(k+1)} = f & \text{in } \Omega_1 \\ u_1^{(k+1)} = g & \text{on } (\partial\Omega_1 \setminus \Gamma)^{\text{in}} \\ u_1^{(k+1)} = \lambda^{(k)} & \text{on } \Gamma^{\text{in}}, \end{cases} \\
 &\text{Solve} \quad \begin{cases} A_2 u_2^{(k+1)} = f & \text{in } \Omega_2 \\ u_2^{(k+1)} = g & \text{on } \partial\Omega_2 \setminus \Gamma \\ -\nu \frac{\partial u_2^{(k+1)}}{\partial n_\Gamma} + \mathbf{b} \cdot \mathbf{n}_\Gamma u_2^{(k+1)} = \mathbf{b} \cdot \mathbf{n}_\Gamma u_1^{(k+1)} & \text{on } \Gamma, \end{cases} \quad (7) \\
 &\text{Compute } \lambda^{(k+1)} = (1 - \vartheta) \lambda^{(k)} + \vartheta u_2^{(k+1)}|_{\Gamma^{\text{in}}}.
 \end{aligned}$$

The coupled advection/advection–diffusion problem has been studied in [30] and alternative interface conditions have been proposed in [21, 23, 24]. In [26] the problem has been solved in the context of virtual control approach. We refer to Sects. 2.2, 2.3, 3.1 for a more detailed analysis and solution of this problem.

Another problem which deserves our attention is the generalized Stokes equation (see [51, Sect. 8.2.1]).

Let us refer to an idealised geometrical situation as depicted in Fig. 4, left.

The bounded domain  $\Omega \subset \mathbb{R}^d$ ,  $d = 2, 3$ , is external to a body whose boundary is  $\Gamma_b$  and we set  $\Gamma_\infty := \partial\Omega \setminus \Gamma_b$ . The problem we are considering reads: find the vector field  $\mathbf{u}$  and the scalar field  $p$  such that

$$\begin{cases} \alpha \mathbf{u} - \nu \Delta \mathbf{u} + \nabla p = \mathbf{f}, & \text{div} \mathbf{u} = 0 & \text{in } \Omega \\ \mathbf{u} = \mathbf{0} & & \text{on } \Gamma_b \\ B \mathbf{u} = \boldsymbol{\varphi}_\infty & & \text{on } \Gamma_\infty, \end{cases} \quad (8)$$

where  $\mathbf{f}$  and  $\boldsymbol{\varphi}_\infty$  are given functions,  $B$  denotes the boundary operator on  $\Gamma_\infty$ , while  $\alpha \geq 0$  is a given parameter. To take  $\alpha = 0$  corresponds to solve the Stokes problem. Nevertheless, this problem may arise in the process of solving the full Navier–Stokes

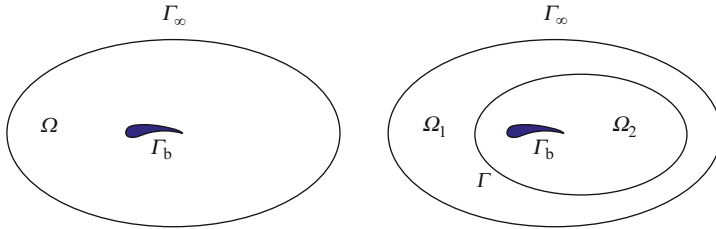


**Fig. 4** The geometrical configuration for an external problem (*left*) and a possible non overlapping decomposition of the computational domain (*right*)

equations, when the discretisation of the time derivative is performed by means of a scheme that is explicit in the non-linear convective term. In this case, the parameter  $\alpha > 0$  represents the inverse of the time-step and the function  $\mathbf{f}$ , in fact, depends on the solution at the previous step, i.e.  $\mathbf{f} = \mathbf{f}(\mathbf{u}^{(n)})$ .

The boundary conditions on  $\Gamma_\infty$  have to be prescribed in a suitable way for assuring well-posedness. In this respect, on a portion  $\Gamma_\infty^{\text{in}}$  of  $\Gamma_\infty$  an onset flow  $\mathbf{u} = \mathbf{u}_\infty^{\text{in}}$  is given. However, assigning conditions on the outflow section  $\Gamma_\infty^{\text{out}}$  may not be simple. It is also clear that all interesting flow features occur in the vicinity of the body due to the role of viscosity in this area.

For this reason, Schenk and Hebeker [56] have proposed the replacement of problem (8) with a reduced one far from the obstacle.

The computational domain  $\Omega$  is partitioned into a subdomain  $\Omega_2$ , next to the body, and a far field subdomain  $\Omega_1$ ; the interface between  $\Omega_1$  and  $\Omega_2$  is denoted by  $\Gamma$ ,  $\mathbf{n}_\Gamma$  is the unit normal vector on  $\Gamma$  directed from  $\Omega_1$  to  $\Omega_2$ , and  $\mathbf{n}$  the unit outward normal vector on  $\partial\Omega$ . The global Stokes equation (8) is replaced with the following coupled problem, where the viscosity  $\nu$  is set to 0 in  $\Omega_1$ :

$$\left\{ \begin{array}{ll} \alpha \mathbf{u}_1 + \nabla p_1 = \mathbf{f}, \quad \text{div} \mathbf{u}_1 = 0 & \text{in } \Omega_1 \\ \mathbf{u}_1 = \mathbf{u}_\infty^{\text{in}} & \text{on } \Gamma_\infty^{\text{in}} \\ p_1 = 0 & \text{on } \Gamma_\infty^{\text{out}} \\ \alpha \mathbf{u}_2 - \nu \Delta \mathbf{u}_2 + \nabla p_2 = \mathbf{f}, \quad \text{div} \mathbf{u}_2 = 0 & \text{in } \Omega_2 \\ \mathbf{u}_2 = \mathbf{0} & \text{on } \Gamma_b, \end{array} \right. \quad (9)$$

or equivalently, by applying the divergence operator to (9)<sub>1</sub>:

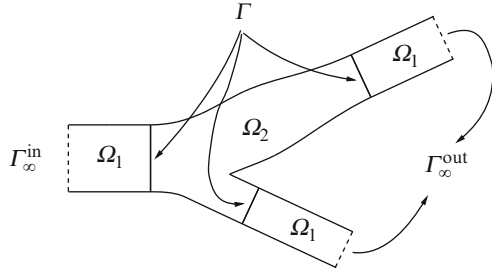
$$\left\{ \begin{array}{ll} \Delta p_1 = \text{div} \mathbf{f} & \text{in } \Omega_1 \\ \frac{\partial p_1}{\partial n} = (\mathbf{f} - \alpha \mathbf{u}_\infty^{\text{in}}) \cdot \mathbf{n} & \text{on } \Gamma_\infty^{\text{in}} \\ p_1 = 0 & \text{on } \Gamma_\infty^{\text{out}} \\ \alpha \mathbf{u}_2 - \nu \Delta \mathbf{u}_2 + \nabla p_2 = \mathbf{f}, \quad \text{div} \mathbf{u}_2 = 0 & \text{in } \Omega_2 \\ \mathbf{u}_2 = \mathbf{0} & \text{on } \Gamma_b. \end{array} \right. \quad (10)$$

Either problem (9) and (10) are incomplete, because the matching conditions that have to be fulfilled on  $\Gamma$  are missing.

In [56] these conditions are recovered through a singular perturbation analysis similar to that carried out for the advection–diffusion problem in [30] and they read:

$$\left\{ \begin{array}{ll} \frac{\partial p_1}{\partial n_\Gamma} = (\mathbf{f} - \alpha \mathbf{u}_2) \cdot \mathbf{n}_\Gamma & \text{on } \Gamma \\ p_1 \mathbf{n}_\Gamma = -\nu (\mathbf{n}_\Gamma \cdot \nabla) \mathbf{u}_2 + p_2 \mathbf{n}_\Gamma & \text{on } \Gamma. \end{array} \right. \quad (11)$$

**Fig. 5** The domain decomposition configuration for an internal problem



The coupled problem (10) and (11) can be used also for the simulation of the fluid motion inside a bounded domain, as depicted in Fig. 5. In this case the domain  $\Omega_1$ , in which the reduced problem is solved, is non-connected and separates the interior domain from both inflow and outflow interfaces.

We observe that the system (10) and (11) models two possible different coupled problems. The first one, when  $\alpha = 0$ , is a Stokes/potential coupling, the vector field  $\mathbf{f}$  is independent of the velocity  $\mathbf{u}$  and the pressure  $p_1$  is independent of the solution  $(\mathbf{u}_2, p_2)$ . Such coupling can be used to model external flows.

The second one, when  $\alpha > 0$ , corresponds to the single step of a time-dependent Navier–Stokes/potential coupling where, as said above, the vector field  $\mathbf{f}$  depends on the solution at the previous step. This is the case of the simulation of either the flow inside a channel (or the blood flow in the carotid) or a far field condition.

As in the case of the advection–diffusion problem, the interface conditions (11) could be used to set-up an iterative algorithm by subdomains as follows.

Assume that  $\widehat{\boldsymbol{\lambda}}^{(0)}$  is given and satisfies  $\int_{\Gamma} \widehat{\boldsymbol{\lambda}}^{(0)} \cdot \mathbf{n}_{\Gamma} = 0$ ; for any  $k \geq 0$  solve

$$\left\{ \begin{array}{ll} \Delta p_1^{(k+1)} = \text{div} \mathbf{f} & \text{in } \Omega_1 \\ \frac{\partial p_1^{(k+1)}}{\partial n} = (\mathbf{f} - \alpha \mathbf{u}_{\infty}^{\text{in}}) \cdot \mathbf{n} & \text{on } \Gamma_{\infty}^{\text{in}} \\ p_1^{(k+1)} = 0 & \text{on } \Gamma_{\infty}^{\text{out}} \\ \frac{\partial p_1^{(k+1)}}{\partial n_{\Gamma}} = (\mathbf{f} - \alpha \widehat{\boldsymbol{\lambda}}^{(k)}) \cdot \mathbf{n}_{\Gamma} & \text{on } \Gamma, \end{array} \right. \quad (12)$$

then solve

$$\left\{ \begin{array}{ll} \alpha \mathbf{u}_2^{(k+1)} - \nu \Delta \mathbf{u}_2^{(k+1)} + \nabla p_2^{(k+1)} = \mathbf{f}, & \text{div} \mathbf{u}_2^{(k+1)} = 0 \text{ in } \Omega_2 \\ \mathbf{u}_2^{(k+1)} = \mathbf{0} & \text{on } \Gamma_b \\ \nu (\mathbf{n}_{\Gamma} \cdot \nabla) \mathbf{u}_2^{(k+1)} - p_2^{(k+1)} \mathbf{n}_{\Gamma} = -p_1^{(k+1)} \mathbf{n}_{\Gamma} & \text{on } \Gamma \end{array} \right. \quad (13)$$

and finally set

$$\widehat{\boldsymbol{\lambda}}^{(k+1)} = (1 - \vartheta)\widehat{\boldsymbol{\lambda}}^{(k)} + \vartheta \mathbf{u}_{2|_F}^{(k+1)}, \quad (14)$$

where  $\vartheta > 0$  is a relaxation parameter.

Since  $\operatorname{div} \mathbf{u}_2^{(k+1)} = 0$  in  $\Omega_2$ , the trace  $\mathbf{u}_{2|_F}^{(k+1)}$  satisfies

$$\int_{\Gamma} \mathbf{u}_{2|_F}^{(k+1)} \cdot \mathbf{n}_{\Gamma} = 0,$$

whence  $\int_{\Gamma} \widehat{\boldsymbol{\lambda}}^{(k)} \cdot \mathbf{n}_{\Gamma} = 0$  for each  $k \geq 0$ .

The analysis of the coupled problem (10) and (11) and the proof of convergence of the above iterative process (12)–(14) are reported in [56]. The analysis can be performed also by writing the problem in terms of the associated Steklov–Poincaré operators, and then proving convergence by applying an abstract result (see [51, Thm 4.2.2]).

Finally, we introduce a coupled free/porous-media flow problem.

The computational domain is a region naturally split into two parts: one occupied by the fluid, the other by the porous media. More precisely, let  $\Omega \subset \mathbb{R}^d$  ( $d = 2, 3$ ) be a bounded domain, partitioned into two non intersecting subdomains  $\Omega_f$  and  $\Omega_p$  separated by an interface  $\Gamma$ , i.e.  $\bar{\Omega} = \bar{\Omega}_f \cup \bar{\Omega}_p$ ,  $\Omega_f \cap \Omega_p = \emptyset$  and  $\bar{\Omega}_f \cap \bar{\Omega}_p = \Gamma$  (Fig. 6). We suppose the boundaries  $\partial\Omega_f$  and  $\partial\Omega_p$  to be Lipschitz continuous. From the physical point of view,  $\Gamma$  is a surface separating the domain  $\Omega_f$  filled by a fluid, from a domain  $\Omega_p$  formed by a porous medium. We assume that  $\Omega_f$  has a fixed surface, i.e., we neglect here the case of free-surface flows. The fluid in  $\Omega_f$  can filtrate through the adjacent porous medium.

The Navier–Stokes equations describe the motion of the fluid in  $\Omega_f$ :  $\forall t > 0$ ,

$$\begin{cases} \partial_t \mathbf{u}_f - \operatorname{div} \mathbf{T}(\mathbf{u}_f, p_f) + (\mathbf{u}_f \cdot \nabla) \mathbf{u}_f = \mathbf{f} & \text{in } \Omega_f \\ \operatorname{div} \mathbf{u}_f = 0 & \text{in } \Omega_f, \end{cases} \quad (15)$$

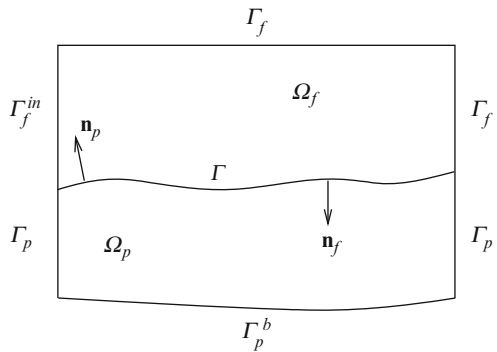


**Fig. 6** Representation of a 2D section of a possible computational domain for the Stokes/Darcy coupling



where  $\mathbf{T}(\mathbf{u}_f, p_f) = \nu(\nabla \mathbf{u}_f + \nabla^T \mathbf{u}_f) - p_f \mathbf{I}$  is the Cauchy stress tensor,  $\mathbf{I}$  being the identity tensor.  $\nu > 0$  is the kinematic viscosity of the fluid,  $\mathbf{f}$  a given volumetric force, while  $\mathbf{u}_f$  and  $p_f$  are the fluid velocity and pressure, respectively.

The filtration of an incompressible fluid through porous media is often described by Darcy's law. The latter provides the simplest linear relation between velocity and pressure in porous media under the physically reasonable assumption that fluid flows are usually very slow and all the inertial (non-linear) terms may be neglected. Darcy's law introduces a fictitious flow velocity, the *Darcy velocity* or *specific discharge*  $\mathbf{q}$  through a given cross section of the porous medium, rather than the true velocity  $\mathbf{u}_p$  with respect to the porous matrix:

$$\mathbf{u}_p = \frac{\mathbf{q}}{n}, \quad (16)$$

with  $n$  being the *volumetric porosity*, defined as the ratio between the volume of void space and the total volume of the porous medium.

To introduce Darcy's law, we define a scalar quantity  $\varphi$  called *piezometric head* which essentially represents the fluid pressure in  $\Omega_p$ :

$$\varphi = z + \frac{p_p}{g}, \quad (17)$$

where  $z$  is the elevation from a reference level, accounting for the potential energy per unit weight of fluid,  $p_p$  is the ratio between the fluid pressure in  $\Omega_p$  and its viscosity  $\rho_f$ , and  $g$  is the gravity acceleration.

Then, Darcy's law can be written as

$$\mathbf{q} = -K \nabla \varphi, \quad (18)$$

where  $K$  is a symmetric positive definite diagonal tensor  $K = (K_{ij})_{i,j=1,\dots,d}$ ,  $K_{ij} \in L^\infty(\Omega_p)$ ,  $K_{ij} > 0$ ,  $K_{ij} = K_{ji}$ , called *hydraulic conductivity tensor*, which depends on the properties of the fluid as well as on the characteristics of the porous medium. Let us denote  $\mathbf{K} = K/n$ .

In conclusion, the motion of an incompressible fluid through a saturated porous medium is described by the following equations:

$$\begin{cases} \mathbf{u}_p = -\mathbf{K} \nabla \varphi & \text{in } \Omega_p \\ \operatorname{div} \mathbf{u}_p = 0 & \text{in } \Omega_p. \end{cases} \quad (19)$$

Finally, to represent the filtration of the free fluid through the porous medium, we have to introduce suitable coupling conditions between the Navier–Stokes and Darcy equations across the common interface  $\Gamma$ . In particular we consider the following three conditions.

1. Continuity of the normal component of the velocity:

$$\mathbf{u}_f \cdot \mathbf{n} = \mathbf{u}_p \cdot \mathbf{n}, \quad (20)$$

where we have indicated  $\mathbf{n} = \mathbf{n}_f = -\mathbf{n}_p$  on  $\Gamma$ . This condition is a consequence of the incompressibility of the fluid.

2. Continuity of the normal stresses across  $\Gamma$  (see, e.g., [36]):

$$-\mathbf{n} \cdot \mathbf{T}(\mathbf{u}_f, p_f) \cdot \mathbf{n} = g\varphi. \quad (21)$$

Remark that pressures may be discontinuous across the interface.

3. Finally, in order to have a completely determined flow in the free-fluid region, we have to specify a further condition on the tangential component of the fluid velocity at the interface. An experimental condition was obtained by Beavers and Joseph stating that the slip velocity at the interface differs from the seepage velocity in the porous domain and it is proportional to the shear rate on  $\Gamma$  [5]:

$$\frac{\nu\alpha_{BJ}}{\sqrt{K}}(\mathbf{u}_f - \mathbf{u}_p)_\tau - (\mathbf{T}(\mathbf{u}_f, p_f) \cdot \mathbf{n})_\tau = 0. \quad (22)$$

By  $(\mathbf{v})_\tau$  we indicate the tangential component to the interface of  $\mathbf{v}$ :

$$(\mathbf{v})_\tau = \mathbf{v} - (\mathbf{v} \cdot \mathbf{n})\mathbf{n}. \quad (23)$$

Since the seepage velocity  $\mathbf{u}_p$  is far smaller than the fluid slip velocity  $\mathbf{u}_f$  at the interface, Saffman proposed to use the following simplified condition (the so-called Beavers–Joseph–Saffman condition) [53]:

$$\frac{\nu\alpha_{BJ}}{\sqrt{K}}(\mathbf{u}_f)_\tau - (\mathbf{T}(\mathbf{u}_f, p_f) \cdot \mathbf{n})_\tau = 0. \quad (24)$$

This condition was later derived mathematically by means of homogenization by Jäger and Mikelić [36–38].

The three coupling conditions described in this section have been extensively studied and analysed also in [17, 19, 46, 49, 52].

In conclusion, the coupled Navier–Stokes/Darcy model reads

$$\left\{ \begin{array}{ll} \partial_t \mathbf{u}_f - \mathbf{div} \mathbf{T}(\mathbf{u}_f, p_f) + (\mathbf{u}_f \cdot \nabla) \mathbf{u}_f = \mathbf{f} & \text{in } \Omega_f \\ \mathbf{div} \mathbf{u}_f = 0 & \text{in } \Omega_f \\ \mathbf{u}_p = -K \nabla \varphi & \text{in } \Omega_p \\ \mathbf{div} \mathbf{u}_p = 0 & \text{in } \Omega_p \\ \mathbf{u}_f \cdot \mathbf{n} = \mathbf{u}_p \cdot \mathbf{n} & \text{on } \Gamma \\ -\mathbf{n} \cdot \mathbf{T}(\mathbf{u}_f, p_f) \cdot \mathbf{n} = g\varphi & \text{on } \Gamma \\ \frac{\nu\alpha_{BJ}}{\sqrt{K}}(\mathbf{u}_f)_\tau - (\mathbf{T}(\mathbf{u}_f, p_f) \cdot \mathbf{n})_\tau = 0 & \text{on } \Gamma. \end{array} \right. \quad (25)$$

Using Darcy's law we can rewrite the system (19) as an elliptic equation for the scalar unknown  $\varphi$ :

$$-\nabla \cdot (\mathbf{K} \nabla \varphi) = 0 \quad \text{in } \Omega_p. \quad (26)$$

In this case, the differential formulation of the coupled Navier–Stokes/Darcy problem becomes

$$\begin{cases} \partial_t \mathbf{u}_f - \operatorname{div} \mathbf{T}(\mathbf{u}_f, p_f) + (\mathbf{u}_f \cdot \nabla) \mathbf{u}_f = \mathbf{f} & \text{in } \Omega_f \\ \operatorname{div} \mathbf{u}_f = 0 & \text{in } \Omega_f \\ -\operatorname{div} (\mathbf{K} \nabla \varphi) = 0 & \text{in } \Omega_p, \end{cases} \quad (27)$$

with the interface conditions on  $\Gamma$ :

$$\begin{cases} \mathbf{u}_f \cdot \mathbf{n} = -\mathbf{K} \frac{\partial \varphi}{\partial n} \\ -\mathbf{n} \cdot \mathbf{T}(\mathbf{u}_f, p_f) \cdot \mathbf{n} = g\varphi \\ \frac{\nu \alpha_{BJ}}{\sqrt{\mathbf{K}}} (\mathbf{u}_f)_\tau - (\mathbf{T}(\mathbf{u}_f, p_f) \cdot \mathbf{n})_\tau = 0. \end{cases} \quad (28)$$

We refer to Sects. 2.6, 2.7, 3.4 for a more exhaustive analysis of the Stokes/Darcy coupling.

## 2 Variational Formulation Approach

The reduced problems presented above will be analysed in this Section in a variational setting, in order to deduce suitable interface conditions which can be rigorously justified. Moreover, different iterative algorithms to solve the reduced problems will be presented.

### 2.1 The Advection–Diffusion Problem

We consider an open bounded domain  $\Omega \subset \mathbb{R}^d$  ( $d = 2, 3$ ) with Lipschitz boundary  $\partial\Omega$ , and we split it into two open subsets  $\Omega_1$  and  $\Omega_2$  such that

$$\overline{\Omega} = \overline{\Omega}_1 \cup \overline{\Omega}_2, \quad \Omega_1 \cap \Omega_2 = \emptyset. \quad (29)$$

Then, we denote by

$$\Gamma = \partial\Omega_1 \cap \partial\Omega_2 \quad (30)$$

the interface between the subdomains (see Fig. 3) and we assume that  $\Gamma$  is of class  $C^{1,1}$ ;  $\overset{\circ}{\Gamma}$  will denote the interior of  $\Gamma$ .

Given two scalar functions  $f$  and  $b_0$  defined in  $\Omega$ , a positive function  $\nu$  defined in  $\Omega_2 \cup \overset{\circ}{\Gamma}$ , a  $d$ -dimensional vector valued function  $\mathbf{b}$  defined in  $\Omega$  satisfying the

following inequalities:

$$\begin{aligned} \exists v_0 \in \mathbb{R} : v(\mathbf{x}) &\geq v_0 > 0 & \forall \mathbf{x} \in \Omega_2 \cup \overset{\circ}{\Gamma}, \\ \exists \sigma_0 \in \mathbb{R} : b_0(\mathbf{x}) + \frac{1}{2} \operatorname{div} \mathbf{b}(\mathbf{x}) &\geq \sigma_0 > 0 & \forall \mathbf{x} \in \Omega, \end{aligned} \quad (31)$$

we are interested in finding two functions  $u_1$  and  $u_2$  (defined in  $\overline{\Omega}_1$  and  $\overline{\Omega}_2$ , respectively) such that  $u_1$  satisfies the advection–reaction equation

$$A_1 u_1 \equiv \operatorname{div}(\mathbf{b} u_1) + b_0 u_1 = f \quad \text{in } \Omega_1, \quad (32)$$

while  $u_2$  satisfies the advection–diffusion–reaction equation

$$A_2 u_2 \equiv -\operatorname{div}(v \nabla u_2) + \operatorname{div}(\mathbf{b} u_2) + b_0 u_2 = f \quad \text{in } \Omega_2. \quad (33)$$

For each subdomain, we distinguish between the *external* (or physical) boundary  $\partial\Omega \cap \partial\Omega_k = \partial\Omega_k \setminus \Gamma$  (for  $k = 1, 2$ ) and the *internal* one, i.e. the interface  $\Gamma$ .

Moreover, for any non-empty subset  $S \subseteq \partial\Omega_1$ , we define

$$\text{The inflow part of } S : S^{\text{in}} = \{\mathbf{x} \in S : \mathbf{b}(\mathbf{x}) \cdot \mathbf{n}(\mathbf{x}) < 0\}, \quad (34)$$

where  $\mathbf{n}(\mathbf{x})$  is the outward unit normal vector on  $S$ ,

$$\text{The outflow part of } S : S^{\text{out}} = \{\mathbf{x} \in S : \mathbf{b}(\mathbf{x}) \cdot \mathbf{n}(\mathbf{x}) \geq 0\}. \quad (35)$$

Boundary conditions for problem (32) must be assigned on  $\partial\Omega_1^{\text{in}}$ .

For a given suitable function  $g$  defined on  $\partial\Omega$ , we denote by  $g_1$  and  $g_2$  the restriction of  $g$  to  $(\partial\Omega_1 \setminus \Gamma)^{\text{in}}$  and  $\partial\Omega_2 \setminus \Gamma$ , respectively, and we set the following Dirichlet boundary conditions on the external boundaries:

$$\begin{aligned} u_1 &= g_1 & \text{on } (\partial\Omega_1 \setminus \Gamma)^{\text{in}}, \\ u_2 &= g_2 & \text{on } \partial\Omega_2 \setminus \Gamma. \end{aligned} \quad (36)$$

Finally, let us denote by  $\mathbf{n}_\Gamma$  the normal vector to  $\Gamma$  oriented from  $\Omega_1$  to  $\Omega_2$ , so that  $\mathbf{n}_\Gamma(\mathbf{x}) = \mathbf{n}_1(\mathbf{x}) = -\mathbf{n}_2(\mathbf{x})$ ,  $\forall \mathbf{x} \in \Gamma$ .

## 2.2 Variational Analysis for the Advection–Diffusion Equation

The basic steps of the analysis carried out in [30] are summarized here.

1. Given a positive function  $v$  in  $\Omega$ , we denote by  $\mathcal{P}_\Omega(v)$  the advection–diffusion problem (1) in  $\Omega$ . For any  $\varepsilon > 0$ , we introduce a smooth function  $v_\varepsilon$  defined in  $\Omega_2$ , which is a regularization of  $v$  according with continuity to  $\varepsilon$  on  $\Gamma$ . Then,  $v_\varepsilon^*$  is the globally defined viscosity defined as (see Fig. 7)

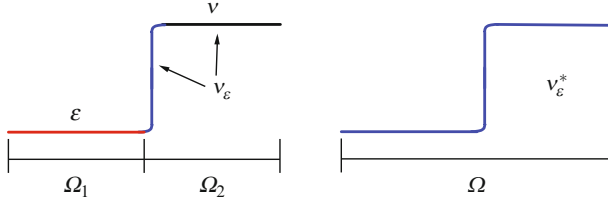


**Fig. 7** The viscosity  $v_\varepsilon^*$  for the regularized problem.  $v_\varepsilon|_{\Omega_2} \rightarrow v$  when  $(\varepsilon \rightarrow 0)$

$$v_\varepsilon^* = \begin{cases} \varepsilon & \text{in } \Omega_1 \\ v_\varepsilon & \text{in } \Omega_2 \end{cases}.$$

We denote by  $\mathcal{P}_\Omega(v_\varepsilon^*) \equiv [\mathcal{P}_{\Omega_1}(\varepsilon)/\mathcal{P}_{\Omega_2}(v_\varepsilon)]$  the following advection–diffusion problem:

$$\begin{cases} -\varepsilon \Delta u_{1,\varepsilon} + \operatorname{div}(\mathbf{b}u_{1,\varepsilon}) + b_0 u_{1,\varepsilon} = f & \text{in } \Omega_1 \\ \operatorname{div}(-v_\varepsilon \nabla u_{2,\varepsilon} + \mathbf{b}u_{2,\varepsilon}) + b_0 u_{2,\varepsilon} = f & \text{in } \Omega_2 \\ \varepsilon \frac{\partial u_{1,\varepsilon}}{\partial n_\Gamma} - \mathbf{b} \cdot \mathbf{n}_\Gamma u_{1,\varepsilon} = v_\varepsilon \frac{\partial u_{2,\varepsilon}}{\partial n_\Gamma} - \mathbf{b} \cdot \mathbf{n}_\Gamma u_{2,\varepsilon} & \text{on } \Gamma \\ u_{1,\varepsilon} = u_{2,\varepsilon} & \text{on } \Gamma \\ u = g & \text{on } \partial\Omega. \end{cases} \quad (37)$$

2. For any  $\varepsilon > 0$ , let  $\mathcal{V}_\Omega(\varepsilon)$  be the variational formulation associated to  $\mathcal{P}_\Omega(\varepsilon)$ . Solving  $\mathcal{V}_\Omega(\varepsilon)$  means to look for the solution  $u_\varepsilon \in V$  of

$$a_\varepsilon(u_\varepsilon, w_\varepsilon) = F(w_\varepsilon), \quad \forall w_\varepsilon \in V. \quad (38)$$

If we take  $g \equiv 0$ , this means to set  $V = H_0^1(\Omega)$  and to solve

$$a_\varepsilon(u_\varepsilon, w_\varepsilon) = \int_\Omega [(\varepsilon \nabla u_\varepsilon - \mathbf{b}u_\varepsilon) \cdot \nabla w_\varepsilon + b_0 u_\varepsilon w_\varepsilon] \, d\mathbf{x}, \quad F(w_\varepsilon) = \int_\Omega f w_\varepsilon \, d\mathbf{x} \quad (39)$$

for any  $w_\varepsilon \in V$ .

Otherwise, if  $g \neq 0$  the formulation is the same, however the right hand side has to be modified as follows:

$$F_g(w_\varepsilon) = F(w_\varepsilon) - a_\varepsilon(R_g, w_\varepsilon),$$

where  $R_g$  is a suitable lifting of the boundary data  $g$ , so that the final solution reads  $u_\varepsilon + R_g$  (see [50]).

3. By asymptotic analysis on  $\mathcal{V}_{\Omega_1}(\varepsilon)$ , recover the reduced problem  $\mathcal{P}_{\Omega_1}(0)$ , so that

$$\mathcal{P}_{\Omega}(v_{\varepsilon}^*) \rightarrow [\mathcal{P}_{\Omega_1}(0)/\mathcal{P}_{\Omega_2}(v)] \quad \text{when } \varepsilon \rightarrow 0.$$

The new coupled problem  $[\mathcal{P}_{\Omega_1}(0)/\mathcal{P}_{\Omega_2}(v)]$  inherits from the limit process a proper set of interface conditions.

According to the analysis performed in [30],  $u_{1,\varepsilon}$  converges weakly in  $L^2(\Omega_1)$  and  $u_{2,\varepsilon}$  converges weakly in  $H^1(\Omega_2)$  when  $\varepsilon \rightarrow 0$ , moreover the limit  $(u_1, u_2) \in L^2(\Omega_1) \times H^1(\Omega_2)$  satisfies the following reduced coupled problem:

$$\begin{cases} \operatorname{div}(\mathbf{b}u_1) + b_0u_1 = f & \text{in } \Omega_1 \\ \operatorname{div}(-v\nabla u_2 + \mathbf{b}u_2) + b_0u_2 = f & \text{in } \Omega_2 \\ -\mathbf{b} \cdot \mathbf{n}_{\Gamma}u_1 = v \frac{\partial u_2}{\partial n_{\Gamma}} - \mathbf{b} \cdot \mathbf{n}_{\Gamma}u_2 & \text{on } \Gamma \\ u_1 = u_2 & \text{on } \Gamma^{\text{in}} \\ u_1 = g_1 & \text{on } (\partial\Omega_1 \setminus \Gamma)^{\text{in}} \\ u_2 = g_2 & \text{on } \partial\Omega_2 \setminus \Gamma. \end{cases} \quad (40)$$

The *interface conditions* (40)<sub>3,4</sub> express the continuity of the flux across the whole interface  $\Gamma$  and the continuity of the solution across the inflow interface  $\Gamma^{\text{in}}$ , respectively. No continuity condition is imposed on  $\Gamma^{\text{out}}$ , as a matter of fact,  $u_1$  and  $u_2$  exhibit a jump across  $\Gamma^{\text{out}}$  which is proportional to  $v|_{\Gamma}$ .

Note that the interface conditions (40)<sub>3,4</sub> can be equivalently expressed as

$$\begin{aligned} u_1 &= u_2 && \text{on } \Gamma^{\text{in}}, \\ \mathbf{b} \cdot \mathbf{n}_{\Gamma}u_1 + v \frac{\partial u_2}{\partial n_{\Gamma}} - \mathbf{b} \cdot \mathbf{n}_{\Gamma}u_2 &= 0 && \text{on } \Gamma^{\text{out}} \\ v \frac{\partial u_2}{\partial n_{\Gamma}} &= 0 && \text{on } \Gamma^{\text{in}}. \end{aligned} \quad (41)$$

In order to proceed with the analysis of the coupled problem, we introduce the following notations. Let  $A$  be an open bounded subset in  $\mathbb{R}^d$ , with Lipschitz continuous boundary. For any open subset  $\Gamma \subset \partial A$ , we define the weighted  $L^2$ -space

$$L_{\mathbf{b}}^2(\Gamma) = \{\varphi : \Gamma \rightarrow \mathbb{R} : \sqrt{|\mathbf{b} \cdot \mathbf{n}_{\Gamma}|}\varphi \in L^2(\Gamma)\}, \quad (42)$$

and the trace space

$$H_{00}^{1/2}(\Gamma) = \{\varphi \in L^2(\Gamma) : \exists \tilde{\varphi} \in H^{1/2}(\partial A) : \tilde{\varphi}|_{\Gamma} = \varphi, \tilde{\varphi}|_{\partial A \setminus \Gamma} = 0\}. \quad (43)$$

The space  $L^2_{\mathbf{b}}(\Gamma)$  endowed with the norm

$$\|\varphi\|_{L^2_{\mathbf{b}}(\Gamma)} = \left( \int_{\Gamma} |\mathbf{b} \cdot \mathbf{n}_{\Gamma}| \varphi^2 d\Gamma \right)^{1/2}$$

is a Hilbert space.

The following result has been proved in [30]:

**Theorem 1.** *Assume the following regularity properties on the data:  $\partial\Omega_1$  and  $\partial\Omega_2$  are Lipschitz continuous, piecewise  $C^{1,1}$ ;  $\Gamma$  is of class  $C^{1,1}$ ;*

$$\begin{aligned} v &\in L^\infty(\Omega_2), \quad \mathbf{b} \in [W^{1,\infty}(\Omega)]^2, \quad b_0 \in L^\infty(\Omega), \quad f \in L^2(\Omega), \\ g &\in H^{-1/2}(\partial\Omega) : g_1 \in L^2_{\mathbf{b}}((\partial\Omega_1 \setminus \Gamma)^{\text{in}}), \quad g_2 \in H^{1/2}(\partial\Omega_2 \setminus \Gamma). \end{aligned} \quad (44)$$

Finally assume (31).

Then there is a unique pair  $(u_1, u_2) \in L^2(\Omega_1) \times H^1(\Omega_2)$  which solves (40), where: (40)<sub>1</sub> and (40)<sub>2</sub> hold in the sense of distributions in  $\Omega_1$  and  $\Omega_2$ , respectively; interface condition (41)<sub>1</sub> holds a.e. on  $\Gamma^{\text{in}}$ , interface condition (41)<sub>2</sub> holds in  $(H^{1/2}_{00}(\Gamma^{\text{out}}))'$ ; interface condition (41)<sub>3</sub> holds in  $(H^{1/2}_{00}(\Gamma^{\text{in}}))'$ . Finally, problem (40) is limit of a family of globally elliptic variational problems.

From now on, the solution  $(u_1, u_2)$  of the heterogeneous problem (40) will be named *heterogeneous solution*.

Other interface conditions have been proposed in the literature to close system (32), (33), (36). For instance, the conditions

$$\begin{aligned} -\mathbf{b} \cdot \mathbf{n}_{\Gamma} u_1 &= v \frac{\partial u_2}{\partial \mathbf{n}_{\Gamma}} - \mathbf{b} \cdot \mathbf{n}_{\Gamma} u_2 \quad \text{on } \Gamma^{\text{out}} \\ u_1 &= u_2, \quad \frac{\partial u_1}{\partial \mathbf{n}_{\Gamma}} = \frac{\partial u_2}{\partial \mathbf{n}_{\Gamma}} \quad \text{on } \Gamma^{\text{in}}, \end{aligned} \quad (45)$$

have been proposed in [21] and are based on absorbing boundary condition theory. The following set (see [23, 24]):

$$\begin{aligned} u_1 &= u_2 \quad \text{on } \Gamma \\ \frac{\partial u_1}{\partial \mathbf{n}_{\Gamma}} &= \frac{\partial u_2}{\partial \mathbf{n}_{\Gamma}} \quad \text{on } \Gamma^{\text{in}} \end{aligned} \quad (46)$$

takes into account the requirement of glueing the solutions across the interface with high regularity.

However, the coupled problem with either one of these set of conditions (45) and (46) cannot be regarded as a limit of the original complete variational problem as the viscosity  $\varepsilon$  tends to zero in  $\Omega_1$ .

Another possible approach to set suitable interface conditions was proposed in [25] for the one-dimensional case with constant coefficients and it is based

on the factorization of the differential operator. To briefly explain it, let us take  $\Omega = (x_1, x_2)$  and let  $x_0 \in \Omega$  denote the position of the interface between  $\Omega_1$  and  $\Omega_2$ , i.e.  $\Omega_1 = (x_1, x_0)$  and  $\Omega_2 = (x_0, x_2)$ . The method consists in the following steps:

- Factorize the differential operator  $A_2 \cdot = -\nu \partial_x^2 \cdot + b \partial_x \cdot + b_0 \cdot$  as

$$A_2 = (b \partial_x - b \lambda^+) \left( -\frac{\nu}{b} \partial_x + \frac{\nu}{b} \lambda^- \right),$$

where  $\lambda^\pm = (b \pm \sqrt{b^2 + 4\nu b_0})/(2\nu)$ , with  $\lambda^+ > 0$  and  $\lambda^- < 0$ .

- Compute the function  $\tilde{u}_1(x) = \tilde{u}_1(x_1) e^{\lambda^+(x-x_1)} + \frac{1}{b} \int_{x_1}^x f(t) e^{\lambda^+(x-t)} dt$ , which is the solution of the modified advection–reaction equation  $\tilde{A}_1 \tilde{u}_1 = b \tilde{u}_1' - b \lambda^+ \tilde{u}_1 = f$  in  $\Omega_1$  with a suitable boundary condition at  $x = x_1$ .
- Solve the advection diffusion problem  $A_2 u_2 = f$  in  $\Omega_2$  with the following interface condition at  $x = x_0$ :

$$-\frac{\nu}{b} u_2'(x_0) + \frac{\nu}{b} \lambda^- u_2(x_0) = \left( -\frac{\nu}{b} u_1'(x_1) + \frac{\nu}{b} \lambda^- u_1(x_1) - \tilde{u}_1(x_1) \right) e^{-\lambda^+ x_1} + \tilde{u}_1(x_0).$$

- Solve the advection reaction problem  $A_1 u_1 = b u_1' + b_0 u_1 = f$  in  $\Omega_1$  with either  $u_1(x_0) = u_2(x_0)$  if  $b < 0$ , or a suitable boundary condition at  $x = x_1$  if  $b > 0$ .

It is shown in [25] that the  $L^2$ –norm error between the heterogeneous solution and the global elliptic one behaves like  $\nu$  (for  $\nu \rightarrow 0$ ) in the domain  $\Omega_1$ , while in  $\Omega_2$  it exponentially decreases with  $\nu$  when  $b < 0$  and it behaves like  $\nu^m$  ( $m = 1, 2, \dots$ ) when  $b > 0$ . The integer  $m$  depends on the accuracy of the boundary condition imposed at  $x = x_1$ .

### 2.3 Domain Decomposition Algorithms for the Solution of the Reduced Advection–Diffusion Problem

In this Section we will present two iterative domain decomposition methods to solve the coupled problem (40), starting from the interface conditions (40)<sub>3,4</sub>. Moreover we will reformulate the heterogeneous problem in terms of the Steklov–Poincaré equation at the interface.

#### 2.3.1 Dirichlet–Neumann algorithm

The interface conditions (40)<sub>3</sub> and (40)<sub>4</sub> provide, respectively, Dirichlet or Neumann data at the interface  $\Gamma$ . Then we can use the condition (40)<sub>3</sub> as an inflow (Dirichlet) condition for the advection problem in  $\Omega_1$  and the condition (40)<sub>4</sub> as a Neumann condition for the elliptic problem in  $\Omega_2$ . The algorithm, named *Dirichlet–Neumann*



(DN) method, produces two sequences of functions  $\{u_1^{(k)}\}$  and  $\{u_2^{(k)}\}$  converging to the solutions  $u_1$  and  $u_2$ , respectively, of the heterogeneous problem as follows.

Given  $\lambda^{(0)} \in L^2_{\mathbf{b}}(\Gamma^{\text{in}})$ , for  $k \geq 0$  do:

$$\begin{aligned} \text{Solve} \quad & \begin{cases} A_1 u_1^{(k+1)} = f & \text{in } \Omega_1 \\ u_1^{(k+1)} = g & \text{on } (\partial\Omega_1 \setminus \Gamma)^{\text{in}} \\ u_1^{(k+1)} = \lambda^{(k)} & \text{on } \Gamma^{\text{in}}, \end{cases} \\ \text{Solve} \quad & \begin{cases} A_2 u_2^{(k+1)} = f & \text{in } \Omega_2 \\ u_2^{(k+1)} = g & \text{on } \partial\Omega_2 \setminus \Gamma \\ -v \frac{\partial u_2^{(k+1)}}{\partial n_\Gamma} + \mathbf{b} \cdot \mathbf{n}_\Gamma u_2^{(k+1)} = \mathbf{b} \cdot \mathbf{n}_\Gamma u_1^{(k+1)} & \text{on } \Gamma, \end{cases} \quad (47) \\ \text{Compute} \quad & \lambda^{(k+1)} = (1 - \vartheta)\lambda^{(k)} + \vartheta u_2^{(k+1)}|_{\Gamma^{\text{in}}}, \end{aligned}$$

where  $\vartheta > 0$  is a suitable relaxation parameter.

The convergence properties of this method are analysed in [30], while several numerical results can be found in [22]. The convergence of DN method is guaranteed by the following theorem [30].

**Theorem 2.** *Let us consider the assumptions of Theorem 1. There exists  $\delta > 0$  such that, if  $\lambda^{(0)} \in L^2_{\mathbf{b}}(\Gamma^{\text{in}})$  and  $\vartheta \in (0, 1 + \delta)$ , then the sequence  $(u_1^{(k)}, u_2^{(k)})$  converges to a limit pair  $(u_1, u_2)$  in the following sense:*

$$u_1^{(k)} \rightarrow u_1 \text{ in } L^2(\Omega_1), \quad u_2^{(k)} \rightarrow u_2 \text{ in } H^1(\Omega_2).$$

The limit pair provides the unique solution to the coupled problem (40).

Other research papers connected with this approach are [2, 9, 29, 55].

We note that, when  $\Gamma^{\text{out}} = \Gamma$ , the DN algorithm (47) converges in one iteration, since the solution in  $\Omega_1$  is independent of the solution in  $\Omega_2$  and, once  $u_1$  is known, the solution in  $\Omega_2$  is obtained by a single “Neumann step”.

On the contrary, when  $\Gamma^{\text{in}} = \Gamma$ , the coupled problem (40) can be solved without iterations. As a matter of fact, by re-writing the interface condition (47)<sub>6</sub> as in (41), we note that the solution in  $\Omega_2$  is uniquely determined, independently of a trace function  $\lambda$  on  $\Gamma$ . Consequently, the solution in  $\Omega_1$  is uniquely defined by the interface condition (41)<sub>1</sub>.

### 2.3.2 Adaptive Robin Neumann Algorithm

Another iterative algorithm, that can be invoked to solve the reduced advection–diffusion problem (40) reads as follows. Given the functions  $\lambda^{(0)} \in L^2_{\mathbf{b}}(\Gamma^{\text{in}})$ ,  $\mu^{(0)} \in L^2_{\mathbf{b}}(\Gamma^{\text{out}})$  and  $u_2^{(0)} \in H^1(\Omega_2)$ , for  $k \geq 0$  do:

$$\begin{aligned}
& \text{Solve} \quad \begin{cases} \operatorname{div}(\mathbf{b}u_1^{(k+1)}) + b_0u_1^{(k+1)} = f & \text{in } \Omega_1 \\ u_1^{(k+1)} = g & \text{on } (\partial\Omega_1 \setminus \Gamma)^{\text{in}} \\ -\mathbf{b} \cdot \mathbf{n}_\Gamma u_1^{(k+1)} = v \frac{\partial u_2^{(k)}}{\partial n_\Gamma} - \mathbf{b} \cdot \mathbf{n}_\Gamma \lambda^{(k)} & \text{on } \Gamma^{\text{in}}, \end{cases} \\
& \text{Solve} \quad \begin{cases} \operatorname{div}(-v \nabla u_2^{(k+1)} + \mathbf{b}u_2^{(k+1)}) + b_0u_2^{(k+1)} = f & \text{in } \Omega_2 \\ u_2^{(k+1)} = g & \text{on } \partial\Omega_2 \setminus \Gamma \\ v \frac{\partial u_2^{(k+1)}}{\partial n_\Gamma} - \mathbf{b} \cdot \mathbf{n}_\Gamma u_2^{(k+1)} = -\mathbf{b} \cdot \mathbf{n}_\Gamma \mu^{(k)} & \text{on } \Gamma^{\text{out}} \\ v \frac{\partial u_2^{(k+1)}}{\partial n_\Gamma} = 0 & \text{on } \Gamma^{\text{in}}, \end{cases} \quad (48) \\
& \text{Compute} \quad \begin{cases} \lambda^{(k+1)} = (1 - \vartheta)\lambda^{(k)} + \vartheta u_2^{(k+1)} & \text{on } \Gamma^{\text{in}} \\ \mu^{(k+1)} = (1 - \vartheta)\mu^{(k)} + \vartheta u_1^{(k+1)} & \text{on } \Gamma^{\text{out}}. \end{cases}
\end{aligned}$$

The algorithm (48) is obtained as the limit, when  $\varepsilon \rightarrow 0$ , of the Adaptive-Robin-Neumann (ARN) method proposed in [10] for the homogeneous global elliptic problem (37). In its original form, ARN method reads given  $\lambda^{(0)}$ ,  $\mu^{(0)}$  and  $u_2^{(0)}$ , for  $k \geq 0$  do

$$\begin{aligned}
& \text{Solve} \quad \begin{cases} -\varepsilon \Delta u_{1,\varepsilon}^{(k+1)} + \operatorname{div}(\mathbf{b}u_{1,\varepsilon}^{(k+1)}) + b_0u_{1,\varepsilon}^{(k+1)} = f & \text{in } \Omega_1 \\ u_{1,\varepsilon}^{(k+1)} = g & \text{on } (\partial\Omega_1 \setminus \Gamma)^{\text{in}} \\ \varepsilon \frac{\partial u_{1,\varepsilon}^{(k+1)}}{\partial n_\Gamma} - \mathbf{b} \cdot \mathbf{n}_\Gamma u_{1,\varepsilon}^{(k+1)} = v_\varepsilon \frac{\partial u_{2,\varepsilon}^{(k)}}{\partial n_\Gamma} - \mathbf{b} \cdot \mathbf{n}_\Gamma \lambda^{(k)} & \text{on } \Gamma_1^{\text{in}} = \Gamma^{\text{in}} \\ \varepsilon \frac{\partial u_{1,\varepsilon}^{(k+1)}}{\partial n_\Gamma} = v_\varepsilon \frac{\partial u_{2,\varepsilon}^{(k)}}{\partial n_\Gamma} & \text{on } \Gamma_1^{\text{out}} = \Gamma^{\text{out}}, \end{cases} \\
& \text{Solve} \quad \begin{cases} \operatorname{div}(-v_\varepsilon \nabla u_{2,\varepsilon}^{(k+1)} + \mathbf{b}u_{2,\varepsilon}^{(k+1)}) + b_0u_{2,\varepsilon}^{(k+1)} = f & \text{in } \Omega_2 \\ u_{2,\varepsilon}^{(k+1)} = g & \text{on } \partial\Omega_2 \setminus \Gamma \\ v_\varepsilon \frac{\partial u_{2,\varepsilon}^{(k+1)}}{\partial n_\Gamma} - \mathbf{b} \cdot \mathbf{n}_\Gamma u_{2,\varepsilon}^{(k+1)} = \varepsilon \frac{\partial u_{1,\varepsilon}^{(k+1)}}{\partial n_\Gamma} - \mathbf{b} \cdot \mathbf{n}_\Gamma \mu^{(k)} & \text{on } \Gamma_2^{\text{in}} = \Gamma^{\text{out}} \\ v_\varepsilon \frac{\partial u_{2,\varepsilon}^{(k+1)}}{\partial n_\Gamma} = \varepsilon \frac{\partial u_{1,\varepsilon}^{(k+1)}}{\partial n_\Gamma} & \text{on } \Gamma_2^{\text{out}} = \Gamma^{\text{in}}, \end{cases} \quad (49) \\
& \text{Compute} \quad \begin{cases} \lambda^{(k+1)} = (1 - \vartheta)\lambda^{(k)} + \vartheta u_{2,\varepsilon}^{(k+1)} & \text{on } \Gamma^{\text{in}} \\ \mu^{(k+1)} = (1 - \vartheta)\mu^{(k)} + \vartheta u_{1,\varepsilon}^{(k+1)} & \text{on } \Gamma^{\text{out}}. \end{cases}
\end{aligned}$$

The idea of this method is to impose a Robin interface condition on the local (i.e. referred to that subdomain) inflow interface  $\Gamma_i^{\text{in}}$  ( $i = 1, 2$ ) and a Neumann interface condition on the local outflow interface  $\Gamma_i^{\text{out}}$  ( $i = 1, 2$ ).

Coming back to the heterogeneous coupling, it is straightforward to prove that, if the choice of  $\vartheta$  guarantees the convergence of ARN method, then the limit solution of ARN (48) coincides with the solution of the heterogeneous problem (40). Moreover, if  $u_2^{(0)}$  is chosen with null normal derivative on the interface  $\Gamma$  and  $\vartheta = 1$ , then ARN (48) and DN (47) methods coincide.

When either  $\Gamma^{\text{in}} = \Gamma$  or  $\Gamma^{\text{out}} = \Gamma$  we can conclude that no iterations are need for ARN method, as for DN.

*Remark 1.* We want to remark here that in the Dirichlet/Neumann method, the Neumann condition (47)<sub>6</sub> is in fact a conormal derivative associated to the differential operator  $A_2$ . On the contrary, in the ARN method the Neumann condition (as (48)<sub>7</sub>) is a pure normal derivative on the interface, while the conormal derivative (48)<sub>6</sub> is called Robin condition, in agreement with the classical definition of Robin boundary condition. Following the latter notation, actually the Dirichlet/Neumann method should be a Dirichlet/Robin method.

### 2.3.3 Steklov–Poincaré Based Solution Algorithms

Let us consider the heterogeneous problem (40) with homogeneous Dirichlet conditions on  $\partial\Omega$ , i.e.,  $g \equiv 0$ . Let  $\lambda \in H_{00}^{1/2}(\Gamma)$  denote the unknown trace of the solution  $u_2$  on  $\Gamma$ . Thanks to the interface condition (40)<sub>4</sub>, the solution  $(u_1, u_2)$  of (40) can be written as

$$u_1 = u_1^\lambda + w_1, \quad u_2 = u_2^\lambda + w_2,$$

where  $w_1$  and  $w_2$  depend on the assigned function  $f$  and are the solution of

$$\begin{cases} A_1 w_1 = f & \text{in } \Omega_1 \\ w_1 = 0 & \text{on } \partial\Omega_1^{\text{in}}, \end{cases} \quad \begin{cases} A_2 w_2 = f & \text{in } \Omega_2 \\ w_2 = 0 & \text{on } \partial\Omega_2, \end{cases} \quad (50)$$

while  $u_1^\lambda$  and  $u_2^\lambda$  are the solutions of

$$\begin{cases} A_1 u_1^\lambda = 0 & \text{in } \Omega_1 \\ u_1^\lambda = 0 & \text{on } (\partial\Omega_1 \setminus \Gamma)^{\text{in}} \\ u_1^\lambda = \lambda|_{\Gamma^{\text{in}}} & \text{on } \Gamma^{\text{in}}, \end{cases} \quad \begin{cases} A_2 u_2^\lambda = 0 & \text{in } \Omega_2 \\ u_2 = 0 & \text{on } \partial\Omega_2 \setminus \Gamma \\ u_2^\lambda = \lambda & \text{on } \Gamma. \end{cases} \quad (51)$$

Given  $\lambda \in H_{00}^{1/2}(\Gamma)$ , we define the Steklov–Poincaré operators  $S_1$  and  $S_2$  such that

$$S_1 \lambda = \begin{cases} \mathbf{b} \cdot \mathbf{n}_\Gamma u_1^\lambda & \text{on } \Gamma^{\text{out}} \\ 0 & \text{on } \Gamma^{\text{in}} \end{cases} \quad (52)$$

and

$$S_2\lambda = \begin{cases} v \frac{\partial u_2^\lambda}{\partial n_\Gamma} - \mathbf{b} \cdot \mathbf{n}_\Gamma u_2^\lambda & \text{on } \Gamma^{\text{out}} \\ v \frac{\partial u_2^\lambda}{\partial n_\Gamma} & \text{on } \Gamma^{\text{in}}. \end{cases} \quad (53)$$

Actually,  $S_1\lambda$  depends only on the values of  $\lambda$  on  $\Gamma^{\text{in}}$ .

Then the interface conditions (40)<sub>3</sub> can be equivalently expressed in terms of Steklov–Poincaré operators as

$$S\lambda \equiv S_1\lambda + S_2\lambda = \chi, \quad (54)$$

where

$$\chi = \begin{cases} -\mathbf{b} \cdot \mathbf{n}_\Gamma w_1 - v \frac{\partial w_2}{\partial n_\Gamma} + \mathbf{b} \cdot \mathbf{n}_\Gamma w_2 & \text{on } \Gamma^{\text{out}} \\ -v \frac{\partial w_2}{\partial n_\Gamma} & \text{on } \Gamma^{\text{in}}. \end{cases} \quad (55)$$

The operator  $S : H_{00}^{1/2}(\Gamma) \rightarrow (H_{00}^{1/2}(\Gamma))'$  is the so-called Steklov–Poincaré operator and the (54) is the Steklov–Poincaré equation associated to the heterogeneous problem (40). The solution of (40) can be reached by sequentially solving the problems (50), (54) and (51).

Several methods may be invoked to solve the Steklov–Poincaré equation (54). To start, let us consider the preconditioned Richardson method

$$\begin{cases} \lambda^{(0)} \text{ given} \\ P(\lambda^{(k+1)} - \lambda^{(k)}) = \vartheta(\chi - S\lambda^{(k)}), \text{ for } k \geq 0, \end{cases} \quad (56)$$

where  $P$  is the preconditioner and  $\vartheta > 0$  an acceleration parameter.

Thanks to the well-posedness of the elliptic problem in  $\Omega_2$ , the operator  $S_2$  is invertible and we can use it as preconditioner, so that (56) becomes

$$\begin{cases} \lambda^{(0)} \text{ given} \\ \lambda^{(k+1)} = (1 - \vartheta)\lambda^{(k)} + \vartheta S_2^{-1}(\chi - S_1\lambda^{(k)}), \text{ for } k \geq 0. \end{cases} \quad (57)$$

By comparing (57) with (47), we recognize that the Dirichlet–Neumann method is equivalent to the Richardson iterative method applied to the Steklov–Poincaré equation (54) with preconditioner  $S_2$ , since the identity  $u_2^{(k+1)}|_\Gamma = S_2^{-1}(\chi - S_1\lambda^{(k)})$  holds.

After a discretization of the heterogeneous problem (by, e.g., finite elements or spectral methods) it is possible to write the discrete counterpart of both the Steklov–Poincaré equation (54) and the Dirichlet–Neumann algorithm (47).

It can be proven that the Dirichlet–Neumann algorithm converges, for suitable choices of the relaxation parameter  $\vartheta$ , independently of the discretization parameter  $h$  for finite elements or  $N$  for spectral methods (see, e.g., [30] for a proof in the

spectral method context). This because the local Steklov–Poincaré operator  $S_2$  is spectrally equivalent to the global Steklov–Poincaré operator  $S$ .

Krylov methods are valid alternatives to Richardson iterations to solve the preconditioned Steklov–Poincaré equation

$$S_2^{-1} S \lambda = S_2^{-1} \chi. \quad (58)$$

In the next section we will provide numerical results about the numerical solution of the coupled problem (40) by using either Dirichlet–Neumann method (47), Adaptive Robin–Neumann method (48) and the preconditioned Bi-CGStab [57] on (58).

## 2.4 Numerical Results for the Advection–Diffusion Problem

In this Section we will provide the numerical solution of a test case in two-dimensional computational domains. The discretization of the differential equation inside each subdomain is performed by quadrilateral conformal Spectral Element Methods (SEM). We refer to [8] for a detailed description of these methods, while here we recall in brief their basic features.

Let  $\mathcal{T} = \{T_m\}_{m=1}^M$  be a partition of the computational domain  $\Omega \subset \mathbb{R}^d$ , where each element  $T_m$  is obtained by a bijective and differentiable transformation  $F_m$  from the reference (or parent) element  $\hat{\Omega}^d = (-1, 1)^d$ . On the reference element we define the finite dimensional space  $\hat{\mathbb{Q}}_N = \text{span}\{\hat{x}_1^{j_1} \cdots \hat{x}_d^{j_d} : 0 \leq j_1, \dots, j_d \leq N\}$  and, for any  $T_m \in \mathcal{T}$ :  $T_m = \mathbf{F}_m(\hat{\Omega}^d)$ , set  $h_m = \text{diam}(T_m)$  and

$$V_{N_m}(T_m) = \{v : v = \hat{v} \circ \mathbf{F}_m^{-1} \text{ for some } \hat{v} \in \hat{\mathbb{Q}}_{N_m}\}.$$

The SEM multidimensional space is

$$X_\delta = \{v \in C^0(\overline{\Omega}) : v|_{T_m} \in V_{N_m}(T_m), \forall T_m \in \mathcal{T}\},$$

where  $\delta$  is an abridged notation for “discrete”, that accounts for the local geometric sizes  $\{h_m\}$  and the local polynomial degrees  $\{N_m\}$ , for  $m = 1, \dots, M$ .

Let us consider the variational formulation (38) and, for simplicity, impose the homogeneous Dirichlet condition on the boundary (i.e.  $g \equiv 0$ ). The SEM approximation of the solution of (38) is the function  $u_\delta \in V_\delta = X_\delta \cap H_0^1(\Omega)$ , such that

$$\sum_m a_{T_m}(u_\delta, v_\delta) = \sum_m (f, v_\delta)_{T_m} \quad \forall v_\delta \in V_\delta \quad (59)$$

holds, where  $a_{T_m}$  and  $(f, v)_{T_m}$  denote the restrictions to  $T_m$  of the bilinear form and the  $L_2$ -inner product (respectively) defined in (39).

Since the high computational cost in evaluating integrals in (59), the bilinear form  $a_{T_m}$  and the  $L_2$ -inner product  $(f, v)_{T_m}$  are often approximated by a discrete bilinear

form  $a_{N_m, T_m}$  and a discrete inner product  $(f, v)_{N_m, T_m}$ , respectively, in which exact integrals are replaced by Numerical Integration (NI) based on Legendre–Gauss–Lobatto formulas.

The SEM-NI approximation of the solution of (38) will be the function  $u_\delta \in V_\delta$  such that

$$\sum_m a_{N_m, T_m}(u_\delta, v_\delta) = \sum_m (f, v_\delta)_{N_m, T_m} \quad \forall v_\delta \in V_\delta. \quad (60)$$

We consider now a test case and we compare the convergence rate of the iterative methods explained in Sect. 2.3. We will denote by DN the Dirichlet Neumann method (47), by ARN the Adaptive Robin–Neumann method (48) and by BiCGStab-SP the preconditioned BiCGstab method applied to the preconditioned Steklov–Poincaré equation (58). Our aim is twofold. From one hand we will represent the numerical solution of the heterogeneous problem (40), on the other hand we want to investigate and compare the convergence rate of the iterative methods versus the magnitude of the viscosity  $\nu$  and the discretization size (i.e. the local geometric sizes  $h_m$  and the local polynomial degrees  $N_m$ ).

*Test case #1:* Let us consider problem (40). The computational domain  $\Omega = (-1, 1)^2$  is split in  $\Omega_1 = (-1, 0.8) \times (-1, 1)$  and  $\Omega_2 = (0.8, 1) \times (-1, 1)$ . The interface is  $\Gamma = \{0.8\} \times (-1, 1)$ . The data of the problem are:  $\mathbf{b} = [y, 0]^t$ ,  $b_0 = 1$ ,  $f = 1$  and the inflow interface is  $\Gamma^{\text{in}} = \{0.8\} \times (-1, 0)$ . Dirichlet boundary conditions are imposed on the vertical sides of  $\Omega$ , precisely  $g = 1$  on  $\{-1\} \times (0, 1)$ ,  $g = 0$  on  $\{1\} \times (-1, 1)$ , while homogeneous Neumann conditions are imposed on the horizontal sides of  $\Omega_2$ . The viscosity will be specified below.

In Fig. 8 the SEM-NI solutions for  $\nu = 10^{-2}$  and  $\nu = 10^{-3}$  are shown. A non-uniform partition in  $3 \times 6$  ( $4 \times 6$ , resp.) quadrilaterals has been considered in  $\Omega_1$  ( $\Omega_2$ , resp.). The same polynomial degree  $N = 8$  has been fixed inside each spectral element. The jump of the solution across  $\Gamma^{\text{out}}$  is evident for  $\nu = 0.01$ , in particular we have obtained  $\|u_1 - u_2\|_{L^\infty(\Gamma^{\text{out}})} \simeq 0.237$  when  $\nu = 0.01$  and  $\|u_1 - u_2\|_{L^\infty(\Gamma^{\text{out}})} \simeq 0.020$  when  $\nu = 0.001$ .

Now we want to compare DN, ARN and BiCGStab-SP methods for what concerns the convergence rate and the computational efficiency.

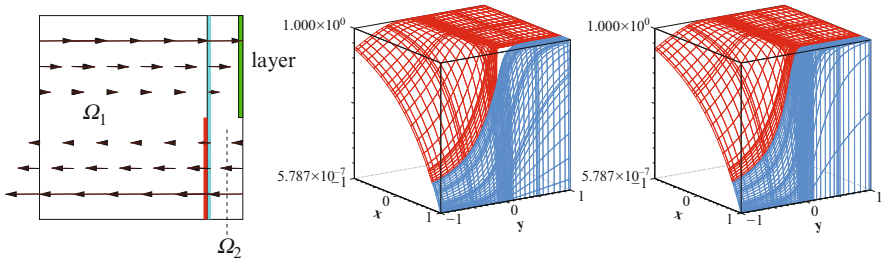


**Fig. 8** Test case #1. The data of the test case (left) and the heterogeneous solution for  $\nu = 0.01$  (center) and  $\nu = 0.001$  (right)

The convergence of both DN and ARN is measured by the stopping test on the difference between two iterates, i.e.

$$\begin{aligned} \|\lambda^{(k+1)} - \lambda^{(k)}\| &\leq \varepsilon && \text{for DN} \\ \max\{\|\lambda^{(k+1)} - \lambda^{(k)}\|, \|\mu^{(k+1)} - \mu^{(k)}\|\} &\leq \varepsilon && \text{for ARN,} \end{aligned} \quad (61)$$

while the convergence of BiCGStab-SP is measured by the stopping test on the residual  $r^{(k+1)} = \chi - S\lambda^{(k+1)}$ , i.e.

$$\frac{\|r^{(k+1)}\|}{\|r^{(0)}\|} \leq \varepsilon. \quad (62)$$

The convergence of both DN and ARN methods depends on the choice of the relaxation parameter  $\vartheta$ , on the contrary, the BiCGStab-SP algorithm does not require to set any acceleration parameter.

In Fig. 9 we report the number of iterations of both DN and ARN methods in order to converge up to a tolerance of  $10^{-6}$  for  $\nu = 0.01$  and we conclude that, for this test case, the optimal value of  $\vartheta$  is  $\vartheta_{opt} = 1$ . Analogous results are obtained for smaller values of the viscosity.

In Table 1 we report the number of iterations needed by every iterative scheme (DN, ARN, BiCGstab-SP) to converge up to a tolerance of  $10^{-6}$ , versus the polynomial degree  $N$ . For both DN and ARN method we set  $\vartheta = 1$ . The partition of  $\Omega$  is not uniform and it coincides with that used to represent the numerical solutions in Fig. 8. The discretization we have used is fine enough to guarantee the absence of spurious oscillations due to large Péclet number.

As we can see, the convergence rate of all methods is independent of both polynomial degree  $N$  and viscosity  $\nu$ .

The BiCGStab-SP method requires the smallest number of iterations, nevertheless each Bi-CGStab iteration costs about two and a half iterations of either DN or ARN. As a matter of fact, each iteration of DN (or equivalently ARN) requires the solution of an advection problem in  $\Omega_1$  plus the solution of an elliptic problem

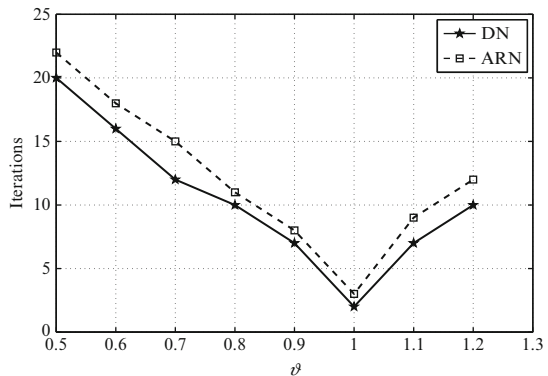


**Fig. 9** Test case #1 with  $\nu = 0.01$ . DN and ARN iterations to satisfy the stopping test (61) versus the relaxation parameter  $\vartheta$

**Table 1** Test case #1. Number of iterations to satisfy stopping test with  $\varepsilon = 10^{-6}$ 

$N$	$\nu = 0.1$			$\nu = 0.01$			$\nu = 0.001$		
	DN	ARN	SP	DN	ARN	SP	DN	ARN	SP
4	2	3	1	2	3	1	2	3	1
6	2	3	1	2	3	1	2	3	1
8	2	3	1	2	3	1	2	3	1
10	2	3	1	2	3	1	2	3	1
12	2	3	1	2	3	1	2	3	1
14	2	3	1	2	3	1	2	3	1
16	2	3	1	2	3	1	2	3	1

The relaxation parameter is  $\vartheta = 1$  in both DN and ARN. SP is an abridged notation for BiCGStab-SP method.

in  $\Omega_2$ . On the contrary, each iteration of BiCGstab-SP requires two matrix vector products to compute the residual  $r^{(k)} = \chi - S\lambda^{(k)}$  plus the solution of two linear systems on the preconditioner  $S_2 z^{(k)} = r^{(k)}$ , meaning that we have to solve two advection problems in  $\Omega_1$  plus three elliptic problems in  $\Omega_2$  at each iteration.

For this test case, we conclude that all three methods are very efficient and their computational costs are comparable. Nevertheless, both DN and ARN methods require a priori knowledge of the optimal relaxation parameter  $\vartheta$ .

## 2.5 Navier–Stokes/Potential Coupled Problem

Models similar to the (Navier–)Stokes/Darcy problem introduced in Sect. 1 can be used in external aerodynamics to describe the motion of an incompressible fluid around a body such as, for example, a ship, a boat or a submerged body in a water basin. In fact, such problems can be studied by decomposing the computational domain into two parts: a region  $\Omega_2$  close to the body where, due to the viscosity effects, all the interesting features of the flow occur, and an outer region  $\Omega_1$  far away from the body where one can neglect the viscosity effects. See, e.g., Fig. 10.

Therefore, suitable heterogeneous differential models comprising Navier–Stokes equations, Euler equations, potential flows and other models from fluid dynamics could be envisaged (see, e.g., [3, 35]).

Here, we present a simple model where in  $\Omega_2$  we consider the full Navier–Stokes equations, while in  $\Omega_1$  we adopt a Laplace equation for the velocity potential.

A coupled heterogeneous model of this kind has been studied in [56] considering a computational domain as in Fig. 11 and the following generalized Stokes problem:

$$\begin{cases} \alpha \mathbf{u}_\varepsilon - \nu_\varepsilon \Delta \mathbf{u}_\varepsilon + \nabla p_\varepsilon = \mathbf{f} & \text{in } \Omega \\ \nabla \cdot \mathbf{u}_\varepsilon = 0 & \text{in } \Omega \\ \mathbf{u}_\varepsilon = \mathbf{0} & \text{on } \Gamma_b, \end{cases} \quad (63)$$



**Fig. 10** Flow around a cylinder computed using a Navier–Stokes/potential coupled problem

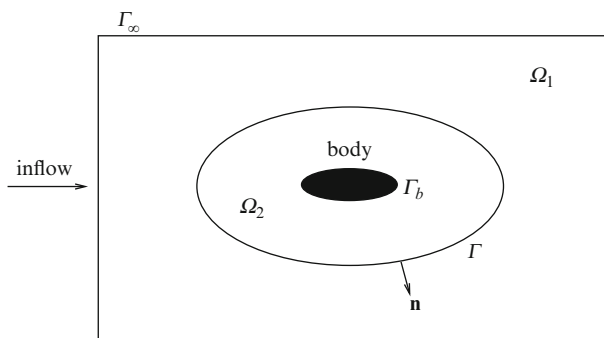
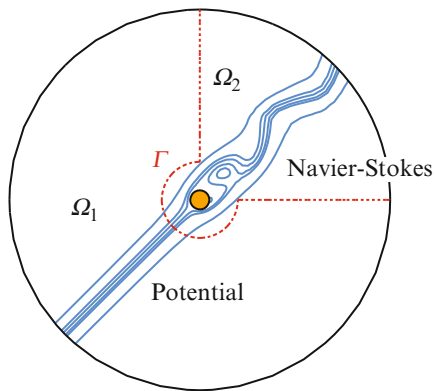


**Fig. 11** Representation of the computational domain for an external aerodynamics problem

with suitable boundary conditions on the outer boundary  $\Gamma_\infty$ . The viscosity is  $\nu_\varepsilon = \nu$  in  $\Omega_2$ , while  $\nu_\varepsilon = \varepsilon$  in  $\Omega_1$ .

In [56] a vanishing viscosity argument is used letting  $\varepsilon \rightarrow 0$  in  $\Omega_1$  in order to set up a suitable global model and to define the correct interface conditions across  $\Gamma$ . Precisely, the following limit coupled problem was characterized:

$$\begin{cases} \alpha \mathbf{u} - \nu \Delta \mathbf{u} + \nabla p = \mathbf{f} & \text{in } \Omega_2 \\ \nabla \cdot \mathbf{u} = 0 & \text{in } \Omega_2 \\ \Delta q = \nabla \cdot \mathbf{f} & \text{in } \Omega_1 \end{cases} \quad (64)$$

with suitable boundary conditions and the coupling conditions across the interface  $\Gamma$

$$\begin{aligned} \frac{\partial q}{\partial \mathbf{n}_\Gamma} &= (\mathbf{f} - \alpha \mathbf{u}) \cdot \mathbf{n}_\Gamma & \text{on } \Gamma \\ -\nu \frac{\partial \mathbf{u}}{\partial \mathbf{n}_\Gamma} + p \mathbf{n}_\Gamma &= q \mathbf{n}_\Gamma & \text{on } \Gamma. \end{aligned} \quad (65)$$

$\mathbf{n}_\Gamma$  denotes the unit normal vector on  $\Gamma$  directed from  $\Omega_2$  to  $\Omega_1$ . We remark that, apart from the physical meaning of the variables, the coupling conditions (65) are similar in their structure to those used for the Navier–Stokes/Darcy coupling (28). In fact, (65)<sub>1</sub> corresponds to (28)<sub>1</sub>, and in (65)<sub>2</sub> the pressure is still discontinuous across the interface, even if there is no distinction between the normal and the tangential components of the stress tensor as in (28)<sub>2</sub> and (28)<sub>3</sub>.

Because of these similarities, the analysis that we shall develop in Sect. 2.6 for the Navier–Stokes/Darcy problem could be accommodated to account also for the heterogenous coupling (64) and (65).

However, one has to keep in mind that the physical meaning of the two coupled problems is very different. In the Navier–Stokes/Darcy case we have two viscous models where Darcy equation and the coupling conditions can be obtained by homogenization in the limit  $\varepsilon \rightarrow 0$  in  $\Omega_p$ , where  $\varepsilon$  represents the size of the pores in the porous medium. On the other hand, the Navier–Stokes/potential model couples viscous and inviscid equations, the latter being obtained in the limit  $\nu \rightarrow 0$  like also the corresponding coupling conditions.

## 2.6 Asymptotic Analysis of the Coupled Navier–Stokes/Darcy Problem

We focus now on the coupled Navier–Stokes/Darcy problem (27) and (28), however we confine ourselves to the steady problem by dropping the time-derivative in the momentum equation (27)<sub>1</sub>:

$$-\operatorname{div} \mathbf{T}(\mathbf{u}_f, p_f) + (\mathbf{u}_f \cdot \nabla) \mathbf{u}_f = \mathbf{f} \quad \text{in } \Omega_f. \quad (66)$$

Even when considering the time-dependent problem, a similar kind of “steady” problem can be found when using an implicit finite difference time-advancing scheme. In that case, however, an extra reaction term  $\alpha \mathbf{u}_f$  would show up on the left-hand side of (66), where the positive coefficient  $\alpha$  plays the role of inverse of the time-step. This reaction term would not affect our forthcoming analysis, though.

To discuss possible boundary conditions on the external boundary of  $\Omega_f$  and  $\Omega_p$ , let us split the boundaries  $\partial\Omega_f$  and  $\partial\Omega_p$  as  $\partial\Omega_f = \Gamma \cup \Gamma_f^{in}$  and  $\partial\Omega_p = \Gamma \cup \Gamma_p \cup \Gamma_p^b$ , as shown in Fig. 6, left.

For the Darcy equation we assign the piezometric head  $\varphi = \varphi_p$  on  $\Gamma_p$ ; moreover, we require that the normal component of the velocity vanishes on the bottom surface, that is,  $\mathbf{u}_p \cdot \mathbf{n}_p = 0$  on  $\Gamma_p^b$ .

For the Navier–Stokes problem, several combinations of boundary conditions are possible, representing different kinds of flow problems. Here, we assign a non-null inflow  $\mathbf{u}_f = \mathbf{u}_{in}$  on  $\Gamma_f^{in}$  and a no-slip condition  $\mathbf{u}_f = \mathbf{0}$  on the remaining boundary  $\Gamma_f$ .

To summarize, the coupled problem (66)–(28) is supplemented with the boundary conditions:

$$\begin{aligned} \mathbf{u}_f &= \mathbf{u}_{in} \text{ on } \Gamma_f^{in}, \quad \mathbf{u}_f = \mathbf{0} \text{ on } \Gamma_f, \\ \varphi &= \varphi_p \text{ on } \Gamma_p, \quad \mathbf{K} \frac{\partial \varphi}{\partial n} = 0 \text{ on } \Gamma_p^b. \end{aligned} \quad (67)$$

We introduce the following functional spaces:

$$\begin{aligned} H_f &= \{\mathbf{v} \in (H^1(\Omega_f))^d : \mathbf{v} = \mathbf{0} \text{ on } \Gamma_f \cup \Gamma_f^{in}\}, \\ \tilde{H}_f &= \{\mathbf{v} \in (H^1(\Omega_f))^d : \mathbf{v} = \mathbf{0} \text{ on } \Gamma_f \cup \Gamma\}, \\ Q &= L^2(\Omega_f), \quad H_p = \{\psi \in H^1(\Omega_p) : \psi = 0 \text{ on } \Gamma_p\}. \end{aligned} \quad (68)$$

We denote by  $|\cdot|_1$  and  $\|\cdot\|_1$  the  $H^1$ -seminorm and norm, respectively, and by  $\|\cdot\|_0$  the  $L^2$ -norm; it will always be clear from the context whether we are referring to spaces on  $\Omega_f$  or  $\Omega_p$ .

The space  $W = H_f \times H_p$  is a Hilbert space with norm

$$\|\underline{w}\|_W = (\|\mathbf{w}\|_1^2 + \|\psi\|_1^2)^{1/2} \quad \forall \underline{w} = (\mathbf{w}, \psi) \in W.$$

Finally, we consider on  $\Gamma$  the trace space  $\Lambda = H_{00}^{1/2}(\Gamma)$  and denote its norm by  $\|\cdot\|_\Lambda$  (see [42]).

We introduce a continuous extension operator

$$E_f: (H^{1/2}(\Gamma_f^{in}))^d \rightarrow \tilde{H}_f. \quad (69)$$

Then  $\forall \mathbf{u}_{in} \in (H_{00}^{1/2}(\Gamma_f^{in}))^d$  we can construct a vector function  $E_f \mathbf{u}_{in} \in \tilde{H}_f$  such that  $E_f \mathbf{u}_{in}|_{\Gamma_f^{in}} = \mathbf{u}_{in}$ .

We introduce another continuous extension operator:

$$E_p: H^{1/2}(\Gamma_p^b) \rightarrow H^1(\Omega_p) \quad \text{such that } E_p \varphi_p = 0 \text{ on } \Gamma. \quad (70)$$

Then, for all  $\varphi \in H^1(\Omega_p)$  we define the function  $\varphi_0 = \varphi - E_p \varphi_p$ .

Finally, we define the following bilinear forms:

$$\begin{aligned} a_f(\mathbf{v}, \mathbf{w}) &= \int_{\Omega_f} \frac{\nu}{2} (\nabla \mathbf{v} + \nabla^T \mathbf{v}) \cdot (\nabla \mathbf{w} + \nabla^T \mathbf{w}) \quad \forall \mathbf{v}, \mathbf{w} \in (H^1(\Omega_f))^d, \\ b_f(\mathbf{v}, q) &= - \int_{\Omega_f} q \operatorname{div} \mathbf{v} \quad \forall \mathbf{v} \in (H^1(\Omega_f))^d, \quad \forall q \in Q, \\ a_p(\varphi, \psi) &= \int_{\Omega_p} \nabla \psi \cdot \mathbf{K} \nabla \varphi \quad \forall \varphi, \psi \in H^1(\Omega_p), \end{aligned} \quad (71)$$

and, for all  $\mathbf{v}, \mathbf{w}, \mathbf{z} \in (H^1(\Omega_f))^d$ , the trilinear form

$$c_f(\mathbf{w}; \mathbf{z}, \mathbf{v}) = \int_{\Omega_f} [(\mathbf{w} \cdot \nabla) \mathbf{z}] \cdot \mathbf{v} = \sum_{i,j=1}^d \int_{\Omega_f} w_j \frac{\partial z_i}{\partial x_j} v_i. \quad (72)$$

Now, if we multiply (66) by  $\mathbf{v} \in H_f$  and integrate by parts we obtain

$$a_f(\mathbf{u}_f, \mathbf{v}) + c_f(\mathbf{u}_f; \mathbf{u}_f, \mathbf{v}) + b_f(\mathbf{v}, p_f) - \int_{\Gamma} \mathbf{n} \cdot \mathbb{T}(\mathbf{u}_f, p_f) \mathbf{v} = \int_{\Omega_f} \mathbf{f} \cdot \mathbf{v}.$$

Notice that we can write

$$- \int_{\Gamma} \mathbf{n} \cdot \mathbb{T}(\mathbf{u}_f, p_f) \mathbf{v} = - \int_{\Gamma} [\mathbf{n} \cdot \mathbb{T}(\mathbf{u}_f, p_f) \cdot \mathbf{n}] \mathbf{v} \cdot \mathbf{n} - \int_{\Gamma} (\mathbb{T}(\mathbf{u}_f, p_f) \cdot \mathbf{n})_{\tau} \cdot (\mathbf{v})_{\tau},$$

so that we can incorporate in weak form the interface conditions (28)<sub>2</sub> and (28)<sub>3</sub> as follows:

$$- \int_{\Gamma} \mathbf{n} \cdot \mathbb{T}(\mathbf{u}_f, p_f) \mathbf{v} = \int_{\Gamma} g \varphi (\mathbf{v} \cdot \mathbf{n}) + \int_{\Gamma} \frac{v \alpha_{BJ}}{\sqrt{K}} (\mathbf{u}_f)_{\tau} \cdot (\mathbf{v})_{\tau}.$$

Finally, we consider the lifting  $E_f \mathbf{u}_{in}$  of the boundary datum and we split  $\mathbf{u}_f = \mathbf{u}_f^0 + E_f \mathbf{u}_{in}$  with  $\mathbf{u}_f^0 \in H_f$ ; we recall that  $E_f \mathbf{u}_{in} = \mathbf{0}$  on  $\Gamma$  and we get

$$\begin{aligned} a_f(\mathbf{u}_f^0, \mathbf{v}) + c_f(\mathbf{u}_f^0 + E_f \mathbf{u}_{in}; \mathbf{u}_f^0 + E_f \mathbf{u}_{in}, \mathbf{v}) + b_f(\mathbf{v}, p_f) \\ + \int_{\Gamma} g \varphi (\mathbf{v} \cdot \mathbf{n}) + \int_{\Gamma} \frac{v \alpha_{BJ}}{\sqrt{K}} (\mathbf{u}_f)_{\tau} \cdot (\mathbf{v})_{\tau} = \int_{\Omega_f} \mathbf{f} \cdot \mathbf{v} - a_f(E_f \mathbf{u}_{in}, \mathbf{v}). \end{aligned} \quad (73)$$

From (27)<sub>2</sub> we find

$$b_f(\mathbf{u}_f^0, q) = -b_f(E_f \mathbf{u}_{in}, q) \quad \forall q \in Q. \quad (74)$$

On the other hand, if we multiply (27)<sub>3</sub> by  $\psi \in H_p$  and integrate by parts we get

$$a_p(\varphi, \psi) + \int_{\Gamma} K \frac{\partial \varphi}{\partial n} \psi = 0.$$

Now we incorporate the interface condition (28)<sub>1</sub> in weak form as

$$a_p(\varphi, \psi) - \int_{\Gamma} (\mathbf{u}_f \cdot \mathbf{n}) \psi = 0,$$

and, considering the splitting  $\varphi = \varphi_0 + E_p \varphi_p$  we obtain

$$a_p(\varphi_0, \psi) - \int_{\Gamma} (\mathbf{u}_f \cdot \mathbf{n}) \psi = -a_p(E_p \varphi_p, \psi). \quad (75)$$

We multiply (75) by  $g$  and sum to (73) and (74); then, we define

$$\begin{aligned} \mathcal{A}(\underline{v}, \underline{w}) = a_f(\mathbf{v}, \mathbf{w}) + g a_p(\varphi, \psi) + \int_{\Gamma} g \varphi (\mathbf{w} \cdot \mathbf{n}) - \int_{\Gamma} g \psi (\mathbf{v} \cdot \mathbf{n}) \\ + \int_{\Gamma} \frac{v \alpha_{BJ}}{\sqrt{K}} (\mathbf{w})_{\tau} \cdot (\mathbf{v})_{\tau}, \end{aligned} \quad (76)$$

$$\mathcal{C}(\underline{v}; \underline{w}, \underline{u}) = c_f(\mathbf{v}; \mathbf{w}, \mathbf{u}),$$

$$\mathcal{B}(\underline{w}, q) = b_f(\mathbf{w}, q),$$

for all  $\underline{v} = (\mathbf{v}, \varphi)$ ,  $\underline{w} = (\mathbf{w}, \psi)$ ,  $\underline{u} = (\mathbf{u}, \xi) \in W$ ,  $q \in Q$ . Finally, we define the following linear functionals:

$$\begin{aligned} \langle \mathcal{F}, \underline{w} \rangle &= \int_{\Omega_f} \mathbf{f} \cdot \mathbf{w} - a_f(E_f \mathbf{u}_{in}, \mathbf{w}) - g a_p(E_p \varphi_p, \psi), \\ \langle \mathcal{G}, q \rangle &= -b_f(E_f \mathbf{u}_{in}, q), \end{aligned} \quad (77)$$

for all  $\underline{w} = (\mathbf{w}, \psi) \in W$ ,  $q \in Q$ .

Adopting these notations, the weak formulation of the coupled Navier–Stokes/Darcy problem reads

find  $\underline{u} = (\mathbf{u}_f^0, \varphi_0) \in W$ ,  $p_f \in Q$  such that

$$\begin{cases} \mathcal{A}(\underline{u}, \underline{v}) + \mathcal{C}(\underline{u} + \underline{u}^*; \underline{u} + \underline{u}^*, \underline{v}) + \mathcal{B}(\underline{v}, p_f) = \langle \mathcal{F}, \underline{v} \rangle & \forall \underline{v} = (\mathbf{v}, \psi) \in W \\ \mathcal{B}(\underline{u}, q) = \langle \mathcal{G}, q \rangle & \forall q \in Q, \end{cases} \quad (78)$$

with  $\underline{u}^* = (E_f \mathbf{u}_{in}, 0) \in \widetilde{H}_f \times H^1(\Omega_p)$ .

Remark that the interface conditions (28) have been incorporated in the weak formulation as natural conditions on  $\Gamma$ : in particular, (28)<sub>2</sub> and (28)<sub>3</sub> are natural conditions for the Navier–Stokes problem, while (28)<sub>1</sub> becomes a natural condition for Darcy’s problem.

The well-posedness of (78) can be proved quite easily in the case of the Stokes/Darcy coupling, i.e. when we neglect the trilinear form  $\mathcal{C}(\cdot; \cdot, \cdot)$ . Indeed, in this case the existence and uniqueness of the solution follows from the classical theory of Brezzi for saddle-point problems after proving the continuity of  $\mathcal{A}(\cdot, \cdot)$ , its coerciveness on the kernel of  $\mathcal{B}(\cdot, \cdot)$  and that an inf-sup condition holds between the spaces  $W$  and  $Q$ . For details of this analysis we refer to [18].

The case of the Navier–Stokes/Darcy problem is more involved. In particular, in this case we could prove the well-posedness only under some hypotheses on the data similar to those required for the sole Navier–Stokes equations. Moreover, uniqueness is guaranteed only in the case of small enough filtration velocities  $\mathbf{u}_f \cdot \mathbf{n}$  across  $\Gamma$ . The analysis that we have carried out is based on classical results for nonlinear saddle-point problems (see, e.g., [31]). We refer the reader to [4, 19]. Similar results have been proved using a different approach in [32].

## 2.7 Solution Techniques for the Navier–Stokes/Darcy Coupling

A possible approach to solve the Navier–Stokes/Darcy problem is to exploit its naturally decoupled structure keeping separated the fluid and the porous media parts and exchanging information between surface and groundwater flows only through

boundary conditions at the interface. From the computational point of view, this strategy is useful at the stage of setting up effective methods to solve the problem numerically.

Therefore, we apply a domain decomposition technique at the differential level to study the Navier–Stokes/Darcy coupled problem. Our aim will be to introduce and analyze a generalized Steklov–Poincaré interface equation (see [51]) associated to our problem, in order to reformulate it solely in terms of interface unknowns. This re-interpretation is crucial to set up iterative procedures between the subdomains  $\Omega_f$  and  $\Omega_p$ , that can be used at the discrete level.

Here we illustrate the main ideas behind this approach, and refer to [19] for a complete analysis.

We choose a suitable governing variable on the interface  $\Gamma$ . Considering the interface conditions (28)<sub>1</sub> and (28)<sub>2</sub>, we can foresee two different strategies to select the interface variable:

1. We can set the interface variable  $\lambda$  as the trace of the normal velocity on the interface:

$$\lambda = \mathbf{u}_f \cdot \mathbf{n} = -\mathbf{K} \frac{\partial \varphi}{\partial n}. \quad (79)$$

2. We can define the interface variable  $\sigma$  as the trace of the piezometric head on  $\Gamma$ :

$$\sigma = \varphi = -\frac{1}{g} \mathbf{n} \cdot \mathbf{T}(\mathbf{u}_f, p_f) \cdot \mathbf{n}. \quad (80)$$

Both choices are suitable from the mathematical viewpoint since they guarantee well-posed subproblems in the fluid and the porous medium part.

We discuss here the approach in the case of the Stokes/Darcy coupling considering the choice of the interface variable  $\lambda$  as in (79). We refer the reader to [15] for the second case (80).

For simplicity, from now on we consider the following condition on the interface:

$$(\mathbf{u}_f)_\tau = 0 \quad \text{on } \Gamma \quad (81)$$

instead of (28)<sub>3</sub>.

Consider the auxiliary problems:

$$\left\{ \begin{array}{ll} -\operatorname{div} \mathbf{T}(\mathbf{u}^*, p^*) = \mathbf{f} & \text{in } \Omega_f \\ \operatorname{div} \mathbf{u}^* = 0 & \text{in } \Omega_f \\ \mathbf{u}^* = \mathbf{u}_{in} & \text{on } \Gamma_f^{in} \\ (\mathbf{u}^*)_\tau = 0 & \text{on } \Gamma \\ \mathbf{u}^* \cdot \mathbf{n} = 0 & \text{on } \Gamma, \end{array} \right. \quad \left\{ \begin{array}{ll} -\operatorname{div} (\mathbf{K} \nabla \varphi^*) = 0 & \text{in } \Omega_p \\ \varphi^* = \varphi_p & \text{on } \Gamma_p \\ \mathbf{K} \frac{\partial \varphi^*}{\partial n} = 0 & \text{on } \Gamma_p^b \\ \mathbf{K} \frac{\partial \varphi^*}{\partial n} = 0 & \text{on } \Gamma. \end{array} \right. \quad (82)$$

Then, assuming to know the value of  $\lambda \in \Lambda_0$ , with

$$\Lambda_0 = \{\mu \in H_{00}^{1/2}(\Gamma) : \int_\Gamma \mu = 0\},$$

we consider the problems:

$$\left\{ \begin{array}{ll} -\operatorname{div} \mathbf{T}(\mathbf{u}^\lambda, p^\lambda) = \mathbf{0} & \text{in } \Omega_f \\ \operatorname{div} \mathbf{u}^\lambda = 0 & \text{in } \Omega_f \\ \mathbf{u}^\lambda = \mathbf{0} & \text{on } \Gamma_f^{in} \\ (\mathbf{u}^\lambda)_\tau = 0 & \text{on } \Gamma \\ \mathbf{u}^\lambda \cdot \mathbf{n} = \lambda & \text{on } \Gamma, \end{array} \right. \quad \left\{ \begin{array}{ll} -\operatorname{div} (\mathbf{K} \nabla \varphi^\lambda) = 0 & \text{in } \Omega_p \\ \varphi^\lambda = 0 & \text{on } \Gamma_p \\ \mathbf{K} \frac{\partial \varphi^\lambda}{\partial n} = 0 & \text{on } \Gamma_p^b \\ \mathbf{K} \frac{\partial \varphi^\lambda}{\partial n} = \lambda & \text{on } \Gamma. \end{array} \right. \quad (83)$$

We can prove that the solution of the Stokes–Darcy problem can be expressed as:  $\mathbf{u}_f = \mathbf{u}^\lambda + \mathbf{u}^*$ ,  $p_f = p^\lambda + p^*$ ,  $\varphi = \varphi^\lambda + \varphi^*$ , where  $\lambda \in \Lambda_0$  is the solution of the Steklov–Poincaré equation

$$(S_f + S_p)\lambda = \chi \quad \text{on } \Gamma. \quad (84)$$

$S_f$  and  $S_p$  are the local Steklov–Poincaré operators formally defined as

$$S_f : \Lambda_0 \rightarrow \Lambda'_0 \text{ such that } S_f \lambda = \mathbf{n} \cdot \mathbf{T}(\mathbf{u}^\lambda, p^\lambda) \cdot \mathbf{n} \text{ on } \Gamma,$$

while

$$S_p : \Lambda_0 \rightarrow \Lambda'_0 \text{ such that } S_p \lambda = g\varphi^\lambda \text{ on } \Gamma.$$

Finally,

$$\chi = -\mathbf{n} \cdot \mathbf{T}(\mathbf{u}^*, p^*) \cdot \mathbf{n} - g\varphi^* \text{ on } \Gamma.$$

The analysis of the operators  $S_f$  and  $S_p$  as well as the study of the well-posedness of the interface equation (84) have been carried out in [18]. In particular, we have proved that the operator  $S_f$  is invertible on the trace space  $\Lambda_0$  and it is spectrally equivalent to  $S_f + S_p$ , i.e., there exist two positive constants  $k_1$  and  $k_2$  (independent of  $\eta$ ) such that

$$k_1 \langle S_f \eta, \eta \rangle \leq \langle S \eta, \eta \rangle \leq k_2 \langle S_f \eta, \eta \rangle \quad \forall \eta \in \Lambda_0.$$

The same property holds at the discrete level considering conforming finite element approximations of  $S_f$  and  $S_p$  with constants  $k_1$  and  $k_2$  that do not depend on the grid size  $h$ . This property makes the operator  $S_f$  an attractive preconditioner to solve the interface problem (84) via an iterative method like, e.g., Richardson or the Conjugate Gradient, yielding a convergence rate independent of  $h$ .

For example, we can consider the following Richardson iterations: given  $\lambda^{(0)} \in \Lambda_0$ , for  $k \geq 0$ ,

$$\lambda^{(k+1)} = \lambda^{(k)} + \vartheta S_f^{-1}(\chi - (S_f + S_p)\lambda^{(k)}) \quad \text{on } \Gamma, \quad (85)$$

where  $0 < \vartheta < 1$  is a suitable relaxation parameter.

This method requires at each step to apply  $S_p$  and  $S_f^{-1}$ , i.e., recalling the definitions of these operators, to solve a Darcy problem in  $\Omega_p$  with given flux across  $\Gamma$  and a Stokes problem in  $\Omega_f$  with assigned normal stress on  $\Gamma$ . More precisely, we can rewrite (85) as: let  $\lambda^{(0)} \in \Lambda$  be an initial guess; for  $k \geq 0$ ,

$$\begin{aligned}
& \text{Solve} \quad \begin{cases} -\operatorname{div}(\mathbf{K}\nabla\varphi^{(k+1)}) = 0 & \text{in } \Omega_p \\ \varphi^{(k+1)} = \varphi_p & \text{on } \Gamma_p \\ \mathbf{K}\frac{\partial\varphi^{(k+1)}}{\partial n} = 0 & \text{on } \Gamma_p^b \\ \mathbf{K}\frac{\partial\varphi^{(k+1)}}{\partial n} = \lambda^{(k)} & \text{on } \Gamma, \end{cases} \\
& \text{Solve} \quad \begin{cases} -\operatorname{div} \mathbf{T}(\mathbf{u}^{(k+1)}, p^{(k+1)}) = \mathbf{f} & \text{in } \Omega_f \\ \operatorname{div} \mathbf{u}^{(k+1)} = 0 & \text{in } \Omega_f \\ \mathbf{u}^{(k+1)} = \mathbf{u}_{in} & \text{on } \Gamma_f^{in} \\ (\mathbf{u}^{(k+1)})_\tau = 0 & \text{on } \Gamma \\ -\mathbf{n} \cdot \mathbf{T}(\mathbf{u}^{(k+1)}, p^{(k+1)}) \cdot \mathbf{n} = g\varphi^{(k+1)} & \text{on } \Gamma, \end{cases} \quad (86) \\
& \text{Compute} \quad \lambda^{(k+1)} = (1 - \vartheta)\lambda^{(k)} + \vartheta \mathbf{u}^{(k+1)} \cdot \mathbf{n} \quad \text{on } \Gamma.
\end{aligned}$$

Remark that this algorithm has the same structure as the Dirichlet–Neumann method in the domain decomposition framework.

Another possible algorithm that we have studied in [20] is a sequential Robin–Robin method which at each iteration requires to solve a Darcy problem in  $\Omega_p$  followed by a Stokes problem in  $\Omega_f$ , both with Robin conditions on  $\Gamma$ . Precisely, the algorithm reads as follows.

Having assigned a trace function  $\eta^0 \in L^2(\Gamma)$ , and two acceleration parameters  $\gamma_f \geq 0$  and  $\gamma_p > 0$ , for each  $k \geq 0$ :

$$\begin{aligned}
& \text{Solve} \quad \begin{cases} -\operatorname{div}(\mathbf{K}\nabla\varphi^{(k+1)}) = 0 & \text{in } \Omega_p \\ \varphi^{(k+1)} = \varphi_p & \text{on } \Gamma_p \\ \mathbf{K}\frac{\partial\varphi^{(k+1)}}{\partial n} = 0 & \text{on } \Gamma_p^b \\ -\gamma_p \mathbf{K}\frac{\partial\varphi^{(k+1)}}{\partial n} + g\varphi|_\Gamma = \eta^{(k)} & \text{on } \Gamma, \end{cases} \\
& \text{Solve} \quad \begin{cases} -\operatorname{div} \mathbf{T}(\mathbf{u}^{(k+1)}, p^{(k+1)}) = \mathbf{f} & \text{in } \Omega_f \\ \operatorname{div} \mathbf{u}^{(k+1)} = 0 & \text{in } \Omega_f \\ \mathbf{u}^{(k+1)} = \mathbf{u}_{in} & \text{on } \Gamma_f^{in} \\ (\mathbf{u}^{(k+1)})_\tau = 0 & \text{on } \Gamma \\ \mathbf{n} \cdot \mathbf{T}(\mathbf{u}_f^{(k+1)}, p_f^{(k+1)}) \cdot \mathbf{n} + \gamma_f \mathbf{u}_f^{(k+1)} \cdot \mathbf{n} \\ \quad = -g\varphi|_\Gamma - \gamma_f \mathbf{K}\frac{\partial\varphi^{(k+1)}}{\partial n} & \text{on } \Gamma, \end{cases} \quad (87)
\end{aligned}$$

$$\text{Compute} \quad \eta^{(k+1)} = -\mathbf{n} \cdot \mathbf{T}(\mathbf{u}_f^{(k+1)}, p_f^{(k+1)}) \cdot \mathbf{n} + \gamma_p \mathbf{u}_f^{(k+1)} \cdot \mathbf{n} \quad \text{on } \Gamma.$$



Both the Stokes problem in  $\Omega_f$  and the Darcy problem in  $\Omega_p$  are well-posed and, at convergence, we recover the solution  $(\mathbf{u}_f, p_f) \in H_f \times Q$  and  $\varphi \in H_p$  of the coupled Stokes/Darcy problem. Indeed, denoting by  $\varphi^*$  the limit of the sequence  $\varphi^k$  in  $H^1(\Omega_p)$  and by  $(\mathbf{u}_f^*, p_f^*)$  that of  $(\mathbf{u}_f^k, p_f^k)$  in  $(H^1(\Omega_f))^d \times Q$ , we obtain

$$-\gamma_p \mathbf{K} \frac{\partial \varphi^*}{\partial n} + g \varphi|_{\Gamma} = -\mathbf{n} \cdot \mathbf{T}(\mathbf{u}_f^*, p_f^*) \cdot \mathbf{n} + \gamma_p \mathbf{u}_f^* \cdot \mathbf{n} \quad \text{on } \Gamma, \quad (88)$$

so that we have

$$(\gamma_f + \gamma_p) \mathbf{u}_f^* \cdot \mathbf{n} = -(\gamma_f + \gamma_p) \mathbf{K} \frac{\partial \varphi^*}{\partial n} \quad \text{on } \Gamma,$$

yielding, since  $\gamma_f + \gamma_p \neq 0$ ,  $\mathbf{u}_f^* \cdot \mathbf{n} = -\mathbf{K} \frac{\partial \varphi^*}{\partial n}$  on  $\Gamma$ , and also, from (88), that  $\mathbf{n} \cdot \mathbf{T}(\mathbf{u}_f^*, p_f^*) \cdot \mathbf{n} = -g \varphi|_{\Gamma}$  on  $\Gamma$ . Thus, the two interface conditions (28)<sub>1</sub> and (28)<sub>2</sub> are satisfied, and we can conclude that the limit functions  $\varphi^* \in H_p$  and  $(\mathbf{u}_f^*, p_f^*) \in H_f \times Q$  are the solutions of the coupled Stokes/Darcy problem.

A proof of convergence is presented in [20] and it follows the guidelines of the theory by Lions [41] for the Robin–Robin method (see also [51, Sect. 4.5]).

A crucial point in the algorithm is the choice of the acceleration parameters  $\gamma_f$  and  $\gamma_p$ . A general strategy is not available, but thanks to a reinterpretation of the Robin–Robin method as an alternating direction scheme à la Peaceman–Rachford (see [48]), we were able to give some hints on how to choose them. We refer to [20].

We will illustrate the numerical behavior of the Dirichlet–Neumann and of the Robin–Robin algorithms in Sect. 2.8.

Finally, we address the case of the Navier–Stokes/Darcy coupling. Also to this nonlinear problem we can associate an interface equation similar to (84) still involving the operator  $S_p$  but a nonlinear operator  $\tilde{S}_f$  analogous to  $S_f$ . Formally, we can represent  $\tilde{S}_f : \Lambda_0 \rightarrow \Lambda'_0$  as the operator associated to the Navier–Stokes problem:

$$\begin{cases} -\operatorname{div} \mathbf{T}(\mathbf{u}^\lambda, p^\lambda) + (\mathbf{u}^\lambda \cdot \nabla) \mathbf{u}^\lambda = \mathbf{0} & \text{in } \Omega_f \\ \operatorname{div} \mathbf{u}^\lambda = 0 & \text{in } \Omega_f \\ \mathbf{u}^\lambda = \mathbf{0} & \text{on } \Gamma_f^{in} \\ (\mathbf{u}^\lambda)_\tau = 0 & \text{on } \Gamma \\ \mathbf{u}^\lambda \cdot \mathbf{n} = \lambda & \text{on } \Gamma, \end{cases} \quad (89)$$

such that  $\tilde{S}_f \lambda = \mathbf{n} \cdot \mathbf{T}(\mathbf{u}^\lambda, p^\lambda) \cdot \mathbf{n}$  on  $\Gamma$ .

Then, we can write the interface problem:

$$\text{find } \lambda \in \Lambda_0 : \quad \tilde{S}_f(\lambda) + S_p \lambda = \chi_p \quad \text{on } \Gamma, \quad (90)$$

with  $\chi_p =$ , and prove its equivalence to the global coupled problem.

A rigorous presentation of this approach can be found in [4].

The set-up of effective iterative methods for the interface problem (90) is not straightforward. In particular, no results are available yet on the characterization of suitable operators spectrally equivalent to  $\tilde{S}_f + S_p$ . In [4, 19] we have proposed and analyzed two classical schemes, fixed-point or Newton, for (90) showing their equivalence to the following algorithms, respectively.

*Fixed-point iterations:* Given  $\mathbf{u}_f^0 \in H_f$ , for  $k \geq 1$ , find  $\mathbf{u}_f^{(k)} \in H_f$ ,  $p_f^{(k)} \in Q$ ,  $\varphi^{(k)} \in H_p$  such that, for all  $\mathbf{v} \in H_f$ ,  $q \in Q$ ,  $\psi \in H_p$ ,

$$\begin{cases} a_f(\mathbf{u}_f^{(k)}, \mathbf{v}) + c_f(\mathbf{u}_f^{(k-1)}; \mathbf{u}_f^{(k)}, \mathbf{v}) + b_f(\mathbf{v}, p_f^{(k)}) \\ \quad + \int_{\Gamma} g \varphi^{(k)}(\mathbf{v} \cdot \mathbf{n}) + \int_{\Gamma} \frac{\nu \alpha_{BJ}}{\sqrt{K}} (\mathbf{u}_f^{(k)})_{\tau} \cdot (\mathbf{v})_{\tau} = \int_{\Omega_f} \mathbf{f} \cdot \mathbf{v} \\ b_f(\mathbf{u}_f^{(k)}, q) = 0 \\ a_p(\varphi^{(k)}, \psi) = \int_{\Gamma} \psi (\mathbf{u}_f^{(k)} \cdot \mathbf{n}). \end{cases} \quad (91)$$

*Newton-like methods:* Let  $\mathbf{u}_f^0 \in H_f$  be given; then, for  $k \geq 1$ , find  $\mathbf{u}_f^{(k)} \in H_f$ ,  $p_f^{(k)} \in Q$ ,  $\varphi^{(k)} \in H_p$  such that, for all  $\mathbf{v} \in H_f$ ,  $q \in Q$ ,  $\psi \in H_p$ ,

$$\begin{cases} a_f(\mathbf{u}_f^{(k)}, \mathbf{v}) + c_f(\mathbf{u}_f^{(k)}; \mathbf{u}_f^{(k-1)}, \mathbf{v}) + c_f(\mathbf{u}_f^{(k-1)}; \mathbf{u}_f^{(k)}, \mathbf{v}) + b_f(\mathbf{v}, p_f^{(k)}) \\ \quad + \int_{\Gamma} g \varphi^{(k)}(\mathbf{v} \cdot \mathbf{n}) + \int_{\Gamma} \frac{\nu \alpha_{BJ}}{\sqrt{K}} (\mathbf{u}_f^{(k)})_{\tau} \cdot (\mathbf{v})_{\tau} \\ \quad = c_f(\mathbf{u}_f^{(k-1)}; \mathbf{u}_f^{(k-1)}, \mathbf{v}) + \int_{\Omega_f} \mathbf{f} \cdot \mathbf{v} \\ b_f(\mathbf{u}_f^{(k)}, q) = 0 \\ a_p(\varphi^{(k)}, \psi) = \int_{\Gamma} \psi (\mathbf{u}_f^{(k)} \cdot \mathbf{n}). \end{cases} \quad (92)$$

Some numerical results will be presented in Sect. 2.8.

## 2.8 Numerical Results for the Navier–Stokes/Darcy Problem

We consider a regular triangulation  $\mathcal{T}_h$  of the domain  $\overline{\Omega}_f \cup \overline{\Omega}_p$ , depending on a positive parameter  $h > 0$ , made up of triangles  $T$ . We assume that the triangulations  $\mathcal{T}_{fh}$  and  $\mathcal{T}_{ph}$  induced on the subdomains  $\Omega_f$  and  $\Omega_p$  are compatible on  $\Gamma$ , that is they share the same edges therein. Finally, we suppose the triangulation induced on  $\Gamma$  to be quasi-uniform (see, e.g., [50]).

Several choices of finite element spaces can be made. If we indicate by  $\mathbf{W}_h$  and  $Q_h$  the finite element spaces which approximate the velocity and pressure fields,

respectively, for the Navier–Stokes problem, there must exist a positive constant  $\beta^* > 0$ , independent of  $h$ , such that the classical inf-sup condition is satisfied, i.e.,  $\forall q_h \in Q_h, \exists \mathbf{v}_h \in \mathbf{W}_h, \mathbf{v}_h \neq \mathbf{0}$ , such that

$$\int_{\Omega_f} q_h \operatorname{div} \mathbf{v}_h \geq \beta^* \|\mathbf{v}_h\|_{H^1(\Omega_f)} \|q_h\|_{L^2(\Omega_f)}.$$

No additional compatibility condition is required when coupling with the Darcy equations. Thus, for our tests we use the  $\mathbb{P}_2 - \mathbb{P}_1$  Taylor–Hood finite elements for Stokes or Navier–Stokes and  $\mathbb{P}_2$  elements for Darcy equation.

We investigate the convergence properties of algorithm (86) (or, equivalently, (85)) and the PCG algorithm for (84) with preconditioner  $S_f^{-1}$ . For the moment we set the physical parameters  $\nu, K, g$  to 1. We consider the computational domain  $\Omega \subset \mathbb{R}^2$  with  $\Omega_f = (0, 1) \times (1, 2)$ ,  $\Omega_p = (0, 1) \times (0, 1)$  and the interface  $\Gamma = (0, 1) \times \{1\}$ . The boundary conditions and the forcing terms are chosen in such a way that the exact solution of the coupled Stokes/Darcy problem is

$$\begin{aligned} (\mathbf{u}_f)_1 &= -\cos\left(\frac{\pi}{2}y\right) \sin\left(\frac{\pi}{2}x\right), & (\mathbf{u}_f)_2 &= \sin\left(\frac{\pi}{2}y\right) \cos\left(\frac{\pi}{2}x\right) - 1 + x, \\ p_f &= 1 - x, & \varphi &= \frac{2}{\pi} \cos\left(\frac{\pi}{2}x\right) \cos\left(\frac{\pi}{2}y\right) - y(x - 1), \end{aligned}$$

where  $(\mathbf{u}_f)_1$  and  $(\mathbf{u}_f)_2$  are the components of the velocity field  $\mathbf{u}_f$  (see [19]).

Four different regular conforming meshes have been considered whose number of elements in  $\Omega$  and of nodes on  $\Gamma$  are reported in Table 2, together with the number of iterations to convergence. A tolerance  $10^{-10}$  has been prescribed for the convergence tests based on the relative residues. In the Dirichlet–Neumann-like algorithm (86) we set the relaxation parameter  $\vartheta = 0.7$ .

Figure 12 shows the computed residues for the adopted iterative methods when using the finest mesh (logarithmic scale on the  $y$ -axis).

These numerical tests show that the discrete preconditioner  $S_f$  is optimal with respect to the grid parameter  $h$  since the corresponding preconditioned methods yield convergence in a number of iterations independent of  $h$ .

We consider now the influence of the physical parameters, which govern the coupled problem, on the convergence rate. We use the PCG method as it embeds the choice of dynamic optimal acceleration parameters. We take the same computational

**Table 2** Number of iterations obtained on different grids

Number of mesh elements	Number of nodes on $\Gamma$	Algorithm (86) ( $\vartheta = 0.7$ )	PCG for (84) (preconditioner $S_f^{-1}$ )
172	13	18	5
688	27	18	5
2,752	55	18	5
11,008	111	18	5

**Fig. 12** Computed relative residues for the interface variable  $\lambda$

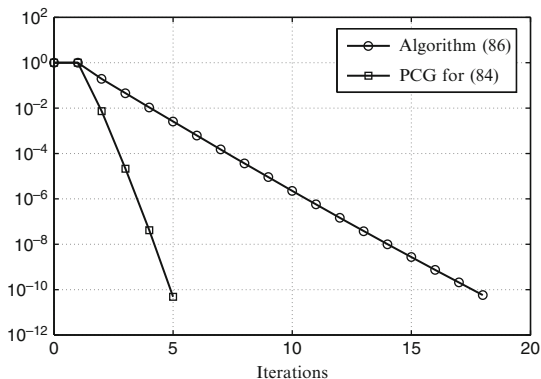


**Table 3** Iterations using the PCG method (preconditioner  $S_f^{-1}$ ) with respect to several values of  $\nu$  and  $K$

$\nu$	$K$	$h = 1/7$	$h = 1/14$	$h = 1/28$	$h = 1/56$
1	1	5	5	5	5
$10^{-1}$	$10^{-1}$	11	11	10	10
$10^{-2}$	$10^{-1}$	15	19	18	17
$10^{-3}$	$10^{-2}$	20	54	73	56
$10^{-4}$	$10^{-3}$	20	59	#	#
$10^{-6}$	$10^{-4}$	20	59	148	#

domain, but here the boundary data and the forcing terms are chosen in such a way that the exact solution of the coupled problem is (see [19]):

$$(\mathbf{u}_f)_1 = y^2 - 2y + 1, \quad (\mathbf{u}_f)_2 = x^2 - x, \quad p_f = 2\nu(x + y - 1) + \frac{g}{3K},$$

$$\varphi = \frac{1}{K} \left( x(1-x)(y-1) + \frac{y^3}{3} - y^2 + y \right) + \frac{2\nu}{g}x.$$

The most relevant physical quantities for the coupling are the fluid viscosity  $\nu$  and the hydraulic conductivity  $K$ . Therefore, we test our algorithms with respect to different values of  $\nu$  and  $K$ , and set the other physical parameters to 1. We consider a convergence test based on the relative residue with tolerance  $10^{-10}$ .

In Table 3 we report the number of iterations necessary for several choices of  $\nu$  and  $K$ . The symbol # indicates that the method did not converge within 150 iterations.

We can see that the convergence of the algorithm is troublesome when the values of  $\nu$  and  $K$  decrease. In fact, in that case the method converges in a large number of iterations which increases when  $h$  decreases, losing its optimality properties. The subdomain iterative method that we have proposed is then effective only when the product  $\nu K$  is sufficiently large, while dealing with small values causes severe difficulties.

**Table 4** Number of iterations to solve problem the modified Stokes/Darcy problem using (93) for different values of  $\nu$ ,  $K$  and  $\gamma$ 

$\nu$	$K$	$\gamma$	Iterations on the mesh with grid size			
			$h = 1/7$	$h = 1/14$	$h = 1/28$	$h = 1/56$
$10^{-3}$	$10^{-2}$	$10$	15	24	28	28
		$10^2$	12	14	16	14
		$10^3$	8	9	9	8
$10^{-6}$	$10^{-4}$	$10^3$	15	23	28	33
		$10^4$	13	14	17	18
		$10^5$	8	9	9	9

**Table 5** Number of iterations using the Robin–Robin method with respect to  $\nu$ ,  $K$  and four different grid sizes  $h$ ; the acceleration parameters are  $\gamma_f = 0.3$  and  $\gamma_p = 0.1$ 

$\nu$	$K$	$h = 1/7$	$h = 1/14$	$h = 1/28$	$h = 1/56$
$10^{-4}$	$10^{-3}$	19	19	19	19
$10^{-6}$	$10^{-4}$	20	20	20	20
$10^{-6}$	$10^{-7}$	20	20	20	20

However, the algorithm still performs well if, instead of the steady Stokes problem, one considers the generalized Stokes momentum equation:

$$\gamma \mathbf{u}_f - \operatorname{div} \mathbf{T}(\mathbf{u}_f, p_f) = \tilde{\mathbf{f}} \quad \text{in } \Omega_f, \quad (93)$$

where  $\gamma$  can represent the inverse of a time step within a time discretization using, e.g., the implicit Euler method. Some numerical results are reported in Table 4 (see also [16]).

On the other hand, the Robin–Robin method (87) performs quite well in presence of small values of  $\nu$  and  $K$ . We present hereafter a test considering the same setting as for Table 3. The analogy with the Peaceman–Rachford method has suggested us to set  $\gamma_f = 0.3$  and  $\gamma_p = 0.1$  (see [15] for more details). In Table 5 we report the number of iterations obtained using the Robin–Robin method for some small values of  $\nu$  and  $K$  and for four different computational grids. A convergence test based on the relative increment of the trace of the discrete normal velocity on the interface  $\mathbf{u}_{fh}^k \cdot \mathbf{n}|_\Gamma$  has been considered with tolerance  $10^{-9}$ . (See [20].)

Finally, we present some numerical tests for the Navier–Stokes/Darcy coupling using the fixed-point and Newton algorithms of Sect. 2.7. The computational domain and the finite element discretization are the same as in the previous tests. (See also [4].)

In a first test, we set the boundary conditions in such a way that the analytical solution for the coupled problem is  $\mathbf{u}_f = (e^{x+y} + y, -e^{x+y} - x)$ ,  $p_f = \cos(\pi x) \cos(\pi y) + x$ ,  $\varphi = e^{x+y} - \cos(\pi x) + xy$ . In order to check the behavior of the iterative methods with respect to the grid parameter  $h$ , we set the physical parameters ( $\nu$ ,  $K$ ,  $g$ ) all equal to 1.

**Table 6** Number of iterations for the iterative methods with respect to  $h$ 

$h$	Fixed-point	Newton
$h = 1/7$	9	5
$h = 1/14$	9	5
$h = 1/28$	9	5

**Table 7** Number of iterations of the fixed-point (FP) and Newton (N) methods with respect to the parameters  $\nu$  and  $K$ 

$\nu$	$K$	$h = 1/7$		$h = 1/14$		$h = 1/28$	
		FP	N	FP	N	FP	N
1	1	7	5	7	5	7	5
1	$10^{-4}$	5	4	5	4	5	4
$10^{-1}$	$10^{-1}$	10	5	10	5	10	5
$10^{-2}$	$10^{-1}$	17	6	17	6	17	6
$10^{-2}$	$10^{-3}$	14	5	14	5	14	5

The algorithms are stopped as soon as  $\|\mathbf{x}^n - \mathbf{x}^{n-1}\|_2 / \|\mathbf{x}^n\|_2 \leq 10^{-10}$ , where  $\|\cdot\|_2$  is the Euclidean norm and  $\mathbf{x}^n$  is the vector of the nodal values of  $(\mathbf{u}_f^n, p_f^n, \varphi^n)$ . Our initial guess is  $\mathbf{u}_f^0 = \mathbf{0}$ .

The number of iterations obtained using the fixed-point algorithm (91), and the Newton method (92) are displayed in Table 6. Both methods converge in a number of iterations which does not depend on  $h$ .

A second test is carried out in order to assess the influence of the physical parameters on the convergence rate of the algorithms. In this case, the analytical solution is  $\mathbf{u}_f = ((y-1)^2 + (y-1) + \sqrt{K}/\alpha_{BJ}, x(x-1))$ ,  $p_f = 2\nu(x+y-1)$ , and  $\varphi = K^{-1}(x(1-x)(y-1) + (y-1)^3/3) + 2\nu x$ . We choose several values for the physical parameters  $\nu$  and  $K$  as indicated in Table 7.

### 3 Virtual Control Approach

The *virtual control* approach represents an alternative approach to the variational asymptotic one, to solve heterogeneous problems.

It is based on the optimal control theory that has been introduced in domain decomposition method with overlapping subdomains to treat both heterogeneous couplings, involving Navier–Stokes and full potential operators [13, 28], and homogeneous problems, either elliptic and parabolic (see [12, 27, 43–45]). In the pioneering papers of Glowinski et al. [12, 27], this method was referred to as a *Least Square* formulation of the multi domain problem.

The basic idea of this approach consists in introducing two “virtual” controls which play the role of unknown Dirichlet data on the interfaces of the decomposition and in minimizing the  $L^2$ -norm of the difference between the hyperbolic and the elliptic solutions (defined inside the two subdomains) on the overlap.

The virtual control approach for heterogeneous advection–diffusion operators was introduced and analysed in [26] and there it has been extended to non-overlapping subdomain decompositions (with sharp interfaces). In the latter situation, the virtual controls are defined on the unique interface and the cost functional to be minimized has to be chosen accurately in order to guarantee the well posedness of the optimal control problem.

Finally, in [1] two different formulations of the heterogeneous advection–diffusion problem with either two and three virtual controls have been analysed for overlapping decompositions.

In the following subsection we will give a detailed description of virtual control approach with either overlapping and non-overlapping decompositions for the heterogeneous problems introduced in Sect. 1.

Here we only note that the virtual control approach without overlap is more efficient than the overlapping version, however the former requires a more definite a priori knowledge on structure of interface conditions. On the contrary, the virtual control approach with overlap is more general and it can be regarded as a rigorous translation of a common practice in engineering community based on solving both problems in a common region and using simple “Dirichlet” type conditions at subdomain boundaries.

### 3.1 Virtual Control Approach Without Overlap for AD Problems

The idea of this approach consists in formulating an optimal control problem [39] featuring both control and observation on the interface  $\Gamma$ . We introduce two functions  $\lambda_1$  and  $\lambda_2$  defined on the interface  $\Gamma$  and called *virtual controls* (Fig. 13), such that they represent the unknown Dirichlet data on  $\Gamma$  for  $u_1$  and  $u_2$ , respectively, i.e.

$$u_1 = \lambda_1 \quad \text{on } \Gamma^{\text{in}}, \quad u_2 = \lambda_2 \quad \text{on } \Gamma. \quad (94)$$

By collecting differential equations (32) and (33), the external boundary conditions (36) and the interface condition (94), we consider the following problem: given  $\lambda_1$ ,  $\lambda_2$ , find  $u_1 = u_1(\lambda_1)$  and  $u_2 = u_2(\lambda_2)$  such that

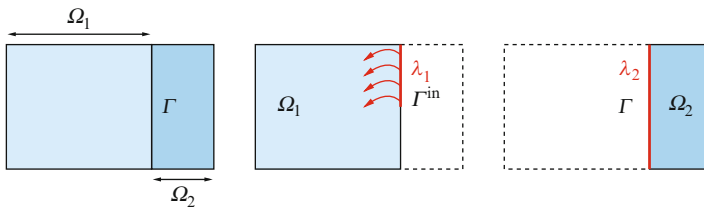


**Fig. 13** Virtual control without overlap

$$\begin{cases} A_1 u_1 = \operatorname{div}(\mathbf{b}u_1) + b_0 u_1 = f & \text{in } \Omega_1 \\ u_1 = g_1 & \text{on } (\partial\Omega_1 \setminus \Gamma)^{\text{in}} \\ u_1 = \lambda_1 & \text{on } \Gamma^{\text{in}} \end{cases} \quad (95)$$

and

$$\begin{cases} A_2 u_2 = -\operatorname{div}(v \nabla u_2) + \operatorname{div}(\mathbf{b}u_2) + b_0 u_2 = f & \text{in } \Omega_2 \\ u_2 = g_2 & \text{on } \partial\Omega_2 \setminus \Gamma \\ u_2 = \lambda_2 & \text{on } \Gamma. \end{cases} \quad (96)$$

In the case where  $\Gamma^{\text{in}} = \emptyset$ , no  $\lambda_1$  is needed since there is no need to prescribe any boundary data on  $\Gamma^{\text{in}}$  for problem (95).

The virtual controls  $\lambda_1$  and  $\lambda_2$  are determined in such a way that the solutions  $u_1$  and  $u_2$  of (95) and (96) adjust in the best possible way on  $\Gamma$ . More precisely, we look for the solution of the minimization problem

$$\inf_{\lambda_1, \lambda_2} J(\lambda_1, \lambda_2), \quad (97)$$

where  $J(\lambda_1, \lambda_2)$  is a suitably chosen cost functional.

Various instances have been proposed and analyzed in [26]. Consider, for example,

$$J(\lambda_1, \lambda_2) = \frac{1}{2} \|u_1(\lambda_1) - u_2(\lambda_2)\|_{L^2_b(\Gamma^{\text{in}})}^2 + \frac{1}{2} \|\varphi_1(\lambda_1) + \varphi_2(\lambda_2)\|_{H^{-1/2}(\Gamma)}^2, \quad (98)$$

where

$$\varphi_1(\lambda_1) = -\mathbf{b} \cdot \mathbf{n}_\Gamma u_1(\lambda_1), \quad \varphi_2(\lambda_2) = -v \frac{\partial u_2(\lambda_2)}{\partial \mathbf{n}_\Gamma} + \mathbf{b} \cdot \mathbf{n}_\Gamma u_2(\lambda_2) \quad (99)$$

are the fluxes on  $\Gamma$  associated to the differential operators  $A_1$  and  $A_2$  (respectively) and  $H^{-1/2}(\Gamma)$  is the dual space of  $H^{1/2}_{00}(\Gamma)$ . Denoting by  $-\Delta_\Gamma$  the Laplace Beltrami operator on  $\Gamma$ , for any  $\psi, \varphi \in H^{-1/2}(\Gamma)$  we define the following inner product (see, e.g., [39]):

$$(\psi, \varphi)_{H^{-1/2}(\Gamma)} = \int_\Gamma (-\Delta_\Gamma)^{-1/4} \psi (-\Delta_\Gamma)^{-1/4} \varphi d\Gamma = \int_\Gamma (-\Delta_\Gamma)^{-1/2} \psi \varphi d\Gamma \quad (100)$$

and the related norm  $\|\psi\|_{H^{-1/2}(\Gamma)} = (\psi, \psi)_{H^{-1/2}(\Gamma)}^{1/2}$ .

We note that the observation is performed on the whole interface  $\Gamma$  for what concerns the gap on the fluxes, whereas it is restricted to the inflow interface  $\Gamma^{\text{in}}$  for that on the velocities.



From now on, by *solution of the virtual control approach* we will mean the solution of the minimization problem (97), with  $J$  defined in (98) and with  $u_i(\lambda_i)$  (for  $i = 1, 2$ ) the solutions of problems (95) and (96), respectively.

Problems (95) and (96) are well posed. As a matter of fact, the following result holds (see, e.g., [30]):

**Theorem 3.** *Under assumptions (44), if  $g_1 \in L^2_{\mathbf{b}}((\partial\Omega_1 \setminus \Gamma)^{\text{in}})$  and  $\lambda_1 \in L^2_{\mathbf{b}}(\Gamma^{\text{in}})$ , then the first-order problem (95) admits a unique solution  $u_1 = u_1(\lambda_1) \in L^2(\Omega_1)$ . Moreover  $u_1 \in L^2_{\mathbf{b}}(\partial\Omega_1)$  and  $\text{div}(\mathbf{b}u_1) \in L^2(\Omega_1)$ .*

As of problem (96), if  $g_2 \in H^{1/2}(\partial\Omega_2 \setminus \Gamma)$  and  $\lambda_2 \in H^{1/2}(\Gamma)$ , and moreover there exists a function  $\mu \in H^{1/2}(\partial\Omega_2)$  with  $g_2 = \mu|_{(\partial\Omega_2 \setminus \Gamma)}$  and  $\lambda_2 = \mu|_{\Gamma}$ , then there exists a unique solution  $u_2(\lambda_2)$  of (96) belonging to  $H^1(\Omega_2)$ . (See, e.g., [30].)

We introduce the following spaces:

$$\begin{aligned} V_1 &= \{w \in L^2(\Omega_1) : \text{div}(\mathbf{b}w) \in L^2(\Omega_1), w|_{\Gamma} \in L^2_{\mathbf{b}}(\Gamma)\}, \quad \Lambda_1 = L^2_{\mathbf{b}}(\Gamma^{\text{in}}), \\ V_2 &= H^1(\Omega_2), \\ \Lambda_2 &= \{\lambda_2 \in H^{1/2}(\Gamma) : \exists \mu \in H^{1/2}(\partial\Omega_2) \text{ s.t. } \lambda_2 = \mu|_{\Gamma} \text{ and } g_2 = \mu|_{\partial\Omega_2 \setminus \Gamma}\}, \\ \mathbf{V} &= V_1 \times V_2, \quad \mathbf{\Lambda} = \Lambda_1 \times \Lambda_2. \end{aligned} \tag{101}$$

In order to prove the existence of solution of the minimization problem (97), we define two pairs of auxiliary problems:

find  $(w_1^f, w_2^f) \in \mathbf{V}$  such that

$$\begin{cases} A_1 w_1^f = f & \text{in } \Omega_1 \\ w_1^f = g_1 & \text{on } (\partial\Omega_1 \setminus \Gamma)^{\text{in}} \\ w_1^f = 0 & \text{on } \Gamma^{\text{in}}, \end{cases} \quad \begin{cases} A_2 w_2^f = f & \text{in } \Omega_2 \\ w_2^f = g_2 & \text{on } \partial\Omega_2 \setminus \Gamma \\ w_2^f = 0 & \text{on } \Gamma, \end{cases} \tag{102}$$

and find  $(u_1^{\lambda_1}, u_2^{\lambda_2}) \in \mathbf{V}$  such that

$$\begin{cases} A_1 u_1^{\lambda_1} = 0 & \text{in } \Omega_1 \\ u_1^{\lambda_1} = 0 & \text{on } (\partial\Omega_1 \setminus \Gamma)^{\text{in}} \\ u_1^{\lambda_1} = \lambda_1 & \text{on } \Gamma^{\text{in}}, \end{cases} \quad \begin{cases} A_2 u_2^{\lambda_2} = 0 & \text{in } \Omega_2 \\ u_2^{\lambda_2} = 0 & \text{on } \partial\Omega_2 \setminus \Gamma \\ u_2^{\lambda_2} = \lambda_2 & \text{on } \Gamma. \end{cases} \tag{103}$$

Moreover we define the fluxes on the interface  $\Gamma$  associated to the solutions  $u_1^{\lambda_1}$  and  $u_2^{\lambda_2}$  as

$$\varphi_1^{\lambda_1} = -\mathbf{b} \cdot \mathbf{n}_{\Gamma} u_1^{\lambda_1}, \quad \varphi_2^{\lambda_2} = -\nu \frac{\partial u_2^{\lambda_2}}{\partial \mathbf{n}_{\Gamma}} + \mathbf{b} \cdot \mathbf{n}_{\Gamma} u_2^{\lambda_2}, \tag{104}$$

while those associated to the solutions  $w_1^f$  and  $w_2^f$  are

$$\chi_1 = -\mathbf{b} \cdot \mathbf{n}_\Gamma w_1^f, \quad \chi_2 = -v \frac{\partial w_2^f}{\partial \mathbf{n}_\Gamma} + \mathbf{b} \cdot \mathbf{n}_\Gamma w_2^f. \quad (105)$$

The cost functional  $J$  can be split as

$$J(\lambda_1, \lambda_2) = J^0(\lambda_1, \lambda_2) + \mathcal{A}(\lambda_1, \lambda_2), \quad (106)$$

where

$$J^0(\lambda_1, \lambda_2) = \frac{1}{2} \|\lambda_1 - \lambda_2\|_{L_b^2(\Gamma^{\text{in}})}^2 + \frac{1}{2} \left\| \varphi_1^{\lambda_1} + \varphi_2^{\lambda_2} \right\|_{H^{-1/2}(\Gamma)}^2,$$

while  $\mathcal{A}$  is an affine functional which reads

$$\mathcal{A}(\lambda_1, \lambda_2) = \frac{1}{2} \|\chi_1 + \chi_2\|_{H^{-1/2}(\Gamma)}^2 + \left( \chi_1 + \chi_2, \varphi_1^{\lambda_1} + \varphi_2^{\lambda_2} \right)_{H^{-1/2}(\Gamma)}.$$

If all data are smooth enough, the existence of  $\boldsymbol{\lambda} = (\lambda_1, \lambda_2)$  achieving  $\inf J(\lambda_1, \lambda_2)$  in a possibly very large abstract space  $\mathbf{\Lambda}$ , follows from the property of  $(J^0(\lambda_1, \lambda_2))^{1/2}$  to be a norm (see [26, Sect. 5]).

### 3.1.1 The Optimality System

By following standard arguments of optimal control theory for elliptic problems (see [39]), we derive now the *optimality system* corresponding to the minimization problem (97).

Let us write the minimization problem (97) in a variational setting, i.e., we look for the solution  $\boldsymbol{\lambda} = (\lambda_1, \lambda_2) \in \mathbf{\Lambda}$  such that

$$\langle \nabla J(\boldsymbol{\lambda}), \boldsymbol{\mu} \rangle = 0 \quad \forall \boldsymbol{\mu} \in \mathbf{\Lambda}. \quad (107)$$

The partial derivative of  $J$  are

$$\begin{aligned} \left\langle \frac{\partial J}{\partial \lambda_1}, \mu_1 \right\rangle &= (\lambda_1 - \lambda_2, \mu_1)_{L_b^2(\Gamma^{\text{in}})} + (\varphi_1(\lambda_1) + \varphi_1(\lambda_2), \varphi_1^{\mu_1})_{H^{-1/2}(\Gamma)} \quad \forall \mu_1 \in \Lambda_1, \\ \left\langle \frac{\partial J}{\partial \lambda_2}, \mu_2 \right\rangle &= -(\lambda_1 - \lambda_2, \mu_2)_{L_b^2(\Gamma^{\text{in}})} + (\varphi_1(\lambda_1) + \varphi_1(\lambda_2), \varphi_2^{\mu_2})_{H^{-1/2}(\Gamma)} \quad \forall \mu_2 \in \Lambda_2, \end{aligned} \quad (108)$$

where, for any  $(\mu_1, \mu_2) \in \mathbf{\Lambda}$ ,  $\varphi_1^{\mu_1}$  and  $\varphi_2^{\mu_2}$  follow the definition of the fluxes as in (104), while  $u_1^{\mu_1}$ ,  $u_2^{\mu_2}$  are defined as in (103).

From the definition (100), for  $i = 1, 2$  we obtain

$$(\varphi_1(\lambda_1) + \varphi_1(\lambda_2), \varphi_i^{\mu_i})_{H^{-1/2}(\Gamma)} = \int_{\Gamma} (-\Delta_{\Gamma})^{-1/2} (\varphi_1(\lambda_1) + \varphi_1(\lambda_2)) \varphi_i^{\mu_i} d\Gamma \quad (109)$$

and, in particular for the flux  $\varphi_1^{\mu_1}$ , it holds

$$\begin{aligned} & \int_{\Gamma} (-\Delta_{\Gamma})^{-1/2} (\varphi_1(\lambda_1) + \varphi_2(\lambda_2)) \varphi_1^{\mu_1} d\Gamma \\ &= \int_{\Gamma^{\text{in}}} (-\Delta_{\Gamma})^{-1/2} (\varphi_1(\lambda_1) + \varphi_2(\lambda_2)) (-\mathbf{b} \cdot \mathbf{n}_{\Gamma}) \mu_1 d\Gamma \\ & \quad + \int_{\Gamma^{\text{out}}} (-\Delta_{\Gamma})^{-1/2} (\varphi_1(\lambda_1) + \varphi_1(\lambda_2)) (-\mathbf{b} \cdot \mathbf{n}_{\Gamma}) u_1^{\mu_1} d\Gamma. \end{aligned} \quad (110)$$

By defining the adjoint problems

$$\begin{cases} A_1^* p_1 \equiv -\mathbf{b} \cdot \nabla p_1 + b_0 p_1 = 0 & \text{in } \Omega_1 \\ p_1 = 0 & \text{on } (\partial\Omega_1 \setminus \Gamma)^{\text{out}} \\ p_1 = (-\Delta_{\Gamma})^{-1/2} (\varphi_1(\lambda_1) + \varphi_2(\lambda_2)) & \text{on } \Gamma^{\text{out}} \end{cases} \quad (111)$$

and

$$\begin{cases} A_2^* p_2 \equiv -\text{div}(v \nabla p_2) - \mathbf{b} \cdot \nabla p_2 + b_0 p_2 = 0 & \text{in } \Omega_2 \\ p_2 = 0 & \text{on } \partial\Omega_2 \setminus \Gamma \\ p_2 = (-\Delta_{\Gamma})^{-1/2} (\varphi_1(\lambda_1) + \varphi_2(\lambda_2)) & \text{on } \Gamma \end{cases} \quad (112)$$

and, by making use of Green's formula, we have

$$\begin{aligned} \int_{\Gamma^{\text{out}}} (-\Delta_{\Gamma})^{-1/2} (\varphi_1(\lambda_1) + \varphi_1(\lambda_2)) (-\mathbf{b} \cdot \mathbf{n}_{\Gamma}) u_1^{\mu_1} d\Gamma &= \int_{\Gamma^{\text{out}}} p_1 (-\mathbf{b} \cdot \mathbf{n}_{\Gamma}) u_1^{\mu_1} d\Gamma \\ &= \int_{\Gamma^{\text{in}}} (\mathbf{b} \cdot \mathbf{n}_{\Gamma}) p_1 \mu_1 d\Gamma \end{aligned}$$

while

$$\begin{aligned} \int_{\Gamma} (-\Delta_{\Gamma})^{-1/2} (\varphi_1(\lambda_1) + \varphi_1(\lambda_2)) \varphi_2^{\mu_2} d\Gamma &= \int_{\Gamma} p_2 \left( -v \frac{\partial u_2^{\mu_2}}{\partial \mathbf{n}_{\Gamma}} + \mathbf{b} \cdot \mathbf{n}_{\Gamma} u_2^{\mu_2} \right) d\Gamma \\ &= - \int_{\Gamma} v \frac{\partial p_2}{\partial \mathbf{n}_{\Gamma}} \mu_2, \end{aligned}$$

whence

$$\begin{aligned} \left\langle \frac{\partial J}{\partial \lambda_1}, \mu_1 \right\rangle &= \int_{\Gamma^{\text{in}}} (-\mathbf{b} \cdot \mathbf{n}_{\Gamma}) [(\lambda_1 - \lambda_2) + (p_2 - p_1)] \mu_1 d\Gamma, \\ \left\langle \frac{\partial J}{\partial \lambda_2}, \mu_2 \right\rangle &= \int_{\Gamma^{\text{in}}} (\mathbf{b} \cdot \mathbf{n}_{\Gamma}) (\lambda_1 - \lambda_2) \mu_2 d\Gamma - \int_{\Gamma} v \frac{\partial p_2}{\partial \mathbf{n}_{\Gamma}} \mu_2 d\Gamma \end{aligned} \quad (113)$$

for any  $\mu_1 \in \Lambda_1$  and  $\mu_2 \in \Lambda_2$ . In conclusion, the solution of the minimization problem (97) satisfies the following *optimality system* (in distributional sense):

$$(OS) \quad \begin{cases} \text{- state equations (95) and (96);} \\ \text{- adjoint equations (111) and (112);} \\ \text{- Euler equations:} \\ (\lambda_1 - \lambda_2) + p_2 - p_1 = 0 & \text{on } \Gamma^{\text{in}} \\ \mathbf{b} \cdot \mathbf{n}_\Gamma (\lambda_1 - \lambda_2) - v \frac{\partial p_2}{\partial \mathbf{n}_\Gamma} = 0 & \text{on } \Gamma^{\text{in}} \\ -v \frac{\partial p_2}{\partial \mathbf{n}_\Gamma} = 0 & \text{on } \Gamma^{\text{out}}. \end{cases}$$

### 3.1.2 Computation of the Laplace–Beltrami Operator

The computation of the discrete counterpart of  $(-\Delta_\Gamma)^{-1/2}(\varphi_1(\lambda_1) + \varphi_2(\lambda_2))$  when  $\Omega \subset \mathbb{R}^2$  can be made as follows.

Given a differentiable function  $u$  in an open neighbourhood of  $\Gamma$ , the tangential gradient of  $u$  is defined by (see, e.g., [11])

$$\nabla_\Gamma u(\mathbf{x}) = \nabla u(\mathbf{x}) - (\nabla u(\mathbf{x}) \cdot \mathbf{n}_\Gamma(\mathbf{x})) \mathbf{n}_\Gamma(\mathbf{x}), \quad \forall \mathbf{x} \in \Gamma, \quad (114)$$

where  $\nabla$  denotes the usual gradient in  $\mathbb{R}^2$ . The *Laplace–Beltrami operator* can be defined through the weak relation:

$$\int_\Gamma -\Delta_\Gamma u \, w \, d\Gamma = \int_\Gamma \nabla_\Gamma u \cdot \nabla_\Gamma w \, d\Gamma, \quad (115)$$

for any function  $w$  differentiable in an open neighbourhood of  $\Gamma$  vanishing at the end-points of  $\Gamma$ . In particular, if  $\Gamma$  is a segment parallel to the  $y$ -axis, it reduces to

$$\int_\Gamma -\Delta_\Gamma u \, w \, d\Gamma = \int_\Gamma \frac{\partial u}{\partial y} \frac{\partial w}{\partial y} \, d\Gamma. \quad (116)$$

In a finite dimensional context, if  $A_{\Gamma,h}$  denotes the symmetric positive definite matrix associated to the discretization of (116), we approximate  $(-\Delta_\Gamma)^{1/2}$  by the square root of  $A_{\Gamma,h}$ , that is the s.p.d. matrix  $A_{\Gamma,h}^{1/2}$  defined by

$$A_{\Gamma,h}^{1/2} = P \Lambda^{1/2} P^T, \quad (117)$$

where  $\Lambda$  and  $P$  are the eigenvalues and eigenvectors matrices, respectively, of  $A_{\Gamma,h}$ .

Alternatively, the fractional Laplace–Beltrami operator  $(-\Delta_\Gamma)^{-1/2}$  can be defined through a Neumann to Dirichlet map defined from  $H^{-1/2}(\Gamma)$  to  $H^{1/2}(\Gamma)$ . Precisely, for any  $\varphi \in H^{-1/2}(\Gamma)$  we solve the problem

$$\begin{cases} -\Delta u + u = 0 & \text{in } \Omega_1 \\ \frac{\partial u}{\partial \mathbf{n}} = 0 & \text{on } \partial\Omega_1 \setminus \Gamma \\ \frac{\partial u}{\partial \mathbf{n}_\Gamma} = \varphi & \text{on } \Gamma \end{cases} \quad (118)$$

and we set  $(-\Delta_\Gamma)^{-1/2}\varphi = u|_\Gamma$ . The differential problem (118) may be solved in  $\Omega_2$  instead of  $\Omega_1$ .

### 3.1.3 Recovering the Interface Conditions

In order to recover the interface conditions we are imposing on the interface  $\Gamma$ , we eliminate the adjoint state variables  $p_1$  and  $p_2$  from the optimality system (OS).

Let us set  $\widehat{\mathbf{b}} = -\mathbf{b}$ ,  $\bar{b}_0 = b_0 - \text{div}\widehat{\mathbf{b}}$  and

$$\Gamma_b^{\text{in}} = \Gamma^{\text{out}}, \quad \Gamma_b^{\text{out}} = \Gamma^{\text{in}}, \quad (\partial\Omega_1 \setminus \Gamma)_b^{\text{in}} = (\partial\Omega_1 \setminus \Gamma)^{\text{out}}.$$

Thanks to (111), (112) and Euler equations in (OS), the functions  $p_1$  and  $p_2$  satisfy the following coupled problem in  $\Omega$ :

$$\begin{cases} \text{div}(\widehat{\mathbf{b}}p_1) + \bar{b}_0p_1 = 0 & \text{in } \Omega_1 \\ -\text{div}(v\nabla p_2) + \text{div}(\widehat{\mathbf{b}}p_2) + \bar{b}_0p_2 = 0 & \text{in } \Omega_2 \\ p_1 = 0 & \text{on } (\partial\Omega_1 \setminus \Gamma)_b^{\text{in}} \\ p_2 = 0 & \text{on } \partial\Omega_2 \setminus \Gamma \\ -v\frac{\partial p_2}{\partial \mathbf{n}_\Gamma} + (\widehat{\mathbf{b}} \cdot \mathbf{n}_\Gamma)p_2 = (\widehat{\mathbf{b}} \cdot \mathbf{n}_\Gamma)p_1 & \text{on } \Gamma_b^{\text{out}} \\ p_1 = p_2 & \text{on } \Gamma_b^{\text{in}} \\ v\frac{\partial p_2}{\partial \mathbf{n}_\Gamma} = 0 & \text{on } \Gamma_b^{\text{in}}. \end{cases} \quad (119)$$

By noting that  $\bar{b}_0 + \frac{1}{2}\text{div}\widehat{\mathbf{b}} = b_0 + \frac{1}{2}\text{div}\mathbf{b} \geq \sigma_0 > 0$  (see (31)) and by applying Theorem 1, problem (119) admits the unique solution  $p_1 = 0$  in  $\Omega_1$ ,  $p_2 = 0$  in  $\Omega_2$ . Therefore, (112)<sub>3</sub> implies  $\varphi_1(\lambda_1) + \varphi_2(\lambda_2) = 0$  on  $\Gamma$ , while the first Euler equation in (OS) implies that  $\lambda_1 - \lambda_2 = 0$  on  $\Gamma^{\text{in}}$ , i.e. the following conditions hold on the interface:

$$\begin{aligned} \varphi_1(\lambda_1) + \varphi_2(\lambda_2) &= 0 & \text{on } \Gamma \\ \lambda_1 &= \lambda_2 & \text{on } \Gamma^{\text{in}}. \end{aligned} \quad (120)$$

In conclusion the following result holds:

**Theorem 4.** *If  $\lambda$  is the solution of the minimization problem (97) with  $J$  defined in (98), then the state solutions  $u_1$  and  $u_2$  of (95) and (96) satisfy the interface conditions (120). Moreover the pair  $(u_1(\lambda_1), u_2(\lambda_2))$ , obtained by the virtual control approach coincides with the solution of the heterogeneous problem (40).*

Thanks to the interface condition (120)<sub>2</sub>, the virtual control problem may be reformulated in terms of a unique control function  $\lambda$  defined on  $\Gamma$  and coinciding with  $\lambda_2$ . The control  $\lambda_1$ , previously introduced, will coincide now with the restriction of  $\lambda$  to  $\Gamma^{\text{in}}$ .

By this reduction, the virtual control problem (97) becomes:  
look for the solution of the minimization problem

$$\inf_{\lambda \in \Lambda_2} J_1(\lambda) \quad \text{with} \quad J_1(\lambda) = \frac{1}{2} \|\varphi_1(\lambda) + \varphi_2(\lambda)\|_{H^{-1/2}(\Gamma)}^2, \quad (121)$$

with

$$\varphi_1(\lambda) = -\mathbf{b} \cdot \mathbf{n}_\Gamma u_1(\lambda), \quad \varphi_2(\lambda) = -v \frac{\partial u_2(\lambda)}{\partial \mathbf{n}_\Gamma} + \mathbf{b} \cdot \mathbf{n}_\Gamma u_2(\lambda) \quad (122)$$

and  $u_1 = u_1(\lambda)$ ,  $u_2 = u_2(\lambda)$  solutions of (95) and (96) with  $\lambda_2 = \lambda$ ,  $\lambda_1 = \lambda|_{\Gamma^{\text{in}}}$ . By working as done for the two-controls formulation, the derivative of the cost functional  $J_1$  reads

$$\begin{aligned} \langle J'_1(\lambda), \mu \rangle &= \int_{\Gamma^{\text{in}}} (-\mathbf{b} \cdot \mathbf{n}_\Gamma)(p_2 - p_1) \mu d\Gamma \\ &\quad - \int_{\Gamma} v \frac{\partial p_2}{\partial \mathbf{n}_\Gamma} \mu d\Gamma \end{aligned} \quad (123)$$

for any  $\mu \in \Lambda_2$ .

The corresponding optimality system (OS1) reads

$$(OS1) \left\{ \begin{array}{l} \text{- state equations (95) and (96) with } \lambda_2 = \lambda, \lambda_1 = \lambda|_{\Gamma^{\text{in}}} \\ \text{- adjoint equations (111) and (112) with } \varphi_i(\lambda) \text{ instead of} \\ \quad \varphi_i(\lambda_i), \text{ for } i = 1, 2; \\ \text{- Euler equations:} \\ \quad (\mathbf{b} \cdot \mathbf{n}_\Gamma)(p_2 - p_1) + v \frac{\partial p_2}{\partial \mathbf{n}_\Gamma} = 0 \quad \text{on } \Gamma^{\text{in}} \\ \quad v \frac{\partial p_2}{\partial \mathbf{n}_\Gamma} = 0 \quad \text{on } \Gamma^{\text{out}}. \end{array} \right.$$

*Remark 2.* Another cost functional proposed in [26] is

$$\tilde{J}(\lambda_1, \lambda_2) = \frac{1}{2} \|u_1(\lambda_1) - u_2(\lambda_2)\|_{L^2_b(\Gamma)}^2 + \frac{1}{2} \|\varphi_1(\lambda_1) + \varphi_2(\lambda_2)\|_{H^{-1/2}(\Gamma)}^2. \quad (124)$$

In this case the observation is performed on the whole interface for both fluxes and velocities. The minimization problem (97), in which the functional  $J$  is replaced by  $\tilde{J}$ , admits a unique solution too (see [26]), however it is not guaranteed that  $\inf \tilde{J}(\lambda_1, \lambda_2) = 0$ , so that no interface conditions are explicitly associated to this minimization problem.

*Remark 3.* We finally remark that the cost functional to be minimized is set up starting from known interface conditions, it is problem dependent and it requires a priori knowledge of the coupled problem. When the latter are not available, it is more suitable to consider the virtual control approach with overlap, that we will introduce in Sect. 3.3.

### 3.1.4 How to Solve the Optimality System

A first intuitive way to solve the optimality system (OS1) consists in invoking a Krylov method to seek the solution  $\lambda$  of the Euler equation of (OS1). Let us write the Euler equation, in distributional sense, as

$$J'_1(\lambda) = 0. \quad (125)$$

When we solve it by a Krylov method, like either GMRES or Bi-CGStab, we have to evaluate the action of the functional  $J'_1$  on the iterate  $\lambda^{(k)}$  at each iteration  $k \geq 0$  and this means to perform the steps summarized in the following algorithm.

*Algorithm 1*

1. solve the primal problems (95) and (96) with  $\lambda^{(k)}$  instead of  $\lambda_i$ , for  $i = 1, 2$ ;
2. compute the fluxes  $\varphi_1(\lambda^{(k)})$ ,  $\varphi_2(\lambda^{(k)})$  and the function  $s^{(k)} = (-\Delta_\Gamma)^{-1/2}(\varphi_1(\lambda^{(k)}) + \varphi_2(\lambda^{(k)}))$
3. solve the dual problems (111), (112) with  $s^{(k)}$  instead of  $(-\Delta_\Gamma)^{-1/2}(\varphi_1(\lambda_1) + \varphi_2(\lambda_2))$
4. compute  $J'_1(\lambda^{(k)})$  by (123), which reads (in distributional sense):

$$J'_1(\lambda) = \begin{cases} (-\mathbf{b} \cdot \mathbf{n}_\Gamma)(p_2 - p_1) - \nu \frac{\partial p_2}{\partial \mathbf{n}_\Gamma} & \text{on } \Gamma^{\text{in}} \\ -\nu \frac{\partial p_2}{\partial \mathbf{n}_\Gamma} & \text{on } \Gamma^{\text{out}}. \end{cases} \quad (126)$$

The solution of the Euler equation  $J'_1(\lambda) = 0$ , by a Krylov method with the use of *Algorithm 1*, is an alternative to the solution of the Steklov–Poincaré equation (54).

By properly replacing the definition of both state and adjoint equations and by correctly writing the derivatives of the cost functional, *Algorithm 1* can be adapted to solve the optimality system associated to the minimization of  $\tilde{J}$ .

Solving  $J'(\lambda) = 0$  is equivalent to solve the Schur complement with respect to the control variable  $\lambda$  derived from the optimal system (OS1).

**Table 8** Test case #1. Comparison between the cost functionals (121) and (124)

$\nu$	$J_1(\lambda)$			$\tilde{J}(\lambda_1, \lambda_2)$		
	$\ u_1 - u_2\ _{L^\infty(\Gamma^{\text{out}})}$	$\inf J_1$	#it	$\ u_1 - u_2\ _{L^\infty(\Gamma^{\text{out}})}$	$\inf \tilde{J}$	#it
0.1	2.330e-1	1.242e-12	18	1.367e-1	5.239e-6	44
0.05	1.221e-1	3.137e-12	27	5.275e-2	3.286e-7	61
0.01	1.346e-2	6.989e-11	60	7.146e-4	6.234e-10	134
0.005	1.075e-2	2.294e-11	82	5.049e-4	8.749e-10	177

#it stands for the number of Bi-CGStab-VC iterations.

### 3.1.5 Numerical Results for Decompositions Without Overlap

Let us consider the Test case #1 introduced in Sect. 2.4. First of all we compare the numerical solutions obtained by the virtual control approach by minimizing either the cost functional  $J_1(\lambda)$  defined in (121) (or, equivalently  $J(\lambda_1, \lambda_2)$  defined in (98)) and  $\tilde{J}(\lambda_1, \lambda_2)$  defined in (124). We have solved both the optimality system (OS1) and that associated to the minimization of  $\tilde{J}$  by Bi-CGStab iterations and by following the steps summarized in *Algorithm 1* (see Sect. 3.1.4). We will name Bi-CGStab-VC this approach.

In Table 8 we report for both the functionals (121) and (124):

- The  $L^\infty$ -norm on  $\Gamma^{\text{out}}$  of the jump of the solution, i.e.,  $[u]_{\Gamma^{\text{out}}} = \|u_1 - u_2\|_{L^\infty(\Gamma^{\text{out}})}$
- The infimum of the minimized cost functional
- The number of Bi-CGStab-VC iterations to converge up a tolerance  $\varepsilon = 10^{-8}$  versus the viscosity  $\nu$

A non-uniform spectral element discretization has been considered to solve the boundary-value problems in both  $\Omega_1$  and  $\Omega_2$ . The domain  $\Omega_1$  ( $\Omega_2$ , resp.) has been split in  $3 \times 6$  ( $4 \times 6$ , resp.) quadrilaterals with the same polynomial degree  $N = 16$  in each spatial direction and in each element.

First of all we note that not only the solution  $(u_1, u_2)$ , obtained by minimizing the cost functional  $J_1$ , features a jump on  $\Gamma^{\text{out}}$  (in fact we know that it is discontinuous on  $\Gamma^{\text{out}}$ ), but also the solution obtained by minimizing the cost functional  $\tilde{J}$  is discontinuous on  $\Gamma^{\text{out}}$ . Moreover, as pointed out in Remark 2, we observe that the value  $\inf \tilde{J}$  is not null for any considered viscosity, however  $\inf \tilde{J} \rightarrow 0$  as  $\nu \rightarrow 0$ . We have observed that the reached value  $\inf J_1$  is independent of the viscosity and it is very close to the machine accuracy.

About the number of Bi-CGStab iterations needed to solve the variational equation  $J'_1(\lambda) = 0$ , we observe that the convergence rate linearly depends on the reciprocal of the viscosity, that the minimization of  $\tilde{J}$  requires twice the iterations to minimize  $J_1$  and that the computational cost of each Bi-CGStab-VC iteration is the same for both the minimization problems. Then we conclude that the minimization of the cost functional  $\tilde{J}$  costs twice that of  $J_1$ .

In Table 9 we report the number of BiCGStab-VC iterations needed to solve the optimality system (OS1) up to a tolerance  $\varepsilon = 10^{-6}$ , versus the polynomial degree  $N$ , for two different values of the viscosity:  $\nu = 0.01$  and 0.005. It emerges that the convergence rate of Bi-CGStab-VC is independent of the polynomial degree.



**Table 9** Number of Bi-CGStab-VC iterations for the minimization of  $J_1(\lambda)$  on the test case #1

$N$	$\nu = 0.01$		$N$	$\nu = 0.005$	
	LB (1)	LB (SP <sup>-1</sup> )		LB (1)	LB (SP <sup>-1</sup> )
4	19	18	4	23	24
6	16	17	6	26	23
8	15	16	8	27	26
10	17	18	10	33	27
12	18	18	12	27	27
14	19	18	14	26	28
16	21	20	16	26	28

The acronym LB(1) stands for the implementation based on the computation of the square root of the discrete Laplace–Beltrami operator, while LB(SP<sup>-1</sup>) stands for the implementation based on the inversion of the Steklov–Poincaré (or Dirichlet to Neumann) operator (see Remark 3.1.2).

### 3.2 Domain Decomposition with Overlap

Let us consider now a decomposition of  $\Omega$  with overlap. Precisely, we introduce two subdomains  $\Omega_1$  and  $\Omega_2$ , such that

$$\overline{\Omega} = \overline{\Omega}_1 \cup \overline{\Omega}_2, \quad \Omega_{12} = \Omega_1 \cap \Omega_2 \neq \emptyset, \quad \Gamma_i = \partial\Omega_i \setminus (\partial\Omega_i \cap \partial\Omega), \quad i = 1, 2 \quad (127)$$

and we denote by  $\mathbf{n}_{\Gamma_i}$  (for  $i = 1, 2$ ) the outward normal vector on  $\Gamma_i$  with respect to  $\Omega_i$ .

In view of the considerations given at the beginning of this section, our aim is to investigate domain decomposition approaches alternative to the sharp-interface one which do not require a priori knowledge of interface conditions.

#### 3.2.1 An Engineering Practice on Overlapping Subdomains

The simpler and, very likely, most largely used approach consists in extending the classical Schwarz method [40, 54] to the heterogeneous coupling, then iterating on the Dirichlet data on the interfaces  $\Gamma_1$  and  $\Gamma_2$ .

For example, if  $A_1$  and  $A_2$  are the differential operators defined in (32) and (33), respectively, the *additive* (or sequential) version of the Schwarz method reads: given  $u_1^{(0)}$  and  $u_2^{(0)}$ , for  $k \geq 0$  do

$$\begin{cases} A_1 u_1^{(k+1)} = f & \text{in } \Omega_1 \\ u_1^{(k+1)} = g_1 & \text{on } (\partial\Omega_1 \setminus \Gamma_1)^{\text{in}} \\ u_1^{(k+1)} = u_2^{(k)} & \text{on } \Gamma_1^{\text{in}}, \end{cases} \quad \begin{cases} A_2 u_2^{(k+1)} = f & \text{in } \Omega_2 \\ u_2^{(k+1)} = g_2 & \text{on } \partial\Omega_2 \setminus \Gamma_2 \\ u_2^{(k+1)} = u_1^{(k+1)} & \text{on } \Gamma_2. \end{cases}$$

If we replace the interface condition  $u_2^{(k+1)} = u_1^{(k+1)}$  with  $u_2^{(k+1)} = u_1^{(k)}$  on  $\Gamma_2$ , we obtain the so-called *multiplicative* (or parallel) version of the Schwarz method.

The convergence of the Schwarz method applied to the global advection–diffusion equation has been largely studied, see, e.g. [6, 7, 33, 47].

In [47], the analysis of the Schwarz alternating method is made for homogeneous singular perturbation problems in which the advection dominates. Precisely, the author proves that if the subdomains can be chosen to *follow the flow*, i.e., if the boundary interface of one of the subdomains corresponds to an outflow boundary for the streamlines of the flow, then the Schwarz iterates converge in the maximum norm with an error reduction factor per iteration that exponentially decays with increasing overlap or decreasing diffusion. On the contrary, if the flow is recirculating and the subdomains are not suitably chosen, numerical evidence shows that there can be some deterioration in the convergence factor of the Schwarz method. No theoretical results however are available in literature about the convergence of Schwarz method for heterogeneous decompositions.

### 3.2.2 Schwarz Method with Dirichlet/Robin Interface Conditions

In [34] a variant of the classical Schwarz method is proposed, always for homogeneous advection–diffusion problems, and it consists in replacing Dirichlet with Robin conditions only on one interface of the decomposition with the aim of accelerating the convergence.

Let us consider again the overlapping decomposition shown in Fig. 14. In [34], Houzeaux and Codina consider the homogenous problem (1) and propose to solve it by a two-domain approach as follows: find the pair  $(u_1, u_2)$  such that

$$\begin{cases} A_2 u_1 = f & \text{in } \Omega_1 \\ u_1 = g & \text{on } \partial\Omega_1 \setminus \Gamma_1 \\ u_1 = u_2 & \text{on } \Gamma_1 \\ \\ A_2 u_2 = f & \text{in } \Omega_2 \\ u_2 = g & \text{on } \partial\Omega_2 \setminus \Gamma_2 \\ v \frac{\partial u_1}{\partial n_{\Gamma_2}} - \frac{1}{2}(\mathbf{b} \cdot \mathbf{n}_{\Gamma_2})u_1 = v \frac{\partial u_2}{\partial n_{\Gamma_2}} - \frac{1}{2}(\mathbf{b} \cdot \mathbf{n}_{\Gamma_2})u_2 & \text{on } \Gamma_2. \end{cases} \quad (128)$$

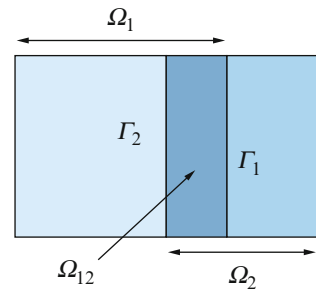


**Fig. 14** The computational domain split in two overlapping subdomains

By introducing Steklov–Poincaré operators on the interfaces, they prove that problem (128) admits a unique solution  $(u_1, u_2)$  such that  $u_1 = u_2$  on  $\Omega_{12}$ . Moreover, the function

$$u = \begin{cases} u_1 & \text{in } (\overline{\Omega_1} \setminus \Omega_{12}) \\ u_2 & \text{in } \Omega_2 \end{cases}$$

coincides with the solution of (1).

However, in [34] an overlapping Dirichlet/Robin method is proposed for the solution of the two advection–diffusion problems, with the purpose of inheriting the robustness properties of the classical Schwarz method, yet allowing the limit case of zero (or extremely small) overlapping, for which Dirichlet/Dirichlet method fails. Note that the interface condition (128)<sub>6</sub> arises from writing the convective term in skew-symmetric form.

Problem (128) can be solved iterating by subdomains. The resulting method is called *Dirichlet–Robin method* and it reads: given  $u_1^{(0)}$  and  $u_2^{(0)}$ , for  $k \geq 0$  do

$$\left\{ \begin{array}{ll} A_2 u_1^{(k+1)} = f & \text{in } \Omega_1 \\ u_1^{(k+1)} = g & \text{on } \partial\Omega_1 \setminus \Gamma_1 \\ u_1^{(k+1)} = \vartheta u_2^{(k)} + (1 - \vartheta) u_1^{(k)} & \text{on } \Gamma_1 \\ A_2 u_2^{(k+1)} = f & \text{in } \Omega_2 \\ u_2^{(k+1)} = g & \text{on } \partial\Omega_2 \setminus \Gamma_2 \\ v \frac{\partial u_2^{(k+1)}}{\partial n_{\Gamma_2}} - \frac{1}{2} (\mathbf{b} \cdot \mathbf{n}_{\Gamma_2}) u_2^{(k+1)} = v \frac{\partial u_1^{(k+1)}}{\partial n_{\Gamma_2}} - \frac{1}{2} (\mathbf{b} \cdot \mathbf{n}_{\Gamma_2}) u_1^{(k+1)} & \text{on } \Gamma_2, \end{array} \right. \quad (129)$$

where  $\vartheta > 0$  is a suitable relaxation parameter. As alternative to the relaxation of Dirichlet data (129)<sub>3</sub>, the authors propose to relax the Robin data (129)<sub>6</sub>. Under suitable choices of the relaxation parameter the Dirichlet–Robin algorithm (129) converges to the solution of the advection–diffusion problem (128).

When the heterogeneous coupling is considered, the Robin interface condition (128)<sub>6</sub> could be replaced by the following one:

$$-\frac{1}{2} (\mathbf{b} \cdot \mathbf{n}_{\Gamma_2}) u_1 = v \frac{\partial u_2}{\partial n_{\Gamma_2}} - \frac{1}{2} (\mathbf{b} \cdot \mathbf{n}_{\Gamma_2}) u_2 \quad \text{on } \Gamma_2, \quad (130)$$

so that the iterative Dirichlet–Robin algorithm for the coupled advection/advection–diffusion problem should read:

given  $u_1^{(0)}$  and  $u_2^{(0)}$ , for  $k \geq 0$  do

$$\begin{cases} A_1 u_1^{(k+1)} = f & \text{in } \Omega_1 \\ u_1^{(k+1)} = g & \text{on } (\partial\Omega_1 \setminus \Gamma_1)^{\text{in}} \\ u_1^{(k+1)} = \vartheta u_2^{(k)} + (1 - \vartheta) u_1^{(k)} & \text{on } \Gamma_1^{\text{in}} \\ A_2 u_2^{(k+1)} = f & \text{in } \Omega_2 \\ u_2^{(k+1)} = g & \text{on } \partial\Omega_2 \setminus \Gamma_2 \\ \nu \frac{\partial u_2^{(k+1)}}{\partial n_{\Gamma_2}} - \frac{1}{2} (\mathbf{b} \cdot \mathbf{n}_{\Gamma_2}) u_2^{(k+1)} = -\frac{1}{2} (\mathbf{b} \cdot \mathbf{n}_{\Gamma_2}) u_1^{(k+1)} & \text{on } \Gamma_2. \end{cases} \quad (131)$$

We note that algorithm (131) coincides with the Dirichlet–Neumann algorithm (47) when the overlap reduces to the empty set. We refer to Remark 1 in Sect. 3.3.2 about the classification of Neumann and Robin interface conditions.

### 3.3 Virtual Control Approach with Overlap for the Advection–Diffusion Equation

Let us consider an overlapping decomposition of  $\Omega$  as in (127). As done for the non-overlapping situation presented in Sect. 3.1, we introduce the Dirichlet *virtual controls*  $\lambda_1 \in L_b^2(\Gamma_1^{\text{in}})$  and  $\lambda_2 \in H^{1/2}(\Gamma_2)$  (Fig. 15) and we look for the solution of the following minimization problem:

$$\inf_{\lambda_1, \lambda_2} \hat{J}(\lambda_1, \lambda_2), \quad (132)$$

with

$$\hat{J}(\lambda_1, \lambda_2) = \int_{\Omega_{12}} (u_1(\lambda_1) - u_2(\lambda_2))^2 d\Omega, \quad (133)$$

and  $u_1 = u_1(\lambda_1)$ ,  $u_2 = u_2(\lambda_2)$  solutions of

$$\begin{cases} A_1 u_1 = f & \text{in } \Omega_1 \\ u_1 = g_1 & \text{on } (\partial\Omega_1 \setminus \Gamma_1)^{\text{in}} \\ u_1 = \lambda_1 & \text{on } \Gamma_1^{\text{in}}, \end{cases} \quad \begin{cases} A_2 u_2 = f & \text{in } \Omega_2 \\ u_2 = g_2 & \text{on } \partial\Omega_2 \setminus \Gamma_2 \\ u_2 = \lambda_2 & \text{on } \Gamma_2. \end{cases} \quad (134)$$

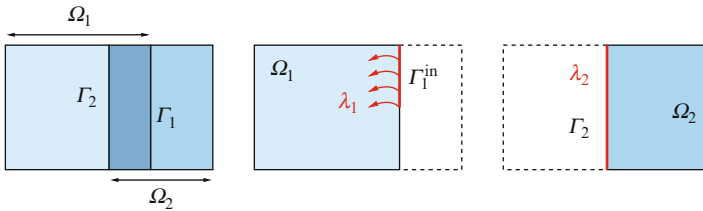


**Fig. 15** Virtual control with overlap

The minimization problem (132) has been studied in [1, 26].

Along this section we set

$$\begin{aligned}\Lambda_1 &= L^2_{\mathbf{b}}(\Gamma_1^{\text{in}}), \\ \Lambda_2 &= \{ \lambda_2 \in H^{1/2}(\Gamma_2) : \exists \mu \in H^{1/2}(\partial\Omega_2) \text{ s.t. } \lambda_2 = \mu|_{\Gamma_2} \text{ and } g_2 = \mu|_{\partial\Omega_2 \setminus \Gamma_2} \},\end{aligned}\tag{135}$$

The following result is stated in [26].

**Proposition 1.** *If the cost functional  $\hat{J}$  can be written as the sum of a quadratic functional  $\hat{J}^0(\lambda_1, \lambda_2)$  and an affine functional  $\mathcal{A}(\lambda_1, \lambda_2)$  (as done in Sect. 3.1), and if the seminorm*

$$\|(\lambda_1, \lambda_2)\| = \left( \hat{J}^0(\lambda_1, \lambda_2) \right)^{1/2}\tag{136}$$

*is indeed a norm, then problem (132) admits a unique solution in the space obtained by completion of  $\Lambda_1 \times \Lambda_2$  with respect to the norm (136).*

The property of (136) being a norm, depends on problem data, i.e. on the convection field  $\mathbf{b}$  and on the domain.

In [1], sufficient conditions which guarantee uniqueness of solution of the minimization problem (132) are furnished.

For simplicity, let us consider the decomposition of  $\Omega$  in two subdomains, as described in (15) and we refer to [1] for more general situations where either the overlapping set  $\Omega_{12} = \Omega_1 \cap \Omega_2$  is not connected or  $\partial\Omega_{12} \cap \partial\Omega = \emptyset$ . We denote by  $\mathbf{n}_{12}$  the outward unit normal to  $\Omega_{12}$ . The sufficient conditions (alternative one to each other) which guarantee uniqueness of solution for (132) are:

- I.  $\mathbf{b} \cdot \mathbf{n}_{12} \neq 0$  on  $\partial\Omega_{12} \cap \partial\Omega$ ,
- II.  $\begin{cases} \mu = b_0 + \text{div}\mathbf{b} \geq 0 \text{ on } \partial\Omega_{12}, \mu \not\equiv 0 \text{ on } \partial\Omega_{12}, \\ \text{the direction } \mathbf{b} \text{ at any point of } \partial\Omega_{12} \text{ forms with the outward normal} \\ \text{to } \partial\Omega_{12} \text{ an acute angle,} \end{cases}$
- III.  $\begin{cases} \mathbf{b} \cdot \mathbf{n}_{12} \neq 0 \text{ on } \partial\Omega_{12}, \frac{\mu}{b_n} - \frac{1}{2} \frac{\partial}{\partial \tau} \left( \frac{b_\tau}{b_n} \right) > 0 \text{ on } \partial\Omega_{12}, \\ \text{where } \frac{\partial}{\partial \tau} \text{ is the derivative along } \partial\Omega_{12}, \text{ while } b_n \text{ and } b_\tau \text{ are the normal} \\ \text{and tangential components, respectively, of } \mathbf{b} \text{ on } \partial\Omega_{12}. \end{cases}$

The previous proposition guarantees, under suitable assumptions, the uniqueness of the virtual controls and then that of the solution  $u_1$  in  $\Omega_1$  and  $u_2$  in  $\Omega_2$ . However in general,  $u_1 \neq u_2$  on the overlap  $\Omega_{12}$ . A natural question is: *how do we recover in  $\Omega_{12}$  a solution of the heterogeneous problem.*

The following result ensures that the difference between  $u_1$  and  $u_2$  in the  $L^2(\Omega_{12})$  norm annihilates when the viscosity vanishes (see [26]).

**Theorem 5.** *If we set*

$$\varphi(v) = \inf_{\lambda_1, \lambda_2} \hat{J}(\lambda_1, \lambda_2) \quad (137)$$

*and if we let  $v \rightarrow 0$ , all other data being fixed, then*

$$\varphi(v) \rightarrow 0 \quad \text{as } v \rightarrow 0. \quad (138)$$

The optimality system associated to the minimization problem (132) can be derived by proceeding as in Sect. 3.1.

For any  $\mu_1 \in \Lambda_1$ ,  $\mu_2 \in \Lambda_2$ , we introduce the auxiliary problems as follows:

$$\begin{cases} A_1 u_1^{\mu_1} = 0 & \text{in } \Omega_1 \\ u_1^{\mu_1} = 0 & \text{on } (\partial\Omega_1 \setminus \Gamma_1)^{\text{in}} \\ u_1^{\mu_1} = \mu_1 & \text{on } \Gamma_1^{\text{in}}, \end{cases} \quad \begin{cases} A_2 u_2^{\mu_2} = 0 & \text{in } \Omega_2 \\ u_2^{\mu_2} = 0 & \text{on } \partial\Omega_2 \setminus \Gamma_2 \\ u_2^{\mu_2} = \mu_2 & \text{on } \Gamma_2, \end{cases} \quad (139)$$

and we differentiate the functional  $\hat{J}$ :

$$\begin{aligned} \left\langle \frac{\partial \hat{J}}{\partial \lambda_1}, \mu_1 \right\rangle &= (u_1(\lambda_1) - u_2(\lambda_2), u_1^{\mu_1})_{L^2(\Omega_{12})} \quad \forall \mu_1 \in \Lambda_1, \\ \left\langle \frac{\partial \hat{J}}{\partial \lambda_2}, \mu_2 \right\rangle &= -(u_1(\lambda_1) - u_2(\lambda_2), u_2^{\mu_2})_{L^2(\Omega_{12})} \quad \forall \mu_2 \in \Lambda_2. \end{aligned} \quad (140)$$

We define the adjoint problems:

$$\begin{cases} A_1^* p_1 = \chi_{12}(u_1(\lambda_1) - u_2(\lambda_2)) & \text{in } \Omega_1 \\ p_1 = 0 & \text{on } \partial\Omega_1^{\text{out}} \end{cases} \quad (141)$$

and

$$\begin{cases} A_2^* p_2 = -\chi_{12}(u_1(\lambda_1) - u_2(\lambda_2)) & \text{in } \Omega_2 \\ p_2 = 0 & \text{on } \partial\Omega_2, \end{cases} \quad (142)$$

(where  $\chi_{12}$  denotes the characteristic function of the overlapping set  $\Omega_{12}$ ) and, by Green's formulas and the boundary conditions set in (139), (141) and (142), the optimality system associated to the minimization problem (132) reads (in distributional sense):

$$(OS2) \quad \begin{cases} \text{- State equations (134);} \\ \text{- Adjoint equations (141) and (142);} \\ \text{- Euler equations:} \\ \quad (-\mathbf{b} \cdot \mathbf{n}_{\Gamma_1}) p_1 = 0 & \text{on } \Gamma_1^{\text{in}} \\ \quad v \frac{\partial p_2}{\partial \mathbf{n}_{\Gamma_2}} = 0 & \text{on } \Gamma_2. \end{cases}$$

The optimality system (OS2) can be solved as described in Sect. 3.1.4 by a Bi-CGStab method.

### 3.3.1 Using Three Virtual Controls

In order to force the solutions  $u_1$  and  $u_2$  to coincide in  $\Omega_{12}$ , a virtual control problem with three controls has been proposed and studied in [1]. Precisely, in addition to the Dirichlet controls  $\lambda_1$  and  $\lambda_2$ , a distributed control  $\lambda_3 \in L^2(\Omega_{12})$  is used as forcing term in the hyperbolic equation in  $\Omega_1$ .

Let  $\Lambda_1$  and  $\Lambda_2$  the spaces defined in (135), then we set

$$\Lambda_3 = L^2(\Omega_{12}). \quad (143)$$

The *three virtual controls problem* is defined as follows. We seek  $\boldsymbol{\lambda} = (\lambda_1, \lambda_2, \lambda_3) \in \Lambda_1 \times \Lambda_2 \times \Lambda_3$  solution of the regularized minimization problem

$$\inf_{\lambda_1, \lambda_2, \lambda_3} \hat{J}_\alpha(\lambda_1, \lambda_2, \lambda_3), \quad (144)$$

where

$$\begin{aligned} \hat{J}_\alpha(\lambda_1, \lambda_2, \lambda_3) &= \frac{1}{2} \int_{\Omega_{12}} (u_1(\lambda_1, \lambda_3) - u_2(\lambda_2))^2 d\Omega \\ &\quad + \frac{\alpha}{2} (\|\lambda_1\|_{\Lambda_1}^2 + \|\lambda_2\|_{\Lambda_2}^2 + \|\omega\lambda_3\|_{\Lambda_3}^2), \end{aligned} \quad (145)$$

$u_1 = u_1(\lambda_1, \lambda_3)$  and  $u_2 = u_2(\lambda_2)$  are the solutions of the state equations

$$\begin{cases} A_1 u_1 = f + \omega \lambda_3 & \text{in } \Omega_1 \\ u_1 = g & \text{on } (\partial\Omega_1 \setminus \Gamma_1)^{\text{in}} \\ u_1 = \lambda_1 & \text{on } \Gamma_1^{\text{in}} \end{cases} \quad \begin{cases} A_2 u_2 = f & \text{in } \Omega_2 \\ u_2 = g & \text{on } \partial\Omega_2 \setminus \Gamma_2 \\ u_2 = \lambda_2 & \text{on } \Gamma_2, \end{cases} \quad (146)$$

$\alpha \geq 0$  is a penalization coefficient and, finally,  $\omega$  is a smooth function in  $\Omega$  such that

$$0 \leq \omega(\mathbf{x}) \leq 1 \text{ in } \Omega, \quad \omega = 0 \text{ in } \Omega \setminus \Omega_{12}, \quad \omega > 0 \text{ in } \Omega_{12}.$$

The optimality system associated to (145) reads (in variational form)

$$(OS3) \quad \begin{cases} \text{- State equations (146);} \\ \text{- Adjoint equations (141) and (142);} \\ \text{- Euler-Lagrange equations:} \\ \quad \begin{cases} (-\mathbf{b} \cdot \mathbf{n}_{\Gamma_1})(p_1 + \alpha\lambda_1) = 0 & \text{on } \Gamma_1^{\text{in}} \\ \nu \frac{\partial p_2}{\partial \mathbf{n}_{\Gamma_2}} + \alpha\lambda_2 = 0 & \text{on } \Gamma_2 \\ \alpha\omega\lambda_3 + \omega p_1 = 0 & \text{in } \Omega_{12}. \end{cases} \end{cases}$$

The following Theorem is proved in [1]:

**Theorem 6.** *For any  $\alpha > 0$ , the minimization problem (144) has a unique solution depending on  $\alpha$ , say  $(\lambda_1, \lambda_2, \lambda_3) = (\lambda_1(\alpha), \lambda_2(\alpha), \lambda_3(\alpha))$ , such that*

$$\|u_1(\lambda_1(\alpha), \lambda_3(\alpha)) - u_2(\lambda_2(\alpha))\|_{L^2(\Omega_{12})} \rightarrow 0 \quad \text{as } \alpha \rightarrow 0. \quad (147)$$

Moreover, if there exists a solution  $(\lambda_1^0, \lambda_2^0, \lambda_3^0)$  of the problem (146) such that the corresponding state functions coincide in  $\Omega_{12}$ , i.e.  $u_1^0(\lambda_1^0, \lambda_3^0) = u_2^0(\lambda_2^0)$  in  $\Omega_{12}$ , then the solution  $(\lambda_1^0, \lambda_2^0, \lambda_3^0)$  is unique and  $\lambda_k(\alpha) \rightarrow \lambda_k^0$  as  $\alpha \rightarrow 0$ , for  $k = 1, 2, 3$ .

*Remark 4.* The third control has been introduced to dump the difference between the hyperbolic and elliptic solutions on the overlap. It is important to highlight that it is added to the right hand side of the hyperbolic equation and not to the right hand side of the elliptic problem. This choice guarantees the uniqueness of solution of the minimization problem (144) when  $\alpha = 0$ , through the application of the uniqueness continuation theorem.

### 3.3.2 Numerical Results on Virtual Control Approaches

In this section we present some numerical results obtained by solving the coupled advection/advection–diffusion problem by two- and three-virtual controls approaches. First of all, we consider the one-dimensional problem

$$\begin{cases} -\nu u''(x) + u'(x) = 1 & 0 < x < 1 \\ u(0) = u(1) = 0, \end{cases} \quad (148)$$

and we set  $\Omega_1 = (0, 0.6)$ ,  $\Omega_2 = (0.3, 1)$ . In Fig. 16 we show the numerical solution obtained with both two-controls (dashed line) and three-controls (solid line), for  $\nu = 1$ , at left and  $\nu = 10^{-2}$  at right. The regularization parameter in  $\hat{J}_\alpha$  is  $\alpha = 0$ . The discretization is performed by spectral elements, precisely, we have decomposed both  $\Omega_1$  and  $\Omega_2$  in two spectral elements and the common element



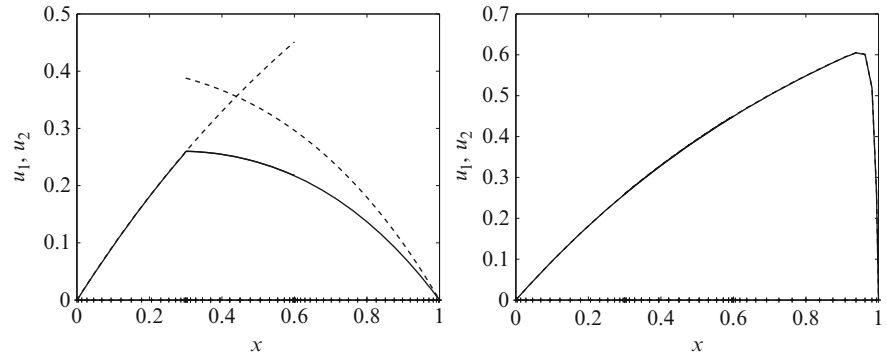


**Fig. 16** Numerical solutions of (148) obtained with two controls (*dashed line*) and three controls (*solid line*) for  $\nu = 1$  at *left* and for  $\nu = 10^{-2}$  at *right*.  $\Omega_1 = (0, 0.6)$ ,  $\Omega_2 = (0.3, 1)$

**Table 10** Test case #1. The number of Bi-CGStab iterations to solve the optimality systems (OS2) and (OS3) and the infimum of the cost functionals  $\hat{J}$  and  $\hat{\hat{J}}_0$  versus the viscosity  $\nu$

$\nu$	Two-controls		Three-controls	
	#it	$\inf \hat{J}(\lambda_1, \lambda_2)$	#it	$\inf \hat{\hat{J}}_0(\lambda_1, \lambda_2, \lambda_3)$
0.1	18	$8.71 \times 10^{-4}$	319	$2.83 \times 10^{-11}$
0.01	15	$5.85 \times 10^{-5}$	276	$1.97 \times 10^{-11}$
0.001	18	$4.92 \times 10^{-7}$	220	$5.81 \times 10^{-11}$
0.0001	18	$9.79 \times 10^{-9}$	190	$2.45 \times 10^{-11}$

discretizes the overlap  $\Omega_{12}$ . The polynomial degree used is  $N = 16$  in each element of both  $\Omega_1$  and  $\Omega_2$  when  $\nu = 1$ , while it is  $N = 16$  in each element of  $\Omega_1$  and  $N = 24$  in  $\Omega_2 \setminus \Omega_{12}$  when  $\nu = 10^{-2}$ . As we can see the solution obtained with three-controls matches on the overlap  $\Omega_{12}$  also with large viscosity  $\nu = 1$ .

Note that the interface  $\Gamma_1$  is an outflow boundary for the hyperbolic problem, so that the control  $\lambda_1$  is not needed. The number of degrees of freedom (i.e. the dimension of the system solved by Bi-CGStab) is one for the two controls approach, while it is of the same order of the number of discretization nodes on the overlap (about  $N$ ) for the three controls approach.

Let us consider now the 2D problem described in the Test case # 1 and let  $\hat{\hat{J}}_0$  denotes the cost functional  $\hat{J}_\alpha$  with  $\alpha = 0$  (i.e. without regularization). In the following table the infimum reached by both the cost functionals  $\hat{J}$  and  $\hat{\hat{J}}_0$  is shown for different values of the viscosity  $\nu$ . It is evident that the minimization of the cost functional with three controls provides a better solution with respect to the two virtual controls approach. Nevertheless, the cost of the three virtual controls approach (in terms of BiCG-Stab iterations needed to solve the optimality system) is very large, as shown in Table 10.

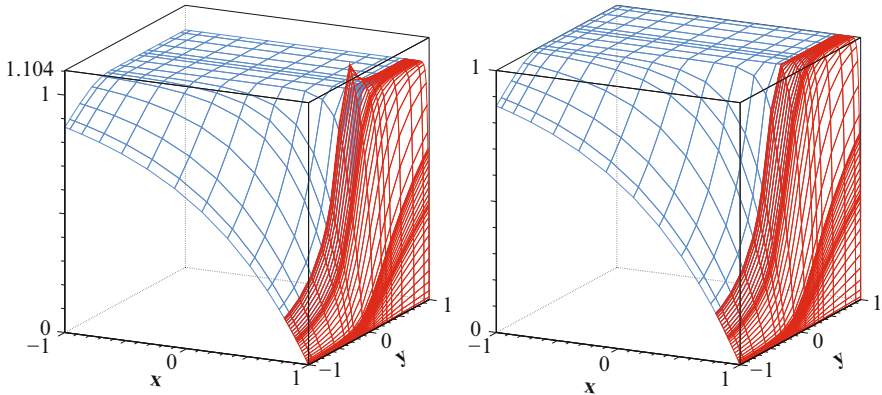


**Fig. 17** Test case #1.  $\nu = 0.01$ . *Left*: the solution obtained by minimizing  $\hat{J}(\lambda_1, \lambda_2)$ . *Right*: the solution obtained by minimizing  $\hat{J}_\alpha(\lambda_1, \lambda_2, \lambda_3)$  with  $\alpha = 0$

The stopping test for Bi-CGStab iterations is performed on the norm of the relative residual with tolerance  $\varepsilon = 10^{-6}$ . We observe that the number of iterations is small and is independent of the viscosity in the case of two virtual controls, while it is very large for the three virtual controls approach, even if it decreases when  $\nu \rightarrow 0$ .

In Fig. 17 we can appreciate the difference between the hyperbolic solution  $u_1$  and the elliptic one  $u_2$  inside the overlapping region  $\Omega_{12}$  for the two-virtual controls approach (left), and the goodness of the solution of the three virtual controls approach (right) when the viscosity is  $\nu = 0.01$ .

*Remark 5.* We conclude this Section by highlighting some features of the virtual control approach with overlap.

The analysis carried out on the virtual control approach with overlap represents a formal mathematical justification to engineering practice, that is to the Schwarz method applied to heterogeneous problems.

The virtual control approach with overlap is more “indifferent” with respect to interface conditions (no a priori information are required, contrary to the virtual control approach without overlap (see Remark 3).)

However, some open questions remain about the setting of the cost functional. In particular it is interesting to know if a “best” functional exists, if it is problem dependent or, again, if it depends on the characteristic parameters of the problem itself.

### 3.4 Virtual Control with Overlap for the Stokes–Darcy Coupling

In this section we apply the virtual control approach with overlap introduced in Sect. 3.3 to the coupled Stokes–Darcy problem that we have considered in Sect. 2.6.

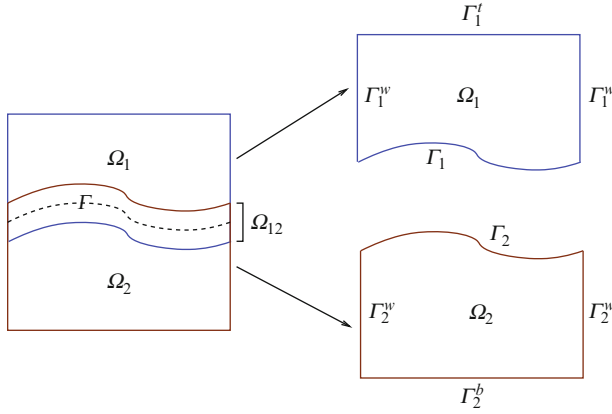


**Fig. 18** Schematic representation of the computational domain

Figure 18 shows our computational domain. In the subdomain  $\Omega_1$  we consider the following Stokes problem: find  $(\mathbf{u}, p) \in [H^1(\Omega_1)]^2 \times L^2(\Omega_1)$  such that

$$\begin{cases} -\nu \Delta \mathbf{u} + \nabla p = \mathbf{f} & \text{in } \Omega_1 \\ \operatorname{div} \mathbf{u} = 0 & \text{in } \Omega_1 \\ \nu \nabla \mathbf{u} \cdot \mathbf{n}_1 - p \mathbf{n}_1 = \mathbf{g} & \text{on } \Gamma_1^t \\ \mathbf{u} = \mathbf{u}^* & \text{on } \Gamma_1^w \\ \mathbf{u} = \boldsymbol{\lambda}_1 & \text{on } \Gamma_1, \end{cases} \quad (149)$$

where  $\mathbf{f}$ ,  $\mathbf{g}$  and  $\mathbf{u}^*$  are suitably chosen enough regular data.

On the other hand, in the subdomain  $\Omega_2$ , we consider the Darcy problem: find the piezometric head  $\varphi \in H^1(\Omega_2)$  such that

$$\begin{cases} -\operatorname{div}(K \nabla \varphi) = 0 & \text{in } \Omega_2 \\ K \nabla \varphi \cdot \mathbf{n}_2 = \boldsymbol{\psi}_N & \text{on } \Gamma_2^w \\ \varphi = \psi_D & \text{on } \Gamma_2^b \\ \varphi = \lambda_2 & \text{on } \Gamma_2, \end{cases} \quad (150)$$

where  $\boldsymbol{\psi}_N$  and  $\psi_D$  are suitable boundary data.

We refer to Fig. 18 for the notation of the boundaries.

$\lambda_1$  and  $\lambda_2$  are the controls variables which have to be seeked in the following spaces, respectively:

$$\Lambda_1 = \{\boldsymbol{\mu} \in [H^{1/2}(\Gamma_1)]^2 : \exists \mathbf{v} \in [H^1(\Omega_1)]^2, \mathbf{v} = \boldsymbol{\mu} \text{ on } \Gamma_1, \mathbf{v} = \mathbf{0} \text{ on } \Gamma_1^w\}, \quad (151)$$

$$\Lambda_2 = \{\mu \in H^{1/2}(\Gamma_2) : \exists \psi \in H^1(\Omega_2), \psi = \mu \text{ on } \Gamma_2, \nabla \varphi \cdot \mathbf{n}_2 = 0 \text{ on } \Gamma_2^w, \psi = 0 \text{ on } \Gamma_2^b\}. \quad (152)$$

$\lambda_1$  and  $\lambda_2$  are the solutions of the following minimization problem:

$$\inf_{\lambda_1, \lambda_2} J(\lambda_1, \lambda_2) \quad \text{with} \quad J(\lambda_1, \lambda_2) = \frac{1}{2} \int_{\Omega_{12}} (\mathbf{u} + K \nabla \varphi)^2. \quad (153)$$

*Remark 6.* Other functionals may be considered for the minimization problem (153) instead of  $J$ . For example, we may minimize the jump of pressures in the overlapping region, thus considering

$$\inf_{\lambda_1, \lambda_2} \bar{J}(\lambda_1, \lambda_2) \quad \text{with} \quad \bar{J}(\lambda_1, \lambda_2) = \frac{1}{2} \int_{\Omega_{12}} (p - g\varphi)^2. \quad (154)$$

Moreover, we could take into account some continuity condition (i.e., the continuity of the normal velocities) on the physical interface  $\Gamma \subset \Omega_{12}$  between the fluid and the porous-media regions. In this case we consider the functional

$$\tilde{J}(\lambda_1, \lambda_2) = \frac{1}{2} \int_{\Gamma} (\mathbf{u} \cdot \mathbf{n} + K \nabla \varphi \cdot \mathbf{n})^2 + \frac{1}{2} \int_{\Omega_{12}} (p - g\varphi)^2, \quad (155)$$

where  $\mathbf{n}$  is the normal unit vector on  $\Gamma$  directed outwards of the fluid domain.

We introduce now the following auxiliary problems:

find  $(\mathbf{u}^f, p^f) \in [H^1(\Omega_1)]^2 \times L^2(\Omega_1)$  such that

$$\begin{cases} -\nu \Delta \mathbf{u}^f + \nabla p^f = \mathbf{f} & \text{in } \Omega_1 \\ \operatorname{div} \mathbf{u}^f = 0 & \text{in } \Omega_1 \\ \nu \nabla \mathbf{u}^f \cdot \mathbf{n}_1 - p^f \mathbf{n}_1 = \mathbf{g} & \text{on } \Gamma_1^t \\ \mathbf{u}^f = \mathbf{u}^* & \text{on } \Gamma_1^w \\ \mathbf{u}^f = \mathbf{0} & \text{on } \Gamma_1, \end{cases} \quad (156)$$

and find  $\varphi^* \in H^1(\Omega_2)$  such that

$$\begin{cases} -\operatorname{div} (K \nabla \varphi^*) = 0 & \text{in } \Omega_2 \\ K \nabla \varphi^* \cdot \mathbf{n}_2 = \psi_N & \text{on } \Gamma_2^w \\ \varphi^* = \psi_D & \text{on } \Gamma_2^b \\ \varphi^* = 0 & \text{on } \Gamma_2. \end{cases} \quad (157)$$

Moreover, we consider the following problems depending only on the control variables:

find  $(\mathbf{u}^{\lambda_1}, p^{\lambda_1}) \in [H^1(\Omega_1)]^2 \times L^2(\Omega_1)$  such that

$$\begin{cases} -\nu \Delta \mathbf{u}^{\lambda_1} + \nabla p^{\lambda_1} = \mathbf{0} & \text{in } \Omega_1 \\ \operatorname{div} \mathbf{u}^{\lambda_1} = 0 & \text{in } \Omega_1 \\ \nu \nabla \mathbf{u}^{\lambda_1} \cdot \mathbf{n}_1 - p^{\lambda_1} \mathbf{n}_1 = \mathbf{0} & \text{on } \Gamma_1^t \\ \mathbf{u}^{\lambda_1} = \mathbf{0} & \text{on } \Gamma_1^w \\ \mathbf{u}^{\lambda_1} = \lambda_1 & \text{on } \Gamma_1, \end{cases} \quad (158)$$

and find  $\varphi^{\lambda_2} \in H^1(\Omega_2)$  such that

$$\begin{cases} -\operatorname{div}(K \nabla \varphi^{\lambda_2}) = 0 & \text{in } \Omega_2 \\ K \nabla \varphi^{\lambda_2} \cdot \mathbf{n}_2 = \mathbf{0} & \text{on } \Gamma_2^w \\ \varphi^{\lambda_2} = 0 & \text{on } \Gamma_2^b \\ \varphi^{\lambda_2} = \lambda_2 & \text{on } \Gamma_2. \end{cases} \quad (159)$$

Then, we can split

$$\mathbf{u} = \mathbf{u}^f + \mathbf{u}^{\lambda_1}, \quad p = p^f + p^{\lambda_1}, \quad \varphi = \varphi^* + \varphi^{\lambda_2}. \quad (160)$$

In this way we can rewrite the functional  $J(\lambda_1, \lambda_2)$  in (153) as

$$J(\lambda_1, \lambda_2) = J^0(\lambda_1, \lambda_2) + \mathcal{A}(\lambda_1, \lambda_2), \quad (161)$$

where  $J^0(\lambda_1, \lambda_2)$  is the quadratic functional

$$J^0(\lambda_1, \lambda_2) = \frac{1}{2} \int_{\Omega_{12}} (\mathbf{u}^{\lambda_1} + K \nabla \varphi^{\lambda_2})^2 \quad (162)$$

while  $\mathcal{A}(\lambda_1, \lambda_2)$  is the affine functional

$$\mathcal{A}(\lambda_1, \lambda_2) = \frac{1}{2} \int_{\Omega_{12}} (\mathbf{u}^f + K \nabla \varphi^*)^2 + \int_{\Omega_{12}} (\mathbf{u}^{\lambda_1} + K \nabla \varphi^{\lambda_2}) \cdot (\mathbf{u}^f + K \nabla \varphi^*). \quad (163)$$

We compute now  $\nabla J = \nabla J^0 + \nabla \mathcal{A}$ .

We have

$$\left\langle \frac{\partial J^0}{\partial \lambda_1}, \mu_1 \right\rangle = \int_{\Omega_{12}} \mathbf{u}^{\mu_1} \cdot (\mathbf{u}^{\lambda_1} + K \nabla \varphi^{\lambda_2}). \quad (164)$$

Considering the dual problem

$$\begin{cases} -\nu \Delta \mathbf{v} + \nabla q = (\mathbf{u}^{\lambda_1} + K \nabla \varphi^{\lambda_2}) \chi_{\Omega_{12}} & \text{in } \Omega_1 \\ \operatorname{div} \mathbf{v} = 0 & \text{in } \Omega_1 \\ \nu \nabla \mathbf{v} \cdot \mathbf{n}_1 - q \mathbf{n}_1 = \mathbf{0} & \text{on } \Gamma_1^f \\ \mathbf{v} = \mathbf{0} & \text{on } \Gamma_1^w \\ \mathbf{v} = \mathbf{0} & \text{on } \Gamma_1, \end{cases} \quad (165)$$

we can characterize the operator (164) as

$$\left\langle \frac{\partial J^0}{\partial \lambda_1}, \mu_1 \right\rangle = - \int_{\Gamma_1} (\nu \nabla \mathbf{v} \cdot \mathbf{n}_1 - q \mathbf{n}_1) \cdot \mu \quad \forall \mu \in A_1. \quad (166)$$

On the other hand, we have

$$\left\langle \frac{\partial J^0}{\partial \lambda_2}, \mu_2 \right\rangle = \int_{\Omega_{12}} -\operatorname{div}(K(\mathbf{u}^{\lambda_1} + K \nabla \varphi^{\lambda_2}) \chi_{\Omega_{12}}) \varphi^{\mu_2}, \quad (167)$$

and, using the dual problem:

$$\begin{cases} -\operatorname{div}(K \nabla \psi) = -\operatorname{div}(K(\mathbf{u}^{\lambda_1} + \nabla \varphi^{\lambda_2}) \chi_{\Omega_{12}}) & \text{in } \Omega_2 \\ K \nabla \psi \cdot \mathbf{n}_2 = \mathbf{0} & \text{on } \Gamma_2^w \\ \psi = 0 & \text{on } \Gamma_2^b \\ \psi = 0 & \text{on } \Gamma_2, \end{cases} \quad (168)$$

we obtain

$$\left\langle \frac{\partial J^0}{\partial \lambda_2}, \mu_2 \right\rangle = - \int_{\Gamma_2} K \nabla \psi \cdot \mathbf{n}_2 \mu_2 \quad \forall \mu_2 \in \Lambda_2. \quad (169)$$

We proceed in a similar way to characterize the affine functional  $\mathcal{A}$ . In this case, we have

$$\left\langle \frac{\partial \mathcal{A}}{\partial \lambda_1}, \mu_1 \right\rangle = - \int_{\Gamma_1} (v \nabla \tilde{\mathbf{v}} \cdot \mathbf{n}_1 - \tilde{q} \mathbf{n}_1) \cdot \boldsymbol{\mu} \quad \forall \boldsymbol{\mu} \in \Lambda_1, \quad (170)$$

$$\left\langle \frac{\partial \mathcal{A}}{\partial \lambda_2}, \mu_2 \right\rangle = - \int_{\Gamma_2} K \nabla \tilde{\psi} \cdot \mathbf{n}_2 \mu_2 \quad \forall \mu_2 \in \Lambda_2. \quad (171)$$

$(\tilde{\mathbf{v}}, \tilde{q}) \in [H^1(\Omega_1)]^2 \times L^2(\Omega_1)$  is the solution of the dual problem (165) with forcing term  $(\mathbf{u}^f + K \nabla \varphi^*) \chi_{\Omega_{12}}$ , while  $\tilde{\psi} \in H^1(\Omega_2)$  is the solution of the dual problem (168) with forcing term  $-\operatorname{div}(K(\mathbf{u}^f + K \nabla \varphi^*) \chi_{\Omega_{12}})$ .

To solve the minimization problem (153) we use the following algorithm:

1. Solve (156) and (157) to get  $\mathbf{u}^f$ ,  $p^f$  and  $\varphi^*$ .
2. Compute  $\nabla \mathcal{A}$ :
  - solve (165) with forcing term  $(\mathbf{u}^f + K \nabla \varphi^*) \chi_{\Omega_{12}}$  and compute (170);
  - solve (168) with forcing term  $-\operatorname{div}(K(\mathbf{u}^f + K \nabla \varphi^*) \chi_{\Omega_{12}})$  and compute (171).
3. Find  $(\lambda_1, \lambda_2) \in \Lambda_1 \times \Lambda_2$  such that  $\nabla J^0 = -\nabla \mathcal{A}$ . To this aim we use an iterative method like Bi-CGStab. At each iteration, to compute  $\nabla J^0(\lambda_1, \lambda_2)$  we do
  - solve (158) and (159);
  - compute  $\mathbf{u}^{\lambda_1} + K \nabla \varphi^{\lambda_2}$  in  $\Omega_{12}$ ;
  - solve (165) to get (166);
  - solve (168) to get (169).
4. Finally, solve (158) and (159) using the functions  $\lambda_1$  and  $\lambda_2$  computed at step 3 and use (160) to obtain the desired solutions.

### 3.4.1 Stokes/Darcy Coupling with Three Virtual Controls

A three virtual controls approach for the Stokes/Darcy coupling with overlap can be formulated as follows:

$$\left\{ \begin{array}{ll} \alpha \mathbf{u} - \nu \Delta \mathbf{u} + (\mathbf{u} \cdot \nabla) \mathbf{u} + \nabla p = \mathbf{0} & \text{in } \Omega_1 \\ \operatorname{div} \mathbf{u} = 0 & \text{in } \Omega_1 \\ \nu \nabla \mathbf{u} \cdot \mathbf{n}_1 - p \mathbf{n}_1 = \mathbf{g} & \text{on } \Gamma_1^t \\ \mathbf{u} = \mathbf{u}^* & \text{on } \Gamma_1^w \\ \mathbf{u} = \lambda_1 & \text{on } \Gamma_1 \\ -\operatorname{div}(K \nabla \varphi) = \chi_{\Omega_{12}} \lambda_3 & \text{in } \Omega_2 \\ K \nabla \varphi \cdot \mathbf{n}_2 = \psi_N & \text{on } \Gamma_2^w \\ \varphi = \psi_D & \text{on } \Gamma_2^b \\ \varphi = \lambda_2 & \text{on } \Gamma_2, \end{array} \right.$$

where  $\lambda_3$  is the third control, while other notations are those introduced in the previous section. It turns out that the virtual controls  $\lambda_1$ ,  $\lambda_2$ , and  $\lambda_3$  are solutions of the minimization problem

$$\inf_{\lambda_1, \lambda_2, \lambda_3} J(\lambda_1, \lambda_2, \lambda_3).$$

Several possible choices can be made for the cost functional  $J$ , e.g.,

$$J(\lambda_1, \lambda_2, \lambda_3) = \int_{\Omega_{12}} (K \nabla \varphi + \mathbf{u})^2 d\Omega.$$

A discussion about this approach (and related ones) is given in [14].

### 3.5 Coupling for Incompressible Flows

The Navier–Stokes/potential coupling introduced in Sect. 2.5 has been considered by Glowinski et al. [12, 13] in the framework of virtual controls with overlapping decomposition.

We denote by  $\Omega_1$  the extended subdomains where we consider the potential model, while let  $\Omega_2$  be the extended subregion where we consider the full Navier–Stokes equations. Finally,  $\Omega_{12} = \Omega_1 \cap \Omega_2$  is the overlapping region, and  $\Gamma_i = \partial\Omega_i \setminus (\partial\Omega_i \cap \partial\Omega)$ , for  $i = 1, 2$ . See Fig. 19.

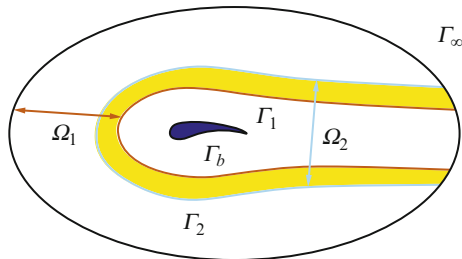


**Fig. 19** Splitting of the computational domain in two overlapping regions for the Navier–Stokes/potential coupling

We consider two control variables  $\lambda_1$  and  $\lambda_2$  in the following spaces, respectively:

$$\begin{aligned} \Lambda_1 &= \left\{ \mu \in H^{1/2}(\Gamma_1) : \exists \psi \in H^1(\Omega_1), \psi = \mu \text{ on } \Gamma_1, \frac{\partial \psi}{\partial \mathbf{n}_\infty} = 0 \text{ on } \Gamma_\infty \right\}, \\ \Lambda_2 &= \left\{ \mu \in [H^{1/2}(\Gamma_2)]^d : \exists \mathbf{v} \in [H^1(\Omega_2)]^d, \mathbf{v} = \mu \text{ on } \Gamma_2, \right. \\ &\quad \left. \mathbf{v} = \mathbf{0} \text{ on } \Gamma_b \cup (\Gamma_\infty \cap \partial\Omega_2), d = 2, 3 \right\}. \end{aligned}$$

$\lambda_1$  and  $\lambda_2$  represent Dirichlet interface conditions for the two subproblems. Indeed, we consider:

$$\begin{cases} \Delta\varphi = 0 & \text{in } \Omega_1 \\ \frac{\partial\varphi}{\partial\mathbf{n}_\infty} = \mathbf{u}_\infty \cdot \mathbf{n}_\infty & \text{on } \Gamma_\infty \cap \partial\Omega_1 \\ \varphi = \lambda_1 & \text{on } \Gamma_1 \end{cases} \quad (172)$$

and

$$\begin{cases} \alpha\mathbf{u} - \nu\Delta\mathbf{u} + (\mathbf{u} \cdot \nabla)\mathbf{u} + \nabla p = \mathbf{f} & \text{in } \Omega_2 \\ \operatorname{div} \mathbf{u} = 0 & \text{in } \Omega_2 \\ \mathbf{u} = \mathbf{0} & \text{on } \Gamma_b \cup (\Gamma_\infty \cap \partial\Omega_2) \\ \mathbf{u} = \lambda_2 & \text{on } \Gamma_2. \end{cases} \quad (173)$$

The unknown Dirichlet data  $\lambda_1$  and  $\lambda_2$  are the solutions of the minimization problem:

$$\inf_{\lambda_1, \lambda_2} J(\lambda_1, \lambda_2) \quad \text{with} \quad J(\lambda_1, \lambda_2) = \frac{1}{2} \int_{\Omega_{12}} (\nabla\varphi - \mathbf{u})^2 d\Omega \quad (174)$$

and satisfying the condition

$$\int_{\Gamma_2} \lambda_2 \cdot \mathbf{n}_{\Gamma_2} d\Gamma + \int_{\Gamma_\infty \cap \partial\Omega_2} \mathbf{u}_\infty \cdot \mathbf{n}_\infty d\Gamma = 0.$$

We refer the interested reader to [12, 13]. A similar approach for the case of compressible flows is presented in [28].

## References

1. V.I. Agoshkov, P. Gervasio, A. Quarteroni, Optimal control in heterogeneous domain decomposition methods for advection-diffusion equations. *Mediterr. J. Math.* **3**(2), 147–176 (2006)
2. G. Aguilar, F. Lisbona, Interface conditions for a kind of non linear elliptic hyperbolic problems, in *Domain Decomposition Methods for Partial Differential Equations*, ed. by A. Quarteroni, J. Périaux, Y.A. Kuznetsov, O.B. Widlund (American Mathematical Society, Providence, 1994), pp. 89–95



3. F. Brezzi, C. Canuto, A. Russo, A self-adaptive formulation for the Euler/Navier–Stokes coupling. *Comput. Meth. Appl. Mech. Eng.* **73**, 317–330 (1989)
4. L. Badea, M. Discacciati, A. Quarteroni, Numerical analysis of the Navier–Stokes/Darcy coupling. *Numer. Math.* **115**(2), 195–227 (2010)
5. G.S. Beavers, D.D. Joseph, Boundary conditions at a naturally permeable wall. *J. Fluid Mech.* **30**, 197–207 (1967)
6. X.C. Cai, Some Domain Decomposition Algorithms for Nonselfadjoint Elliptic and Parabolic Partial Differential Equations. Technical Report TR-461, Department of Computer Science, Courant Institute, 1989
7. X.-C. Cai, Additive Schwarz algorithms for parabolic convection-diffusion equations. *Numer. Math.* **60**(1), 41–61 (1991)
8. C. Canuto, M.Y. Hussaini, A. Quarteroni, T.A. Zang, *Spectral Methods. Evolution to Complex Geometries and Applications to Fluid Dynamics* (Springer, Heidelberg, 2007)
9. T.F. Chan, T.P. Mathew, Domain decomposition algorithms, in *Acta Numer.* (Cambridge University Press, Cambridge, 1994), pp. 61–143
10. C. Carlenzoli, A. Quarteroni, Adaptive domain decomposition methods for advection-diffusion problems, in *Modeling, Mesh Generation, and Adaptive Numerical Methods for Partial Differential Equations* (Minneapolis, MN, 1993), *IMA Volumes in Mathematics and its Applications*, vol. 75 (Springer, New York, 1995), pp. 165–186
11. K. Deckelnick, G. Dziuk, C.M. Elliott, Computation of geometric partial differential equations and mean curvature flow. *Acta Numer.* **14**, 139–232 (2005)
12. Q.V. Dinh, R. Glowinski, J. Périaux, Applications of domain decomposition techniques to the numerical solution of the Navier–Stokes equations, in *Numerical Methods for Engineering*, vol. 1 (Dunod, Paris, 1980), pp. 383–404
13. Q.V. Dinh, R. Glowinski, J. Périaux, G. Terrasson, On the coupling of viscous and inviscid models for incompressible fluid flows via domain decomposition, in *First Conf. on Domain Decomposition Methods for Partial Differential Equations*, ed. by G.A. Meurant, R. Glowinski, G.H. Golub, J. Périaux (SIAM, Philadelphia, 1988), pp. 350–368
14. M. Discacciati, P. Gervasio, A. Quarteroni, Virtual controls for heterogeneous problems. Technical Report, in progress.
15. M. Discacciati, *Domain Decomposition Methods for the Coupling of Surface and Groundwater Flows*. Ph.D. thesis, Ecole Polytechnique Fédérale de Lausanne, Switzerland, 2004
16. M. Discacciati, Iterative methods for Stokes/Darcy coupling, in *Domain Decomposition Methods in Science and Engineering. Lecture Notes in Computational Science and Engineering* (40), ed. by R. Kornhuber et al. (Springer, Berlin and Heidelberg, 2004) pp. 563–570
17. M. Discacciati, E. Miglio, A. Quarteroni, Mathematical and numerical models for coupling surface and groundwater flows. *Appl. Numer. Math.* **43**, 57–74 (2002)
18. M. Discacciati, A. Quarteroni, Analysis of a domain decomposition method for the coupling of Stokes and Darcy equations, in *Numerical Mathematics and Advanced Applications, ENUMATH 2001* ed. by F. Brezzi, A. Buffa, S. Corsaro, A. Murli (Springer, Milan, 2003), pp. 3–20
19. M. Discacciati, A. Quarteroni, Navier–Stokes/Darcy coupling: modeling, analysis, and numerical approximation. *Rev. Mat. Complut.* **22**(2), 315–426 (2009)
20. M. Discacciati, A. Quarteroni, A. Valli, Robin–Robin domain decomposition methods for the Stokes–Darcy coupling. *SIAM J. Numer. Anal.* **45**(3), 1246–1268 (electronic) (2007)
21. E. Dubach, Contribution à la résolution des équations fluides en domaine non borné. Ph.D. thesis, Université Paris 13, 1993
22. A. Frati, F. Pasquarelli, A. Quarteroni, Spectral approximation to advection-diffusion problems by the fictitious interface method. *J. Comput. Phys.* **107**(2), 201–211 (1993)
23. M.J. Gander, L. Halpern, C. Japhet, Optimized Schwarz algorithms for coupling convection and convection-diffusion problems, in *Domain Decomposition Methods in Science and Engineering* (Lyon, 2000), ed. by N. Debit, M. Garbey, R. Hoppe, J. Périaux, D. Keyes, Y. Kuznetsov, *Theory Eng. Appl. Comput. Methods, Internat. Center Numer. Methods Eng.* (CIMNE, Barcelona, 2002), pp. 255–262.

24. M.J. Gander, L. Halpern, C. Japhet, V. Martin, Advection diffusion problems with pure advection approximation in subregions, in *Domain Decomposition Methods in Science and Engineering XVI, Lecture Notes in Computer Science and Engineering*, vol. 55 ed. by O. Widlund and D. Keyes, (Springer, Berlin, 2007), pp. 239–246
25. M.J. Gander, L. Halpern, C. Japhet, V. Martin, Viscous problems with a vanishing viscosity approximation in subregions: a new approach based on operator factorization, in *Proceedings of ESAIM, CANUM2008*, Saint Jean de Monts, Vendée, France, vol. 27, 2009, pp. 272–288
26. P. Gervasio, J.-L. Lions, A. Quarteroni, Heterogeneous coupling by virtual control methods. *Numer. Math.* **90**(2), 241–264 (2001)
27. R. Glowinski, J. Périaux, Q.V. Dinh, Domain decomposition methods for non linear problems in fluid dynamics. Technical Report RR-0147, INRIA, 07 1982
28. R. Glowinski, J. Périaux, G. Terrasson, On the coupling of viscous and inviscid models for compressible fluid flows via domain decomposition, in *Third International Symposium on Domain Decomposition Methods for Partial Differential Equations*, Houston, TX, 1989, ed. by T.F. Chan, R. Glowinski, J. Périaux, O.B. Widlund, (SIAM, Philadelphia, PA, 1990), pp. 64–97
29. F. Gastaldi, A. Quarteroni, On the coupling of hyperbolic and parabolic systems: analytical and numerical approach. *Appl. Numer. Math.* **6**(1), 3–31 (1989)
30. F. Gastaldi, A. Quarteroni, G. Sacchi Landriani, On the coupling of two dimensional hyperbolic and elliptic equations: analytical and numerical approach, in *Third International Symposium on Domain Decomposition Methods for Partial Differential Equations*, Houston, TX, 1989, ed. by J. Périaux, T.F. Chan, R. Glowinski, O.B. Widlund, (SIAM, Philadelphia, 1990), pp. 22–63
31. V. Girault, P.A. Raviart, *Finite Element Methods for Navier–Stokes Equations. Theory and Algorithms* (Springer, Berlin, 1986)
32. V. Girault, B. Rivière, DG approximation of coupled Navier–Stokes and Darcy equations by Beaver–Joseph–Saffman interface condition. Technical Report TR-MATH 07-09, University of Pittsburgh, Department of Mathematics, 2007
33. G. Houzeaux, R. Codina, *A Geometrical Domain Decomposition Method in Computational Fluid Dynamics, Monograph CIMNE*, vol. 70 (International Center for Numerical Methods in Engineering (CIMNE), Barcelona, 2002)
34. G. Houzeaux, R. Codina, An iteration-by-subdomain overlapping Dirichlet/Robin domain decomposition method for advection-diffusion problems. *J. Comput. Appl. Math.* **158**(2), 243–276 (2003)
35. A. Iafraiti, E.F. Campana, A domain decomposition approach to compute wave breaking (wave-breaking flows). *Int. J. Numer. Meth. Fluids* **41**, 419–445 (2003)
36. W. Jäger and A. Mikelić, On the boundary conditions at the contact interface between a porous medium and a free fluid. *Ann. Scuola Norm. Sup. Pisa Cl. Sci.* **23**, 403–465 (1996)
37. W. Jäger, A. Mikelić, On the interface boundary condition of Beavers, Joseph and Saffman. *SIAM J. Appl. Math.*, **60**(4):1111–1127 (2000)
38. W. Jäger, A. Mikelić, N. Neuss, Asymptotic analysis of the laminar viscous flow over a porous bed. *SIAM J. Sci. Comput.*, **22**(6):2006–2028 (2001)
39. J.-L. Lions, *Optimal Control of Systems Governed by Partial Differential Equations*. (Springer, New York, 1971)
40. P.-L. Lions, On the Schwarz alternating method. I, in *First International Symposium on Domain Decomposition Methods for Partial Differential Equations*, Paris, 1987 (SIAM, Philadelphia, PA, 1988), pp. 1–42
41. P.L. Lions, On the Schwarz alternating method III: a variant for non-overlapping subdomains, in *Third International Symposium on Domain Decomposition Methods for Partial Differential Equations* ed. by T.F. Chan et al., (SIAM, Philadelphia, 1990), pp. 202–231
42. J.L. Lions, E. Magenes, *Problèmes aux Limites Non Homogènes et Applications*, vol. 1 (Dunod, Paris, 1968)
43. J.-L. Lions, O. Pironneau, Algorithmes parallèles pour la solution de problèmes aux limites. *C. R. Acad. Sci. Paris Sér. I Math.* **327**, 947–952 (1998)
44. J.-L. Lions, O. Pironneau, Sur le contrôle parallèle des systèmes distribués. *C. R. Acad. Sci. Paris Sér. I Math.* **327**, 993–998 (1998)

45. J.-L. Lions, O. Pironneau, Domain decomposition methods for CAD. *C. R. Acad. Sci. Paris Sér. I Math.* **328**, 73–80 (1999)
46. W.L. Layton, F. Schieweck, I. Yotov, Coupling fluid flow with porous media flow. *SIAM J. Num. Anal.* **40**, 2195–2218 (2003)
47. T.P. Mathew, Uniform convergence of the Schwarz alternating method for solving singularly perturbed advection-diffusion equations. *SIAM J. Numer. Anal.* **35**(4), 1663–1683 (1998)
48. D. Peaceman, H. Rachford, The numerical solution of parabolic and elliptic differential equations. *J. SIAM* **3**, 28–41 (1955)
49. L.E. Payne, B. Straughan, Analysis of the boundary condition at the interface between a viscous fluid and a porous medium and related modelling questions. *J. Math. Pures Appl.* **77**, 317–354 (1998)
50. A. Quarteroni, *Numerical Models for Differential Problems. Series MS&A.* vol. 2 (Springer, Milan, 2009)
51. A. Quarteroni, A. Valli, *Domain Decomposition Methods for Partial Differential Equations. Numerical Mathematics and Scientific Computation.* (The Clarendon Press, Oxford University Press, New York, 1999)
52. B. Rivière, I. Yotov, Locally conservative coupling of Stokes and Darcy flows. *SIAM J. Numer. Anal.* **42**(5), 1959–1977 (2005)
53. P.G. Saffman, On the boundary condition at the interface of a porous medium. *Stud. Appl. Math.* **1**, 93–101 (1971)
54. H.A. Schwarz, Über einige abbildungsaufgaben. *Ges. Math. Abh.* **11**, 65–83 (1869)
55. J.S. Scroggs, A parallel algorithm for nonlinear convection-diffusion equations, in *Third International Symposium on Domain Decomposition Methods for Partial Differential Equations*, Houston, TX, 1989 (SIAM, Philadelphia, PA, 1990), pp. 373–384
56. K. Schenk and F.K. Hebekker, Coupling of two dimensional viscous and inviscid incompressible Stokes equations. Technical Report Preprint 93-68 (SFB 359), Heidelberg University, 1993
57. H.A. van der Vorst, Bi-CGSTAB: a fast and smoothly converging variant of Bi-CG for the solution of nonsymmetric linear systems. *SIAM J. Sci. Statist. Comput.* **13**(2), 631–644 (1992)

Multiscale and Adaptivity: Modeling, Numerics and  
Applications

C.I.M.E. Summer School, Cetraro, Italy 2009

Bertoluzza, S.; Nochetto, R.H.; Quarteroni, A.; Siebert,  
K.G.; Veese, A. - Naldi, G.; Russo, G. (Eds.)

2012, XII, 314 p. 72 illus., 24 illus. in color., Softcover

ISBN: 978-3-642-24078-2